

dRICH SiPM photodetector electronics and integration

Roberto Preghenella

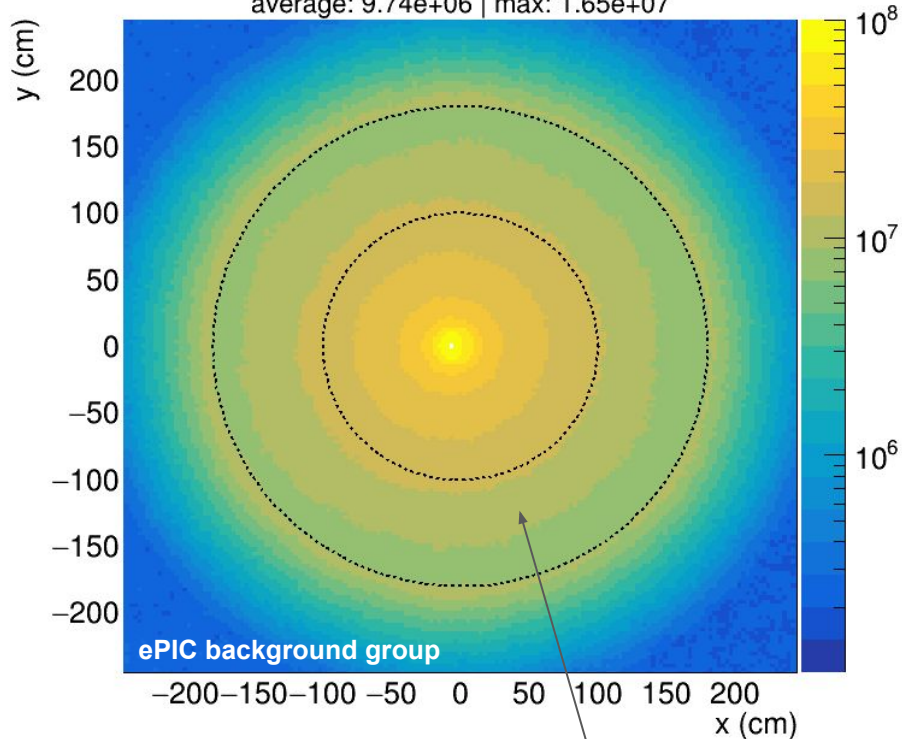
INFN Bologna

Summer 2024 Joint EICUG/ePIC Collaboration Meeting
PID Parallel Session at Lehigh Collaboration Meeting
25 July 2024, Lehigh University in Bethlehem, PA

Radiation damage estimates (March 1st, 2024 update)

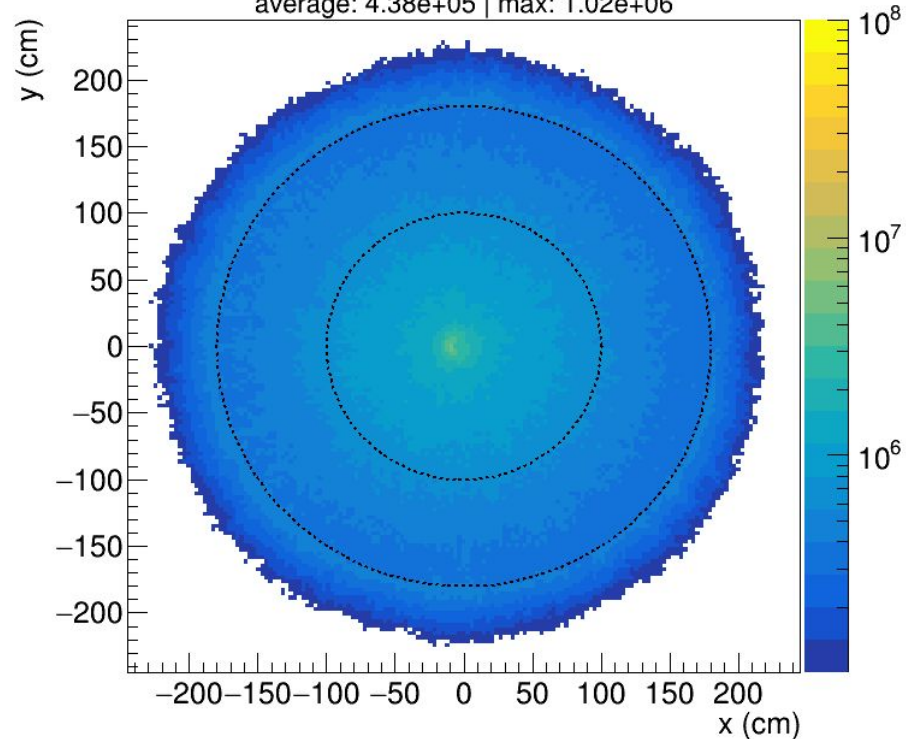
1 MEQ neutron equivalent fluence ($\text{cm}^{-2}/\text{fb}^{-1}$)
 minimum-bias PYTHIA e+p events at 10x275 GeV

average: $9.74\text{e}+06$ | max: $1.65\text{e}+07$



1 MEQ neutron equivalent fluence ($\text{cm}^{-2}/\text{fb}^{-1}$)
 275 GeV proton beam+gas events @ 35 kHz

average: $4.38\text{e}+05$ | max: $1.02\text{e}+06$

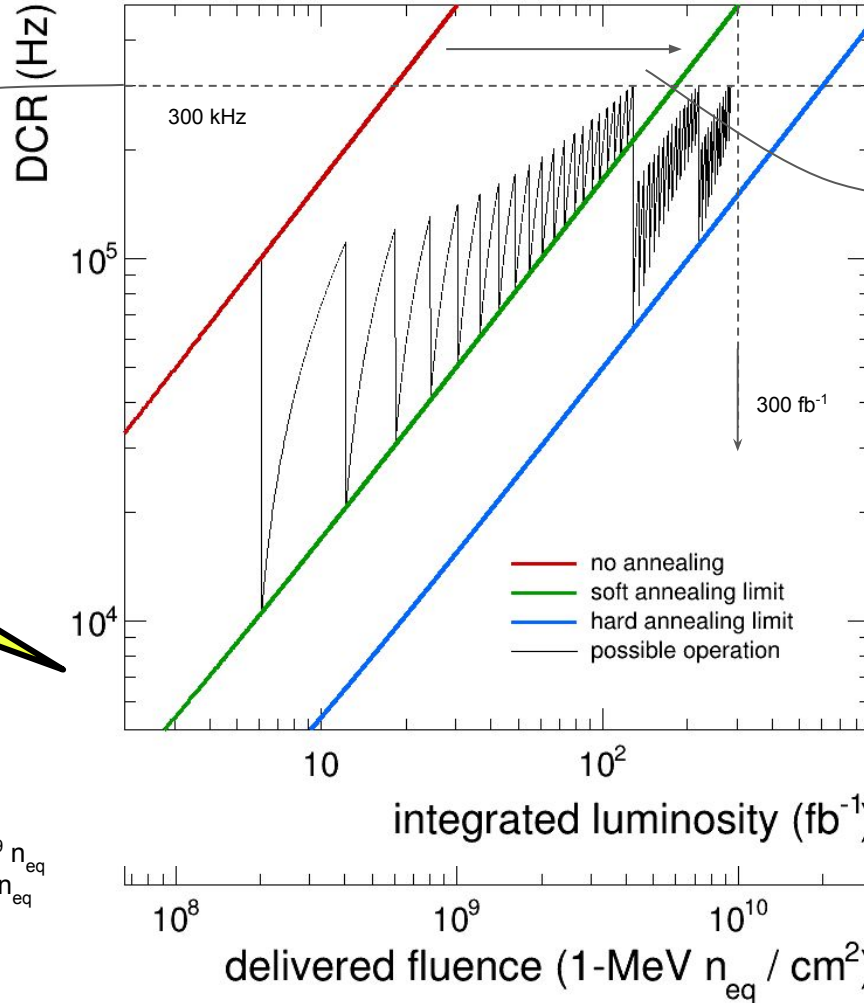


max fluence = $1.75 \cdot 10^7 \text{ neq}/\text{fb}^{-1}$ at the location of dRICH photosensors
 $210 < z < 260 \text{ cm}$, $100 < R < 180$, including fluence from proton beam-background interactions

Ageing model

max acceptable DCR for
Physics performance
~ 10 noise hits / sector **within 500 ps**

**the "possible operation"
scenario shown here has 44
soft-annealing cycles and 3
hard-annealing cycles**



in-situ annealing
significantly extends
SiPM lifetime

up to 300 fb⁻¹ without need
of touching/replacing SiPM
working on optimisation of
annealing protocol, maybe one
could reach beyond that

these predictions are according to
present knowledge / tested solutions
there are more handles to
further mitigate DCR
lower Vover, 3V
lower T operation -40 C or below

model input from R&D measurements (up to 2022)

- DCR increase: 500 kHz/10⁹ n_{eq}
- residual DCR (online annealing): 50 kHz/10⁹ n_{eq}
- residual DCR (oven annealing): 15 kHz/10⁹ n_{eq}

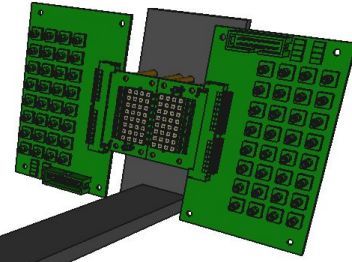
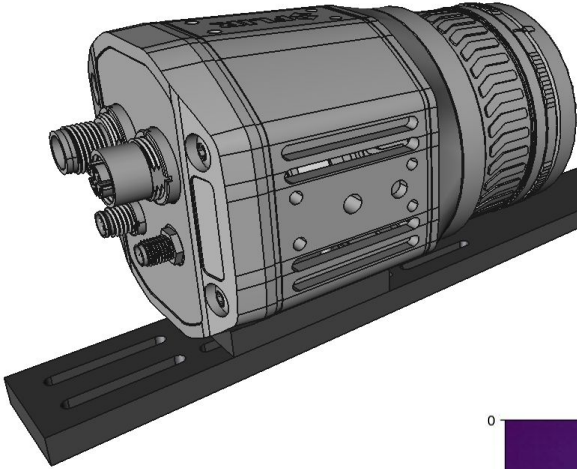
1-MeV neq fluence from background group

- 1.75 · 10⁷ n_{eq} / fb⁻¹
- add an extra 2x safety factor

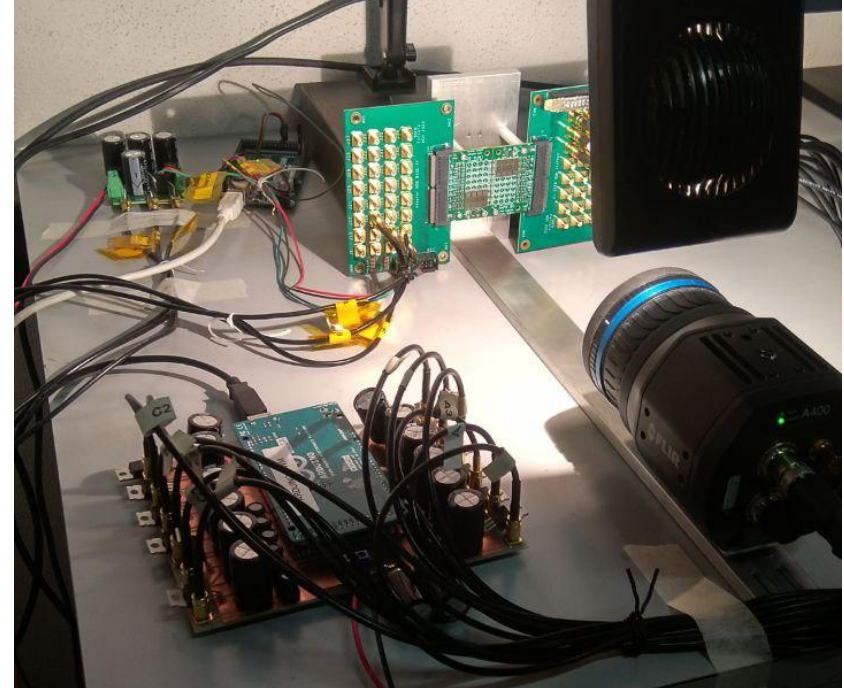
Automated multiple SiPM online self-annealing

system for online self-annealing with temperature monitor and control of each individual SiPM

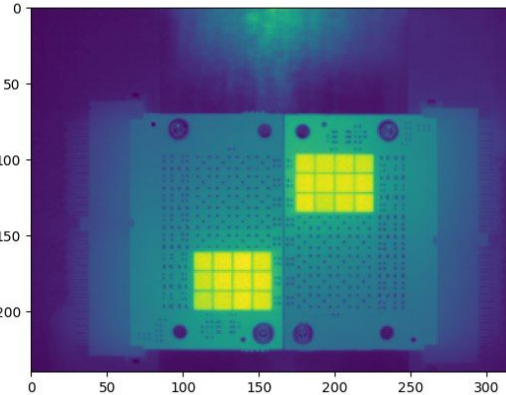
thermal camera



SiPM sensors & control electronics



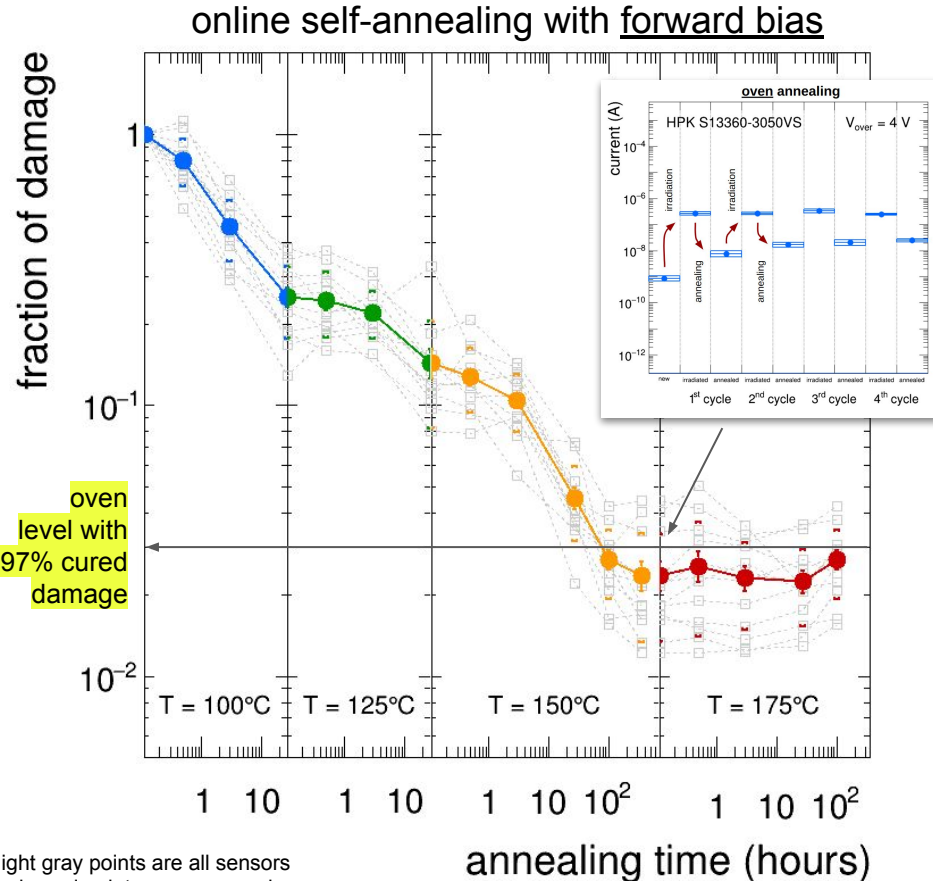
thermal image



monitor and logging system



Detailed studies of SiPM online self-annealing



**test on a large number SiPM sensors
how much damage is cured as a
function of temperature and time**

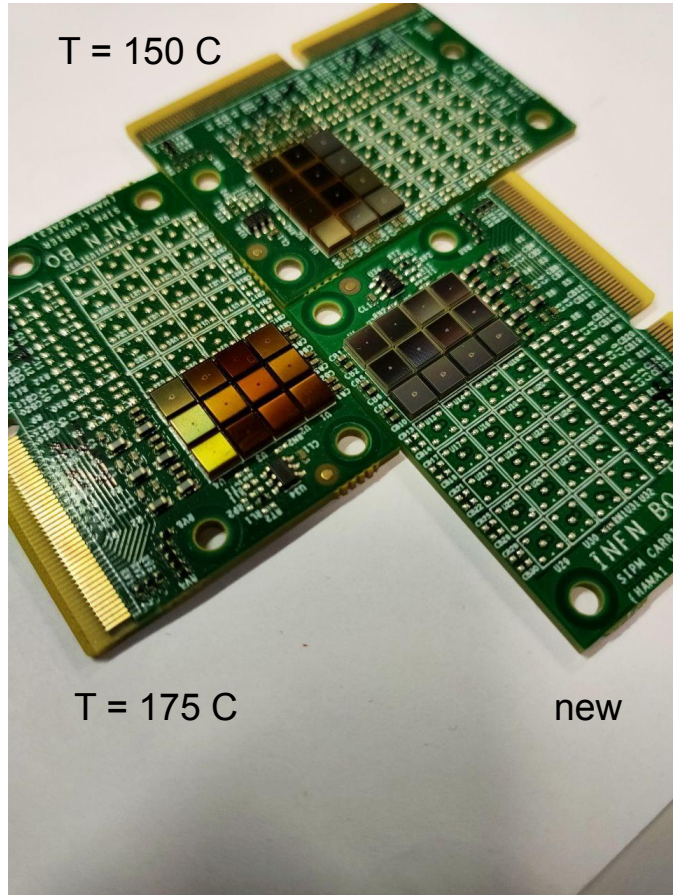
the same sensors have undergone self-annealing
increasing temperature steps
increasing integrated time steps

- started with T = 100 C annealing
 - performed 4 steps up to 30 hours integrated
- followed by T = 125, 150 and 175 C

**fraction of residual damage
seems to saturate at 2-3%
after ~ 300 hours at T = 150 C**
continuing at higher T = 175 C seems
not to cure more than that

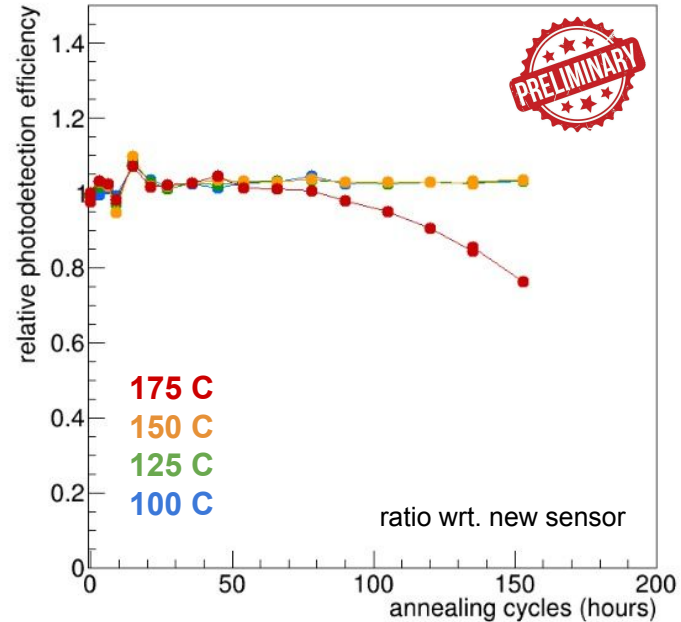
light gray points are all sensors
coloured points are averaged over sensors
coloured brackets is the RMS

Detailed studies of SiPM online self-annealing



after many hours of online annealing

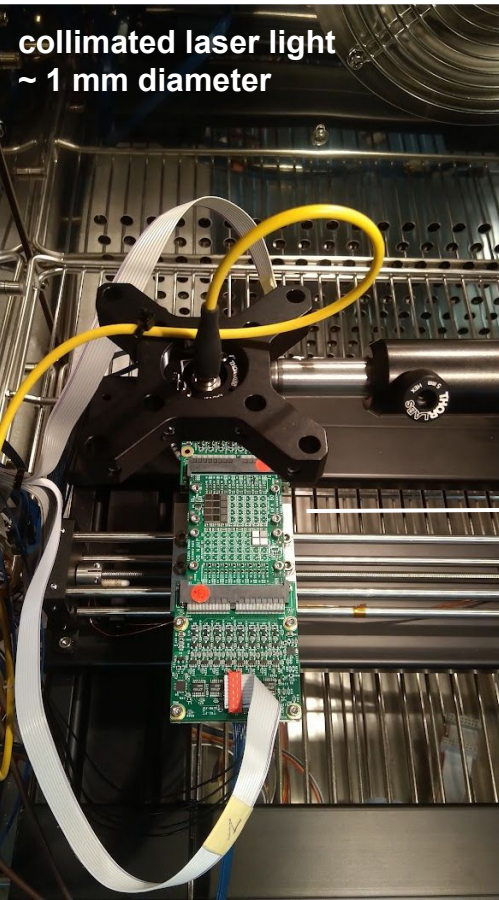
we noticed alterations on the SiPM windows
 in particular in one board that underwent
 500 hours of online annealing at $T = 175\text{ C}$
 the sensors appear "yellowish" when compared to new



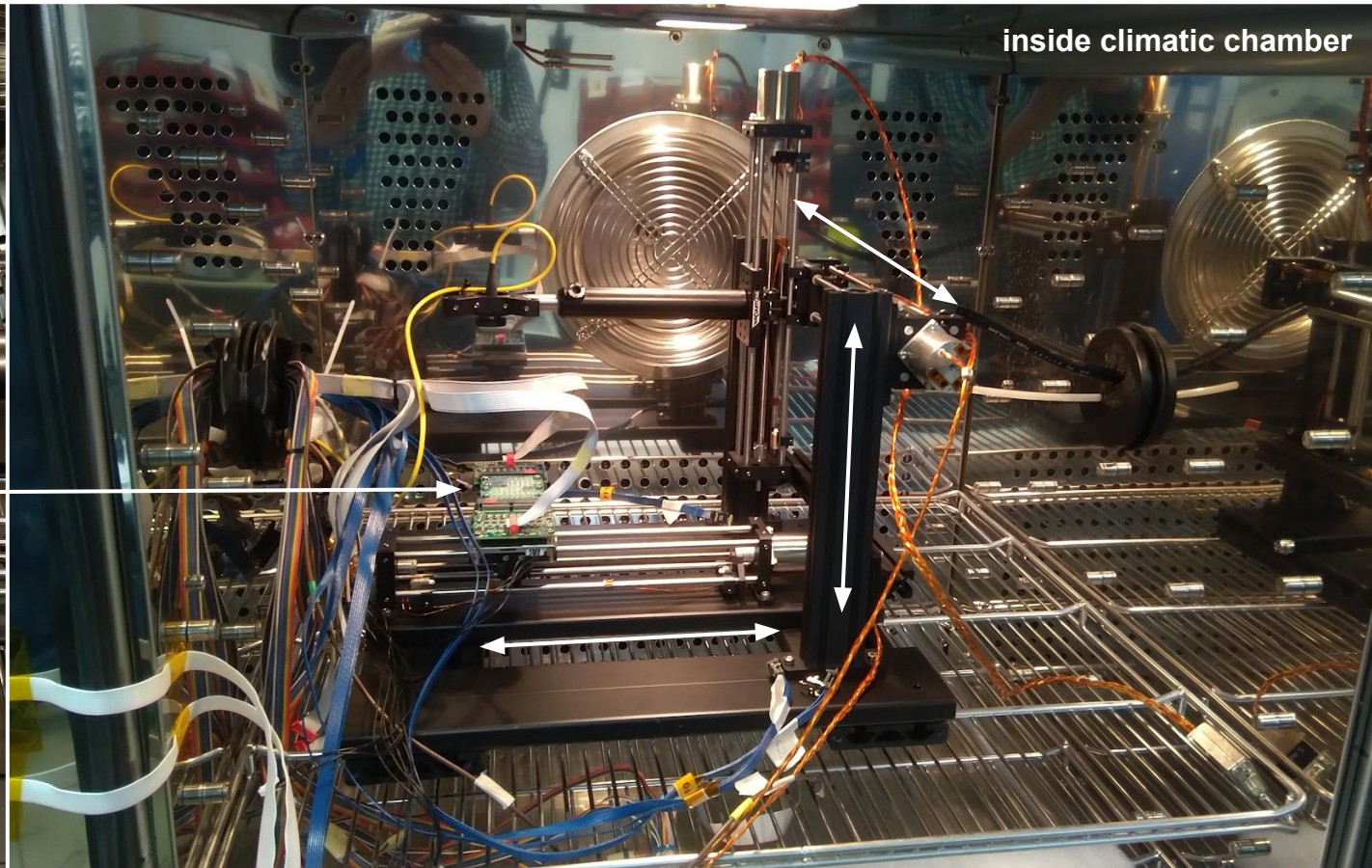
detailed studies are ongoing, preliminary results indicate efficiency loss after 100 hours of annealing at $T = 175\text{ C}$. lower temperatures unaffected up to 150 hours

Upgraded laser setup at INFN Bologna

new xyz moving stage that can operate at low temperature (down to $T = -40\text{ C}$) within a 200 mm range



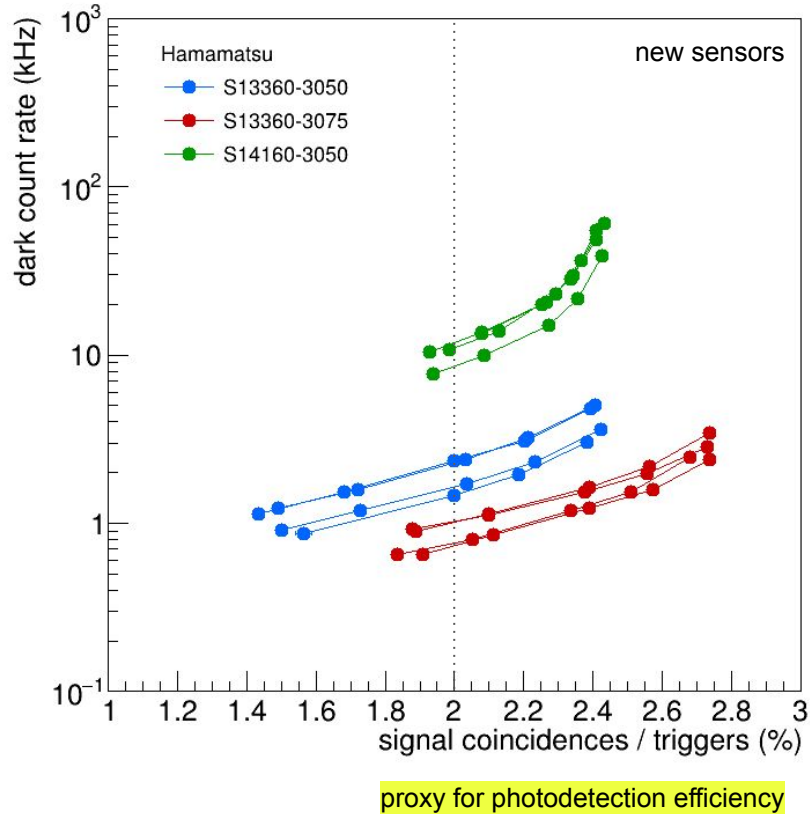
collimated laser light
~ 1 mm diameter



inside climatic chamber

DCR vs. PDE comparison between sensors

3 Hamamatsu sensor types, 4 sensors each measured as NEW



at the same level of detection efficiency
namely, the probability to detect light from laser pulse
different sensors have different DCR level

best: S13360-3075

most promising sensors, large pitch SPADs (75 μm)

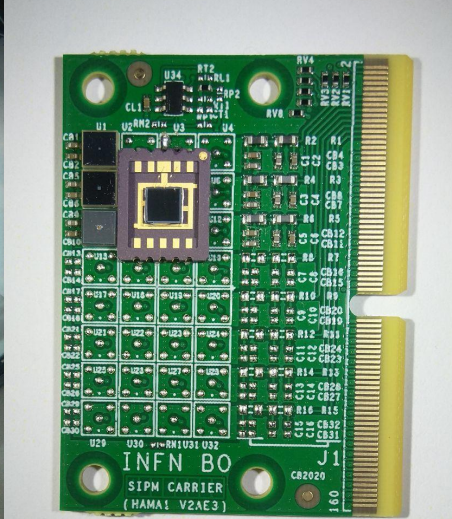
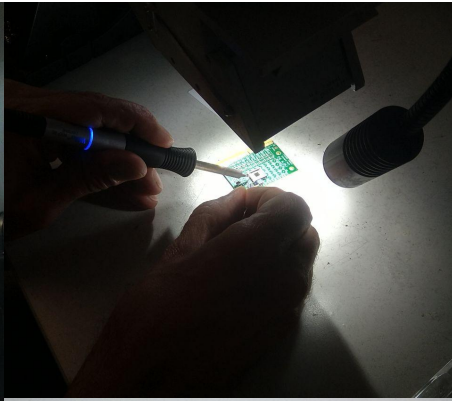
second: S13360-3050

same technology, medium pitch SPADs (50 μm)

worst: S14160-3050

different technology, medium pitch SPADs (50 μm)

New Hamamatsu SiPM prototypes



S13360-3050UVE

newly-developed Hamamatsu SiPM sensors

based on S13360 series

few samples of 50 μm and 75 μm SPAD sensors

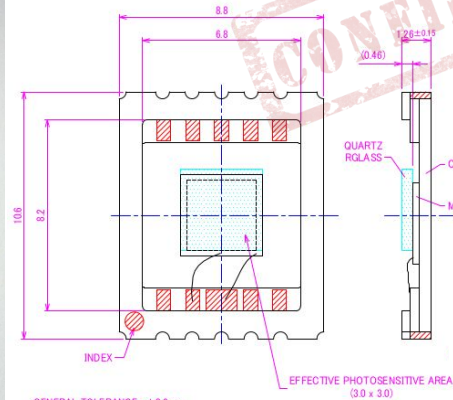
on paper they look VERY promising

- improved NUV sensitivity
- improved signal shape
- improved recharge time

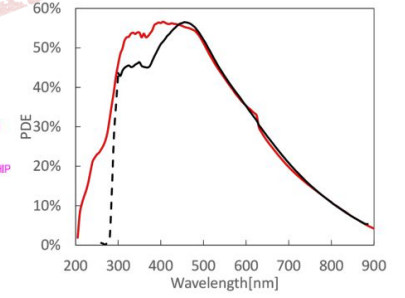
mounted on EIC SiPM test boards

we will characterise and test them in full

irradiation, annealing, laser, ...



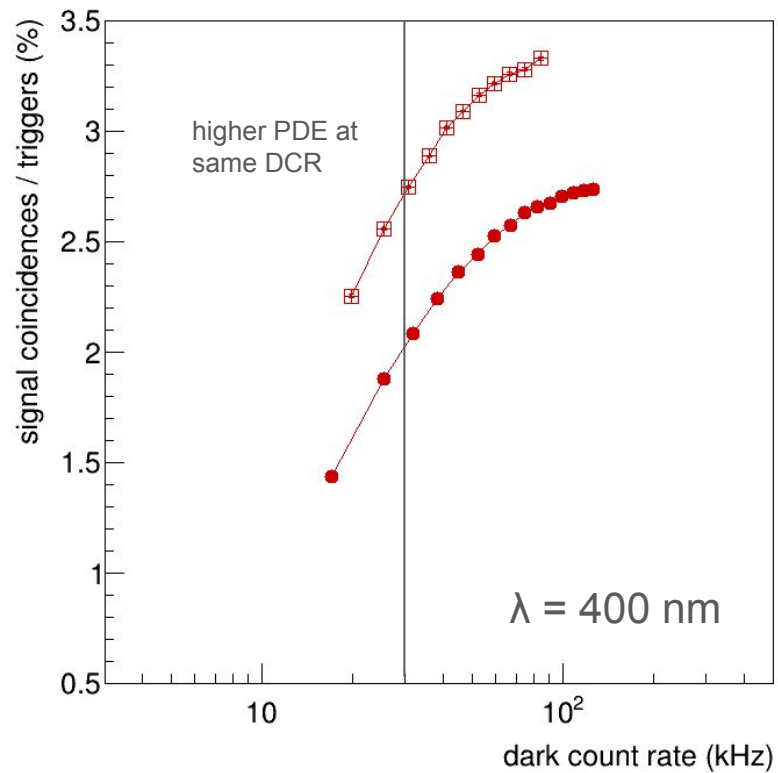
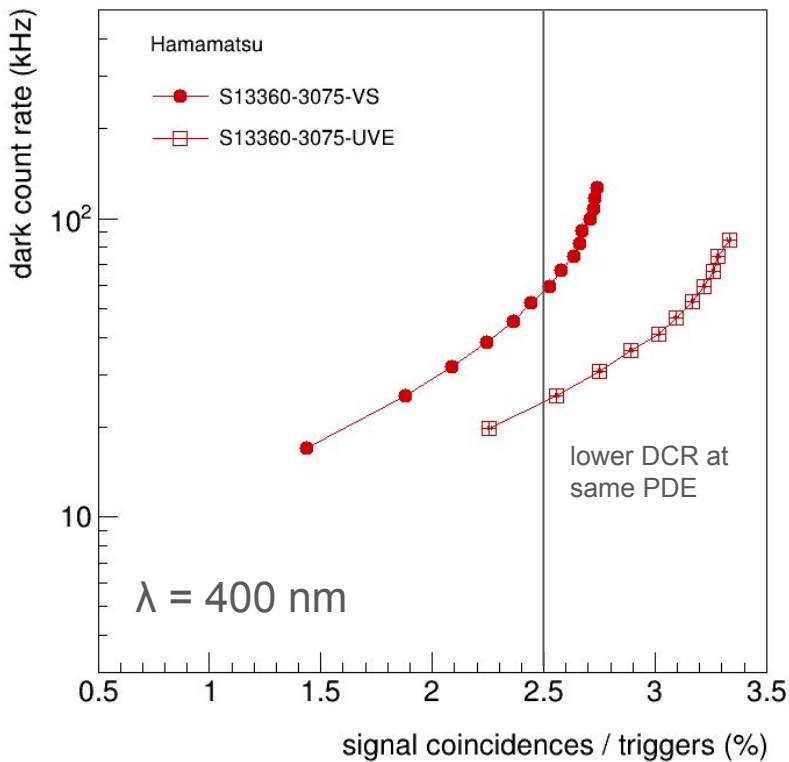
-GENERAL TOLERANCE: $\pm 0.3\text{mm}$
 -Au-WIRES ARE NOT PROTECTED.



— Prototype : based on S13360 series (75 μm)
 — Conventional : S14520 series (75 μm)

CONFIDENTIAL

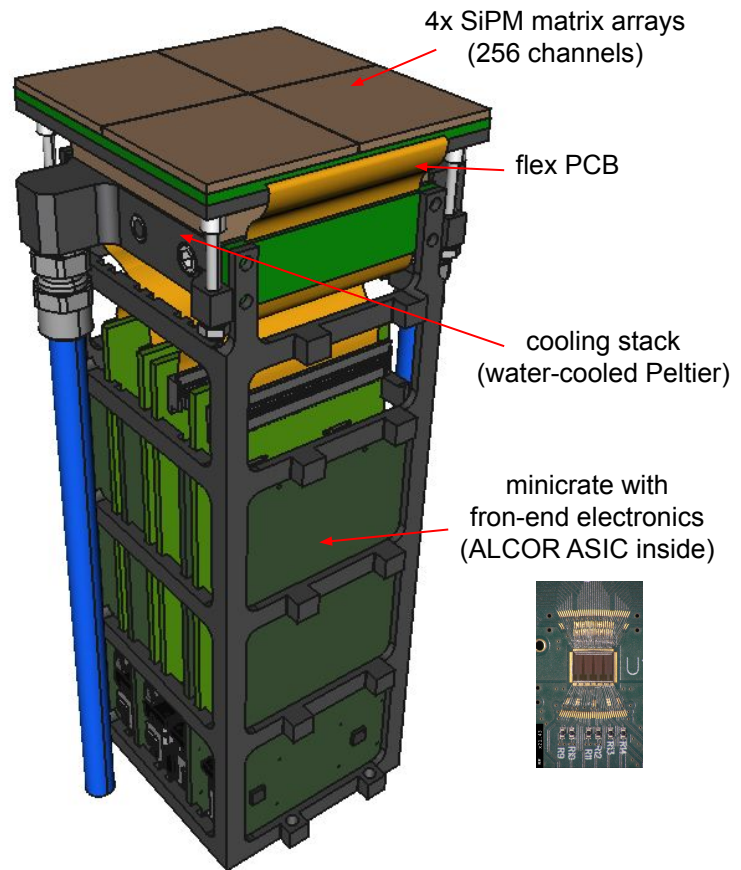
prototype Hamamatsu sensors (10^9 neq after oven annealing)



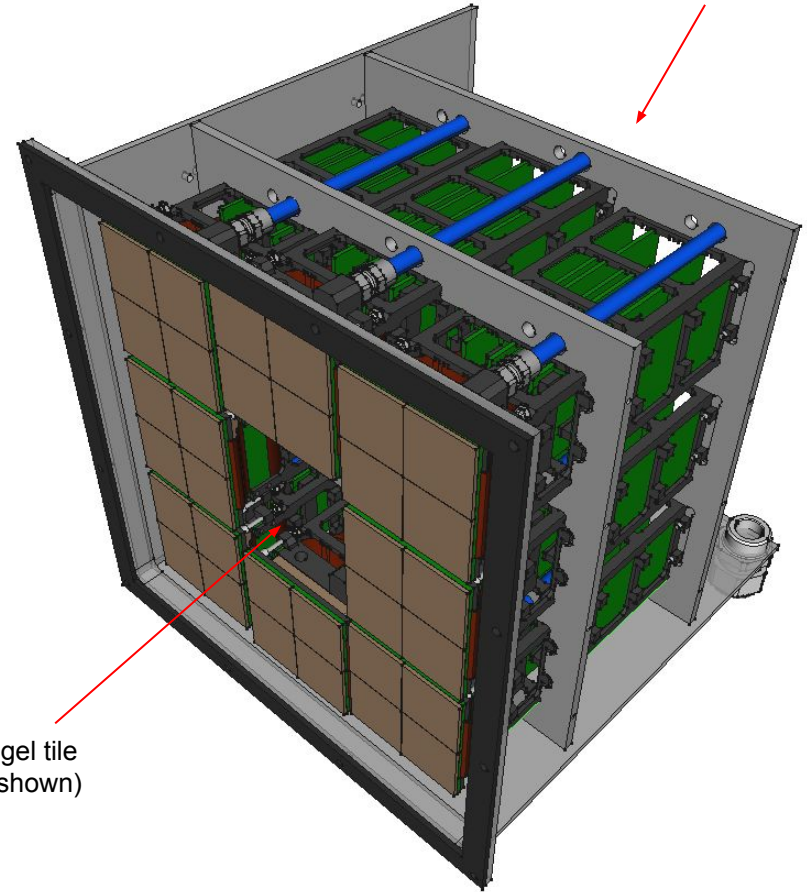
prototype Hamamatsu UVE sensors have significantly higher efficiency than standard sensors
 caveat: we only measure PDE at the fixed **laser wavelength of ~400 nm**, larger PDE expected because...
 prototype sensors have a NUV-enhanced behaviour.
 we will study them further, currently asking Hamamatsu status for production and quotation of this product

detector prototype
and beam tests

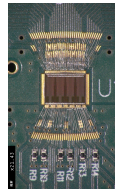
EIC ePIC-dRICH SiPM photodetector prototype



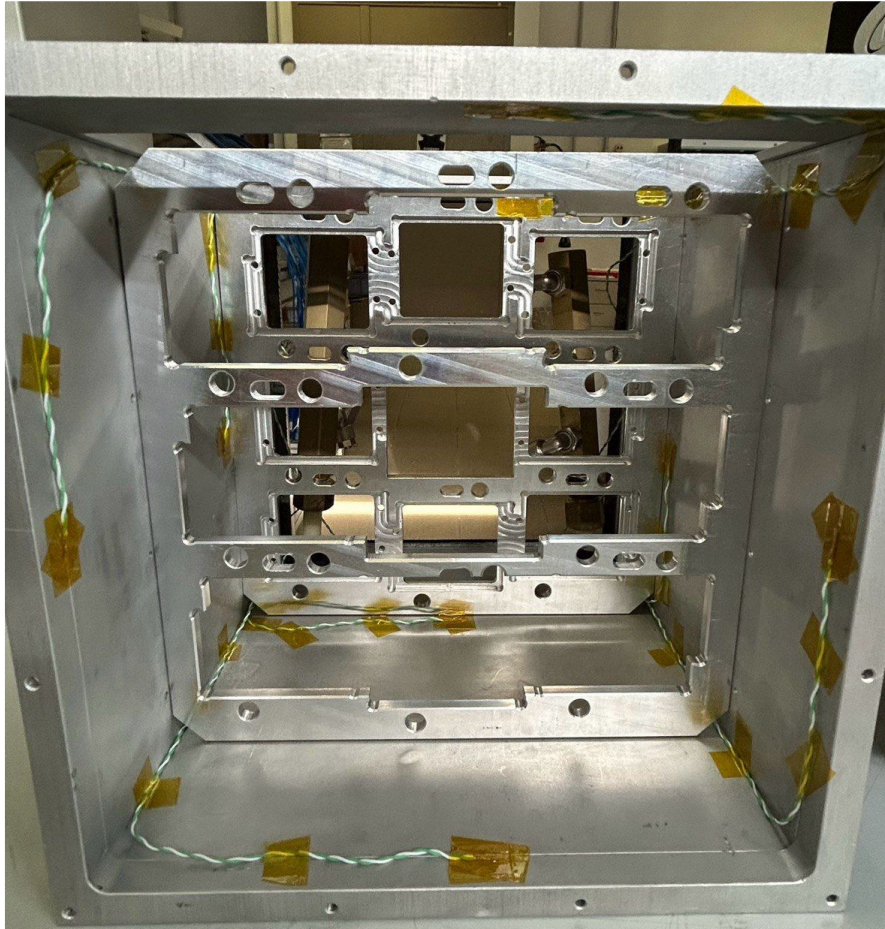
PhotoDetector Unit (PDU)



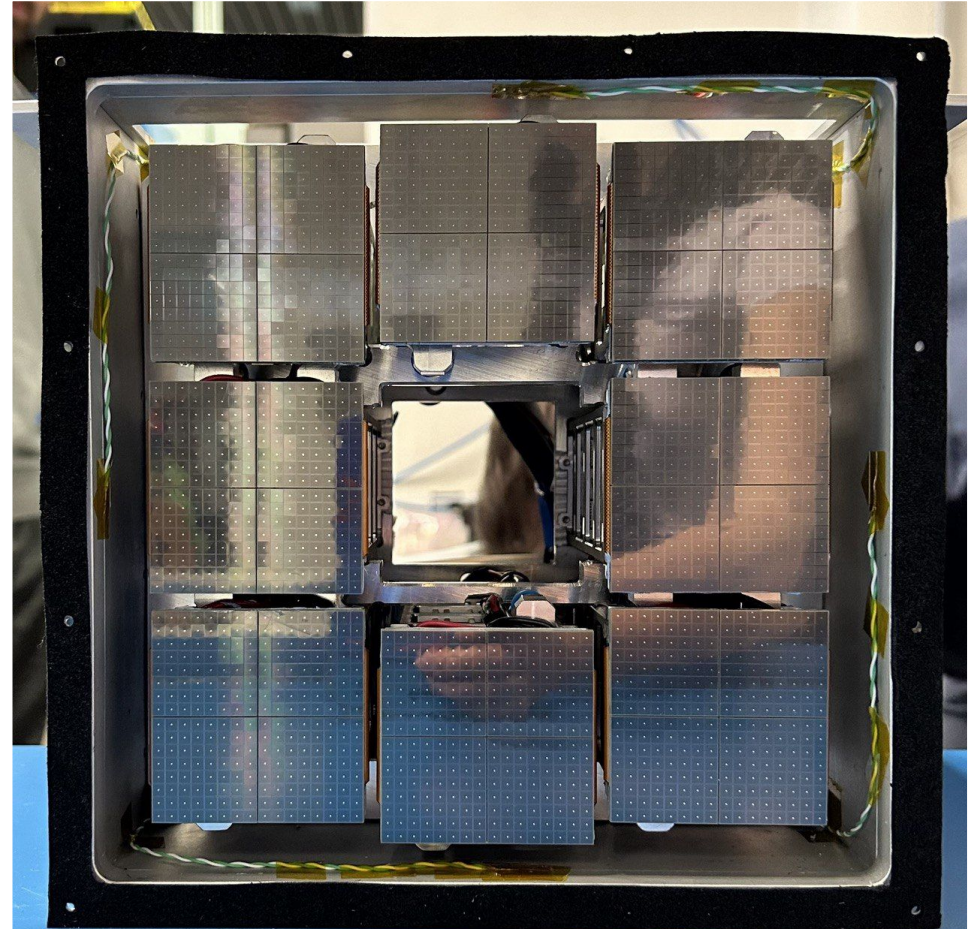
Readout Box



From an empty box to a full detector



empty readout box with PDU housing and monitor thermocouples



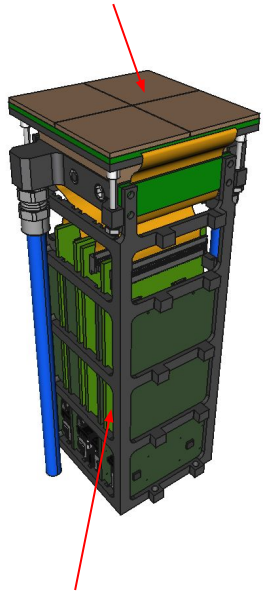
readout box filled with 8 PDUs ready to go

2024 test beam at CERN-PS

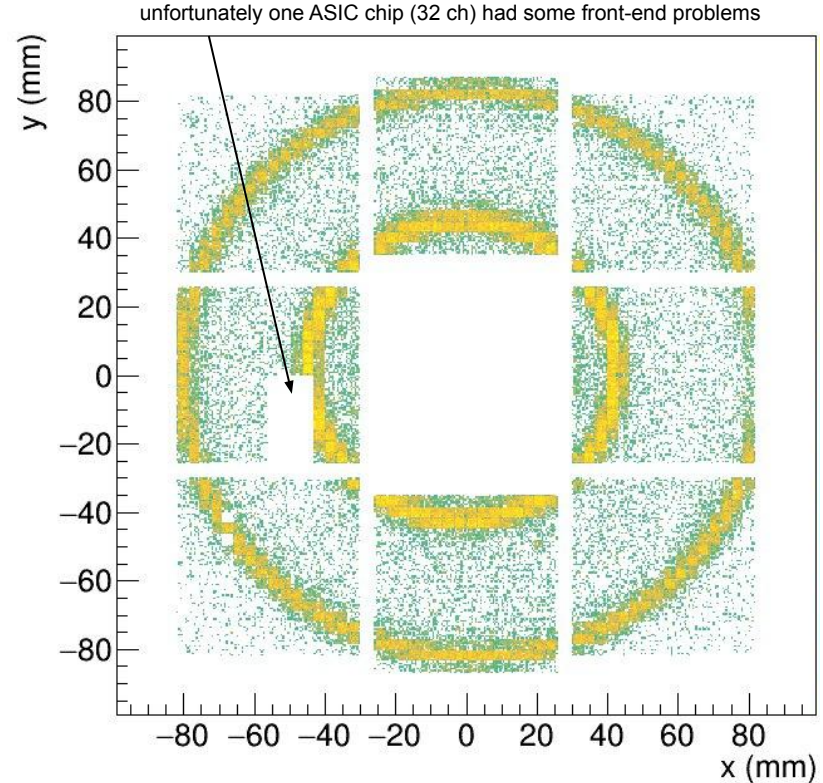
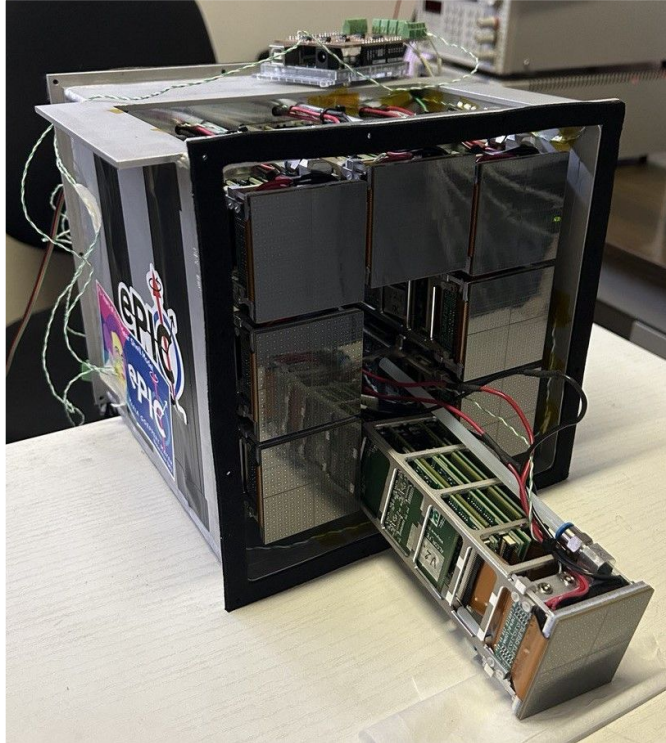
another successful beam test with prototype SiPM photodetector units (CERN-PS, ended on 5th June)

PDU

4x SiPM matrix arrays
(256 channels)



front-end electronics
(ALCOR ASIC inside)

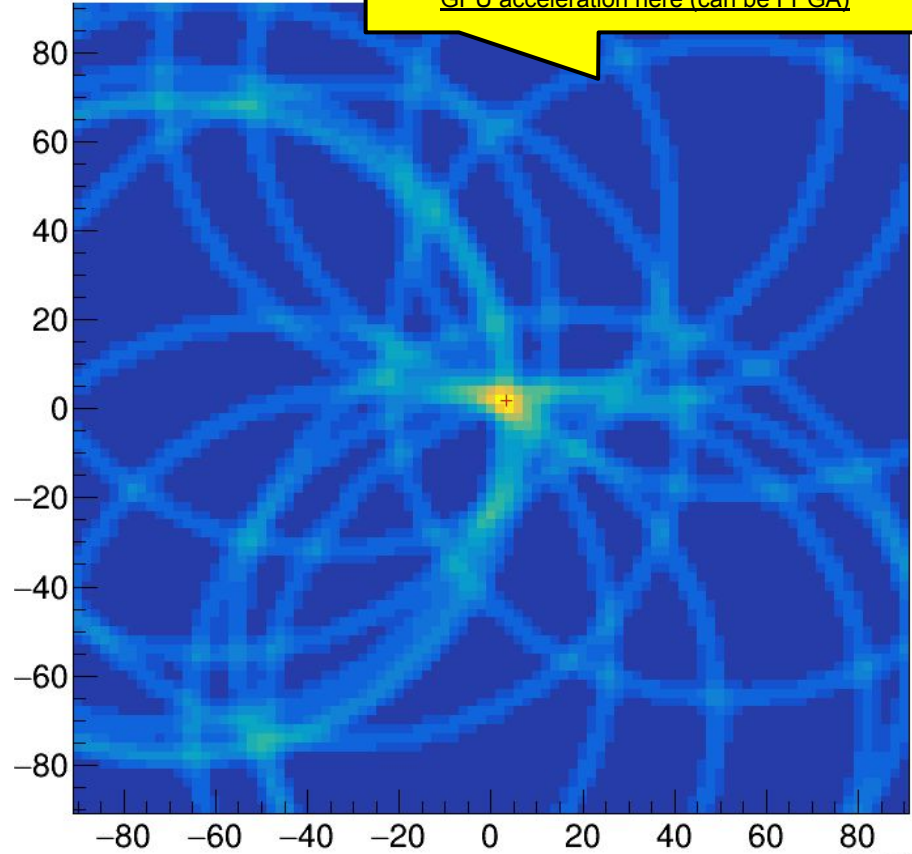
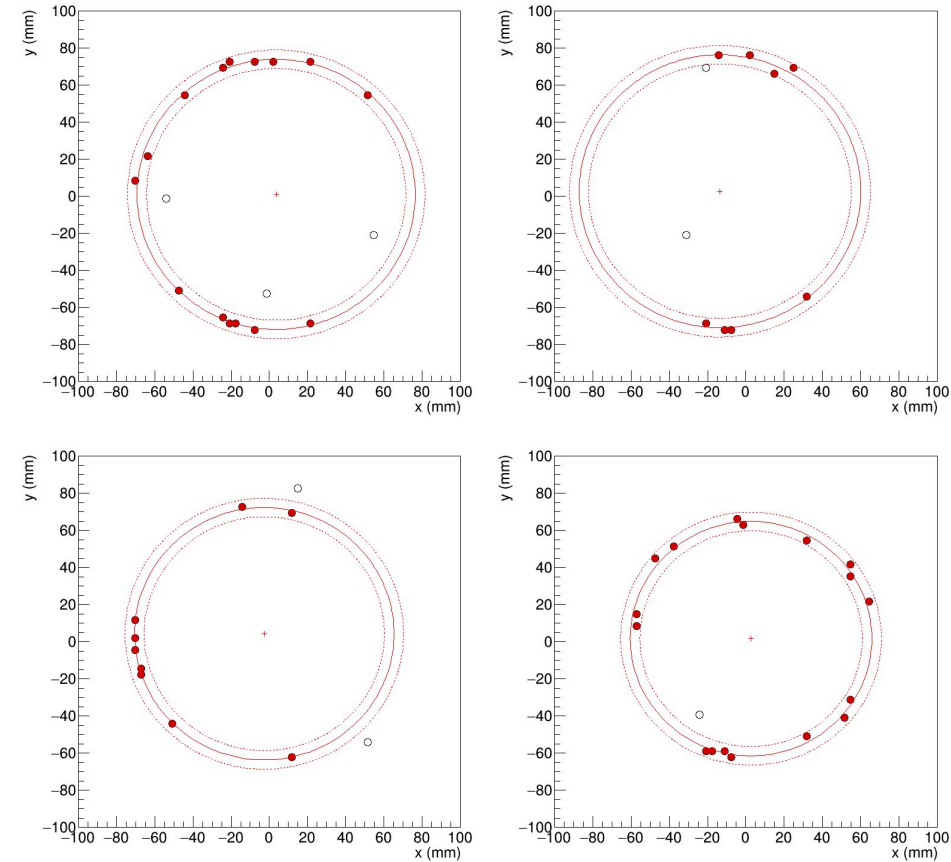


all the rest was rather full of photons
> 2000 SiPMs with TDC readout at work

Test beam data analysis is ongoing

event-by-event pattern recognition with Hough Transform Method

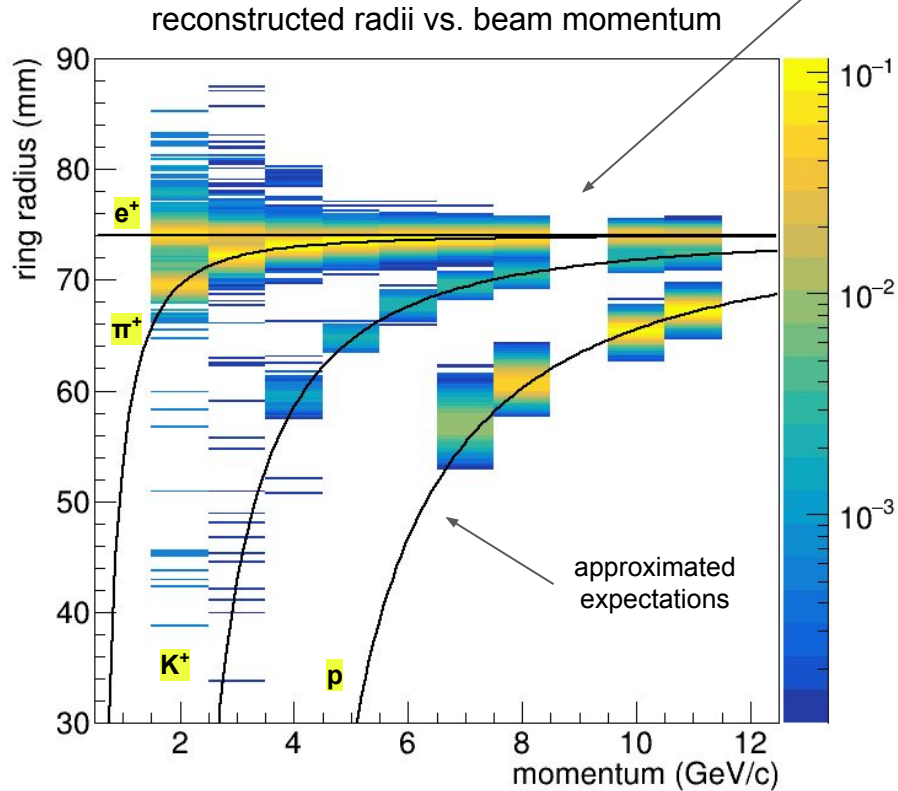
4D (including time) Hough transform can detect rings in a streaming detector
GPU acceleration here (can be FPGA)



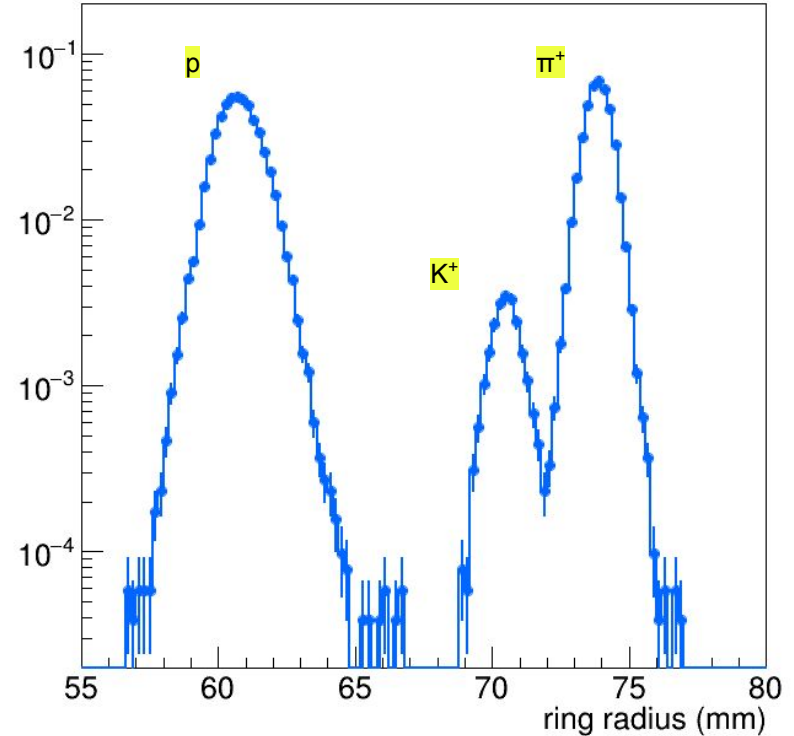
Beam momentum scan

positive particles, aerogel only

something went wrong with the beam configuration for 9 GeV
(that's a pity, data seems not good)



reconstructed ring radius at 8 GeV/c beam momentum

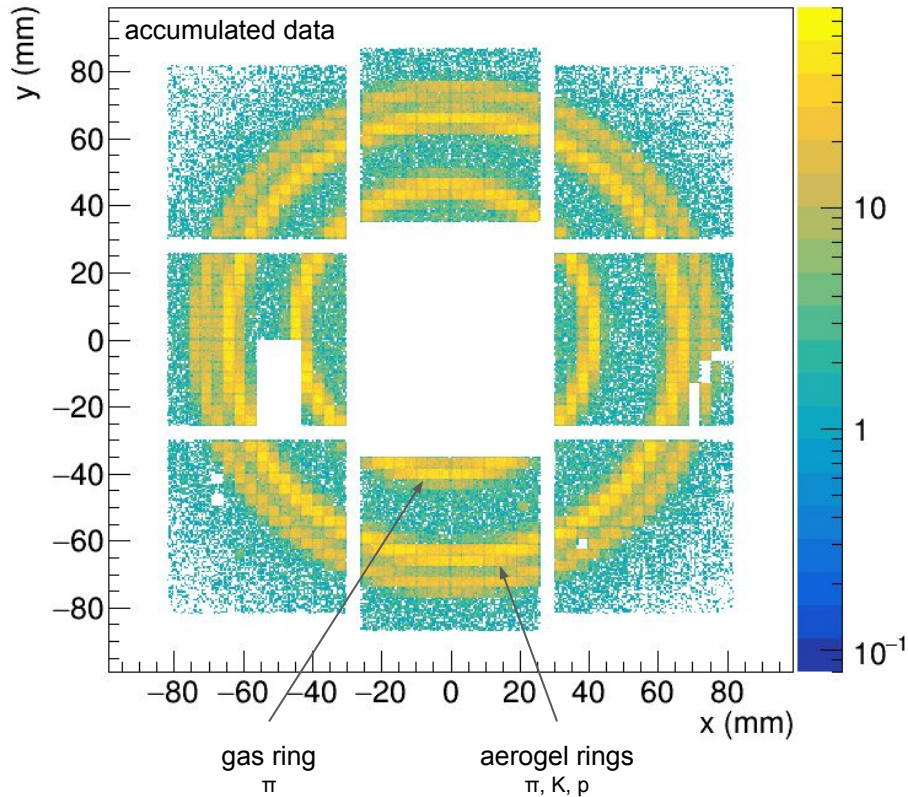


Nicola Rubini

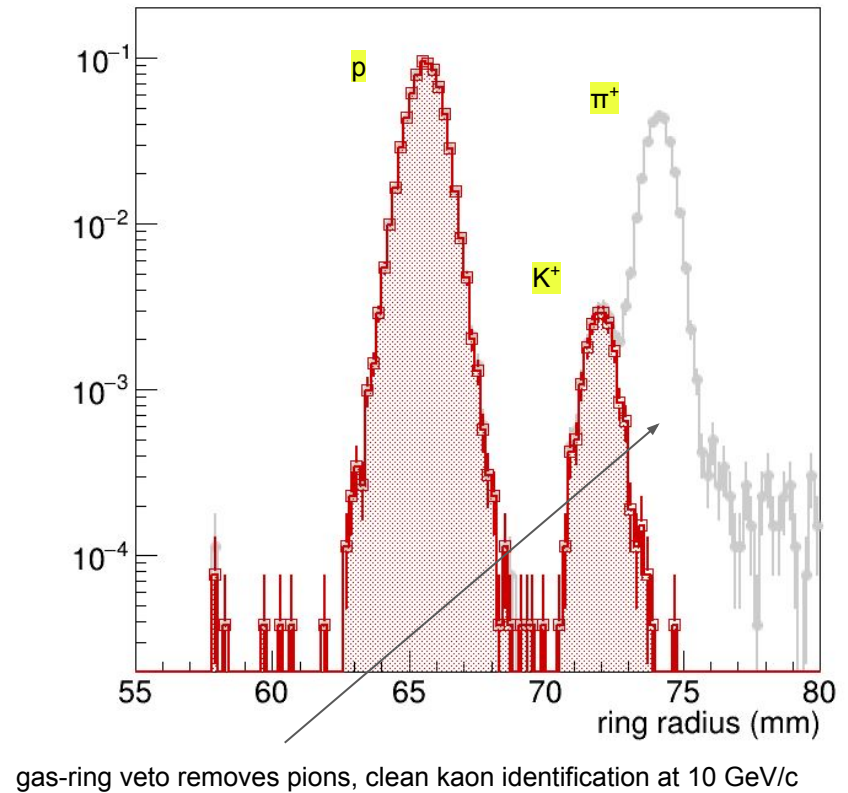
Interplay between aerogel and gas radiators

gas ring tags pions, at 10 GeV/c kaons and protons are below C_2F_6 gas threshold

10 GeV/c positive beam with no selection applied



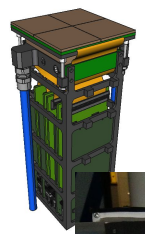
reconstructed ring radius at 10 GeV/c with gas veto



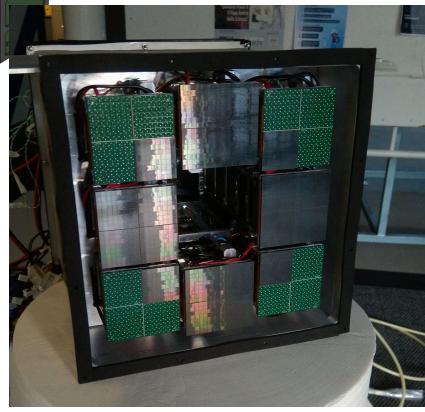


towards construction →

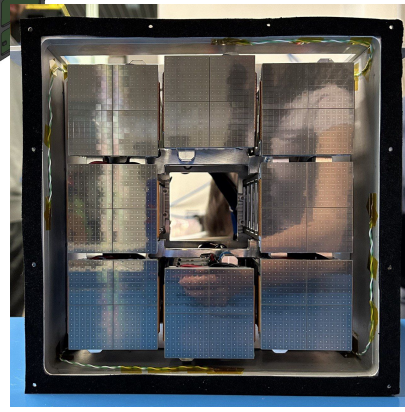
2022
electronics v1



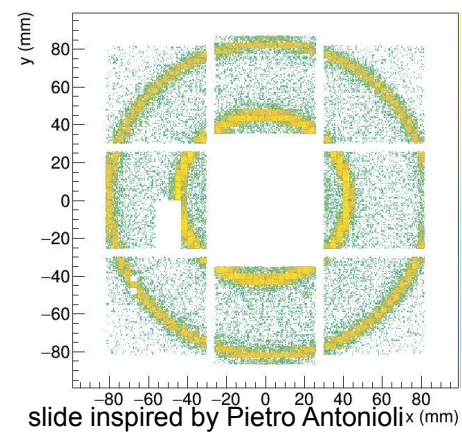
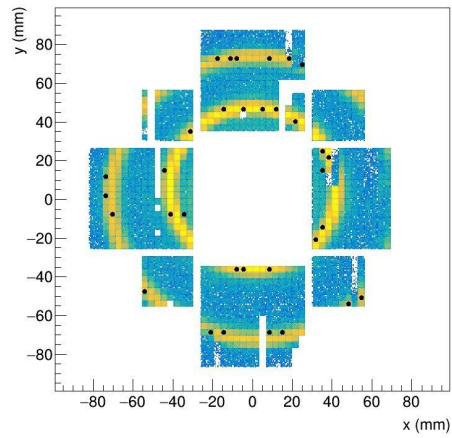
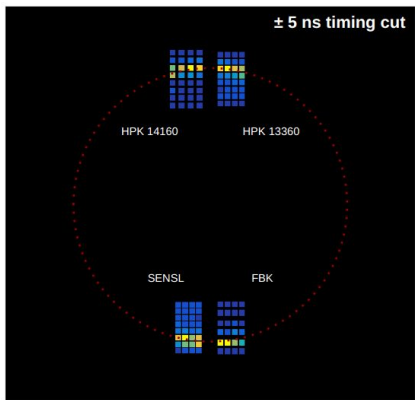
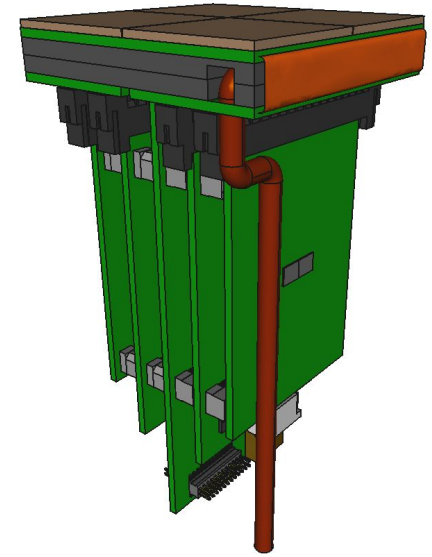
2023
electronics v2



2024
electronics v2.1



2025
electronics v3
final prototype

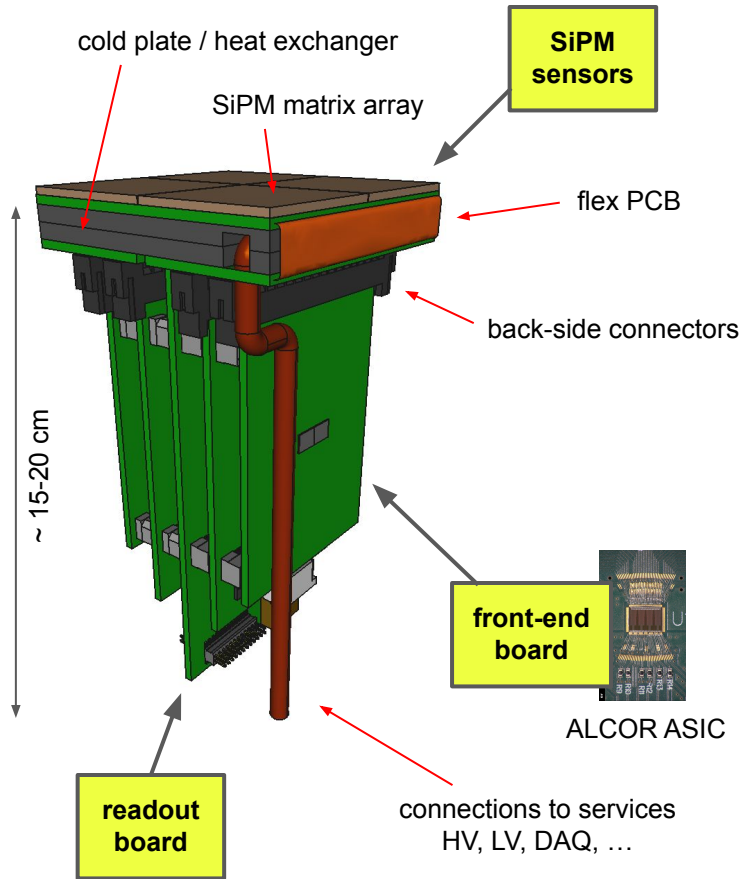


slide inspired by Pietro Antonioli

detector integration
and electronics

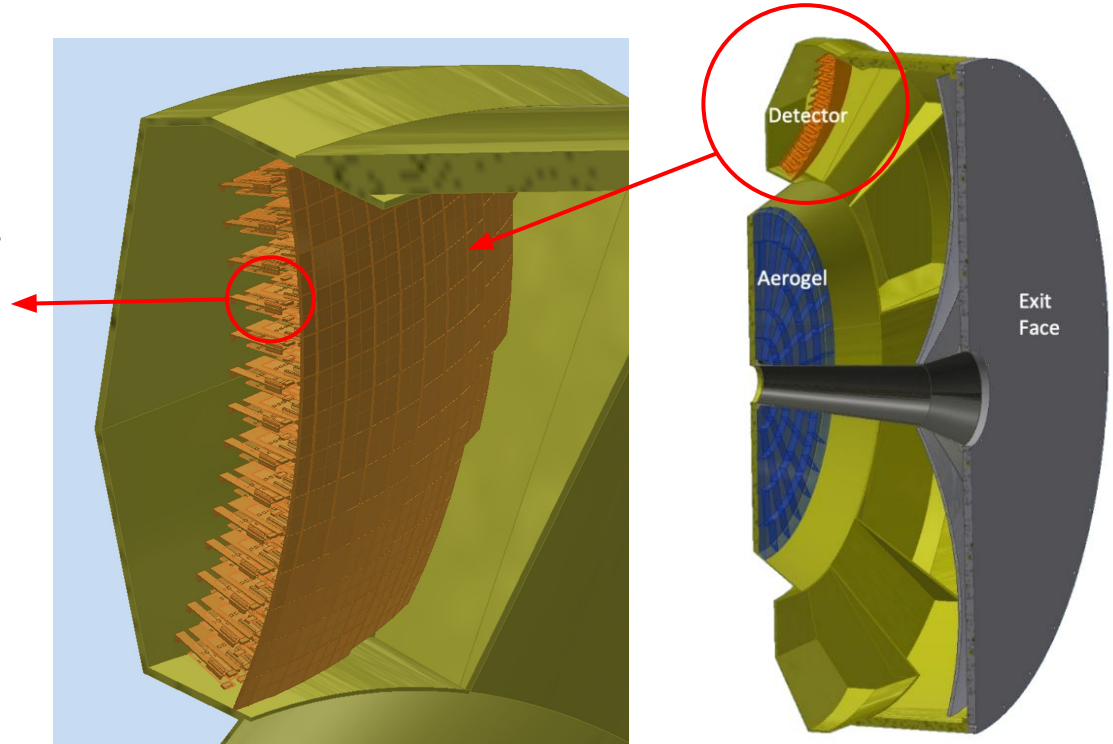
Photodetector unit

conceptual design of PDU layout



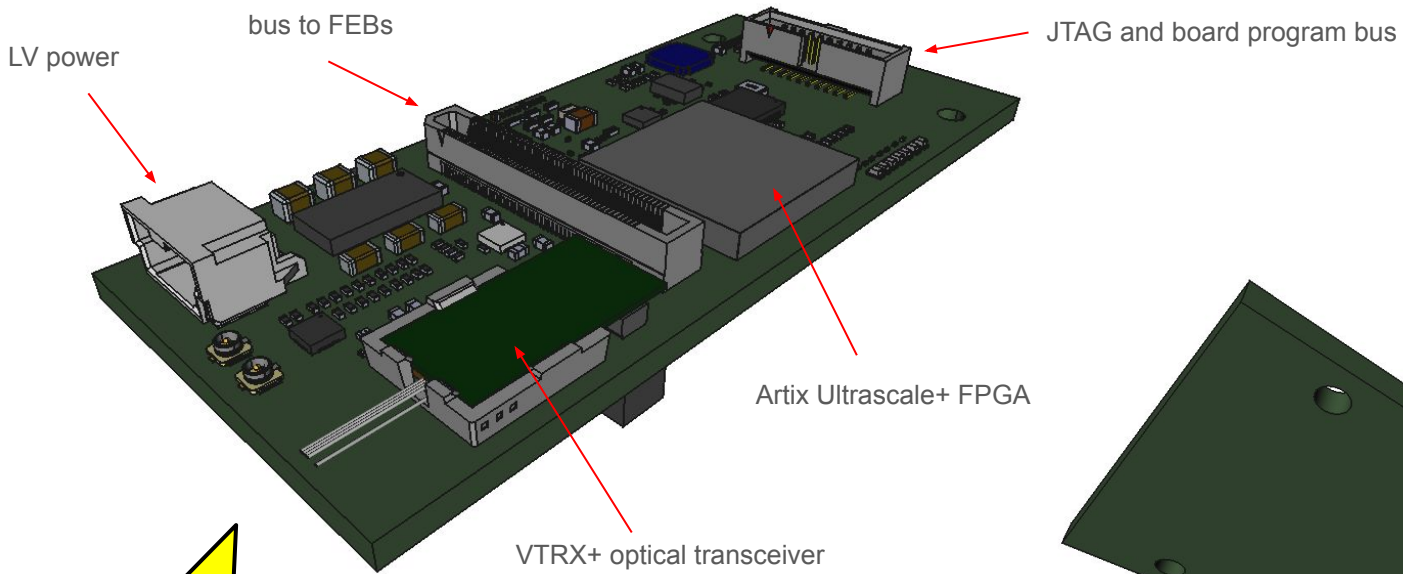
SiPM sensor matrices mounted on carrier PCB board

- 4x 64-channel SiPM array device (256 channels) for each unit
 - need modularity to realise curved readout surface
- 1248 photodetector units for full dRICH readout
 - 4992 SiPM matrix arrays (8x8)
 - 319488 readout channels



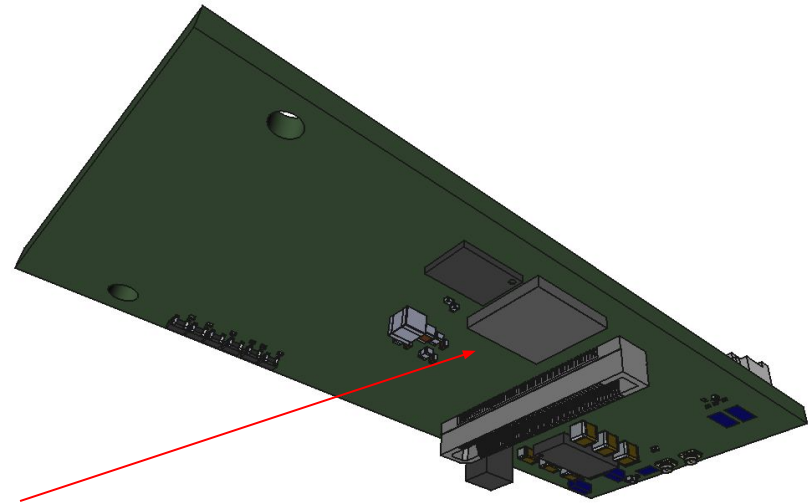
RDO is in advanced design stage

project will be soon sent for board layout by external company and production of first prototypes



Daive Falchieri

RDO



RDO readout architecture for next beam test

- 8x stacks of electronics each with
- 1 RDO
 - 4 "fake" FEBS

"fake" FEBS

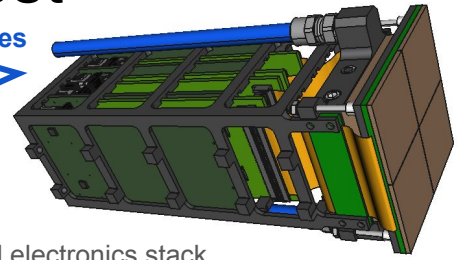
RDO

VTRX+ optical link to commercial SFP

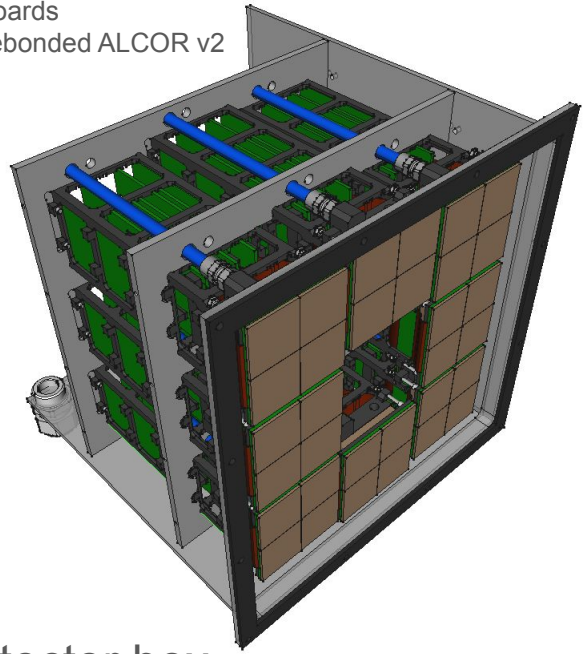


high-performance computer with 8 SFP optical links

8x FireFly cables



existing front-end electronics stack
4 ALCOR-dual boards
each with 2x wirebonded ALCOR v2

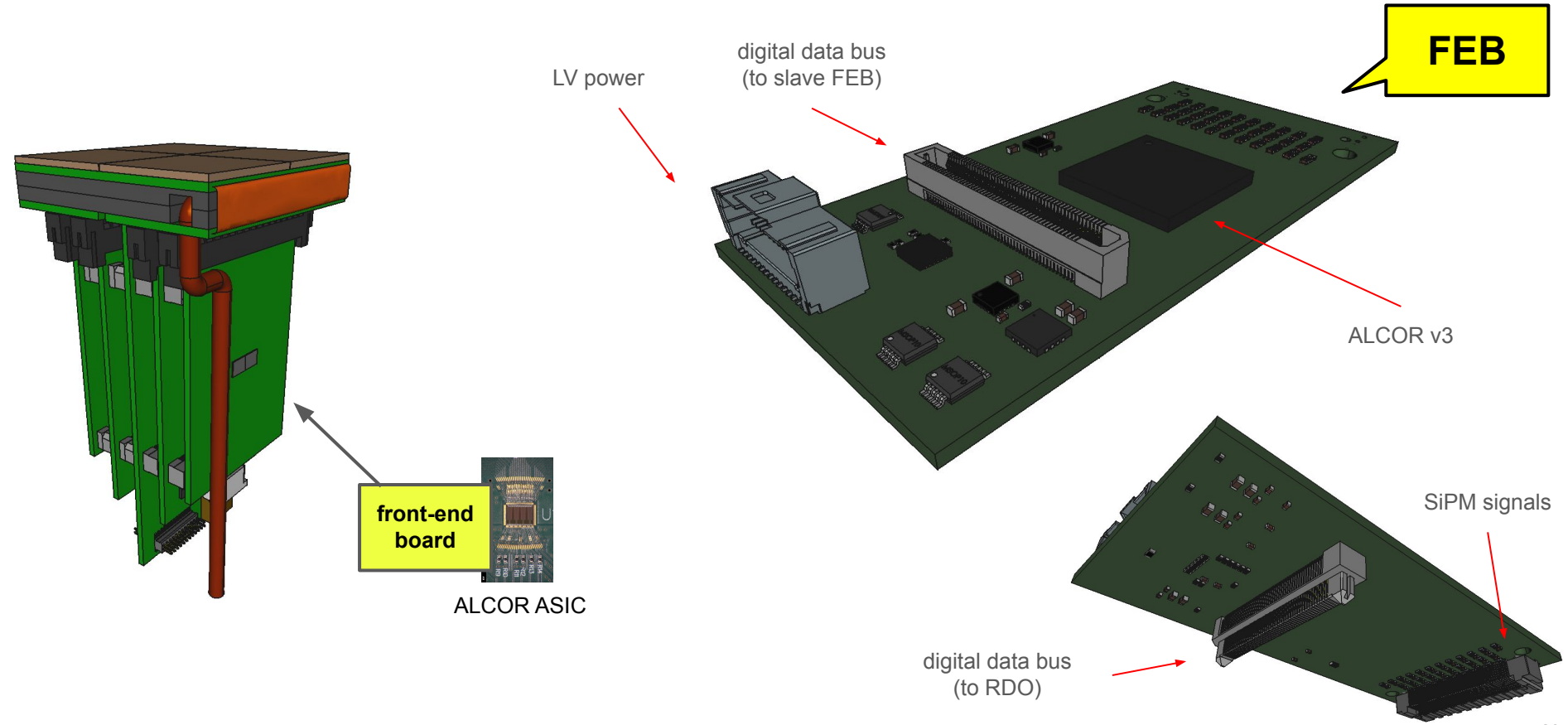


outside

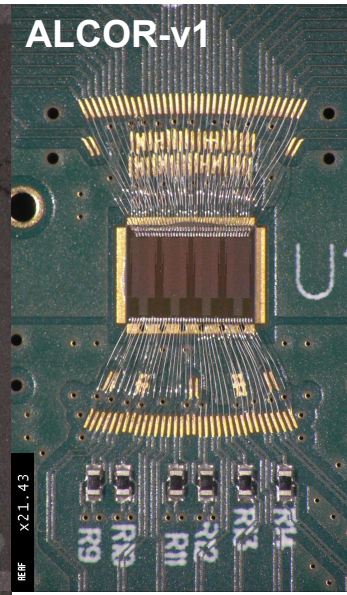
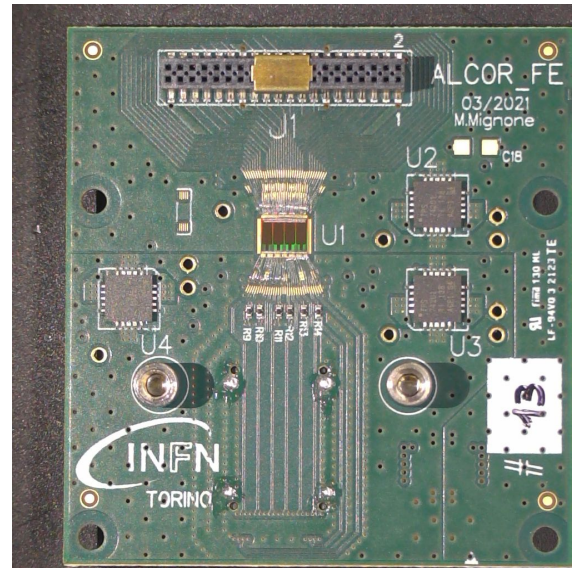
inside detector box

The front-end board (FEB) and ALCOR v3

taking ALCOR chip to the ultimate dRICH requirement with 64 channels and a BGA package



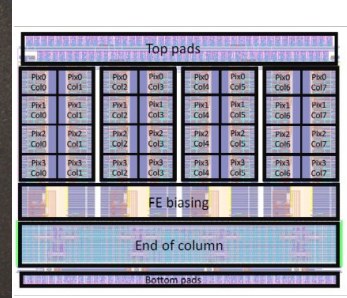
ALCOR ASIC: integrated front-end and TDC



developed by INFN-TO

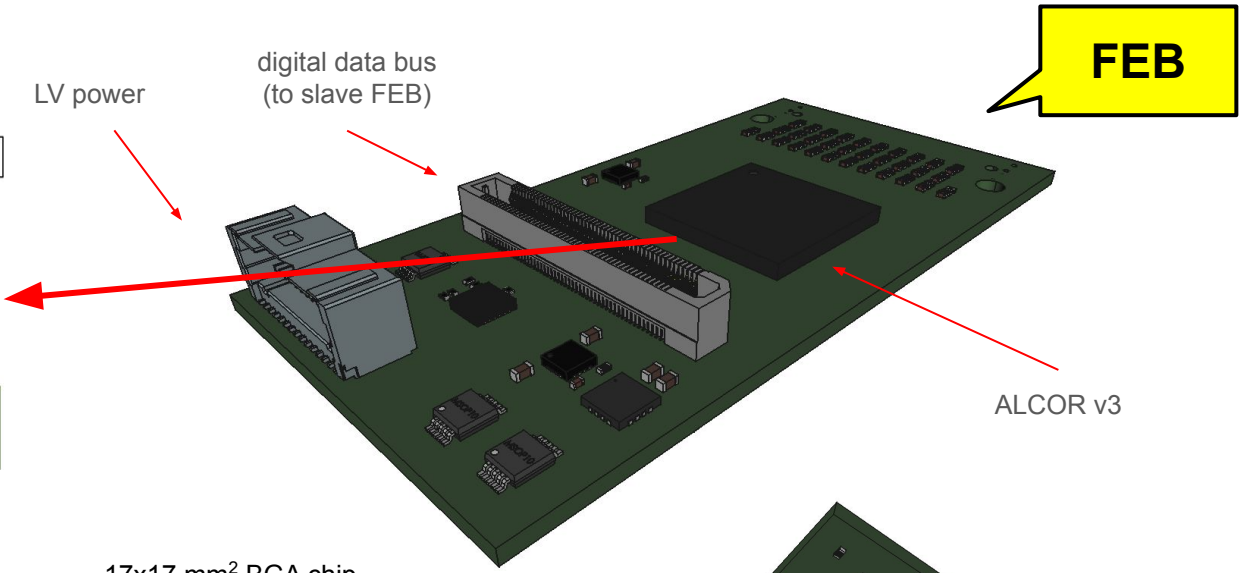
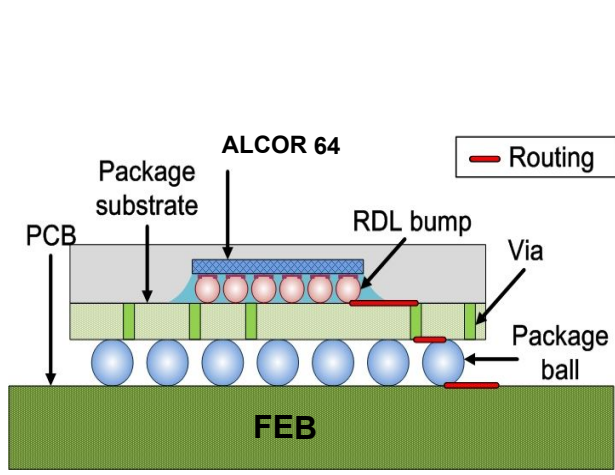
64-pixel matrix mixed-signal ASIC
 current versions (v1,v2,v2.1) have 32 channels, wirebonded
 final version will have 64 channels, BGA package, 394.08 MHz clock

- **the chip performs**
 - signal amplification
 - conditioning and event digitisation
- **each pixel features**
 - 2 leading-edge discriminators
 - 4 TDCs based on analogue interpolation
 - 20 or 40 ps LSB (@ 394 MHz)
 - digital shutter to enable TDC digitisation
 - suppress out-of-gate DCR hits
 - 1-2 ns timing window
 - programmable delay, sub ns accuracy
- **single-photon time-tagging mode**
 - continuous readout
 - also with Time-Over-Threshold
- **fully digital output**
 - 8 LVDS TX data links



The front-end board (FEB) and ALCOR v3

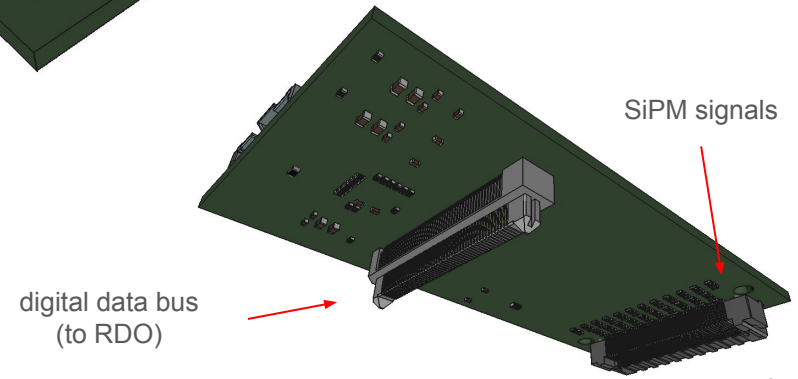
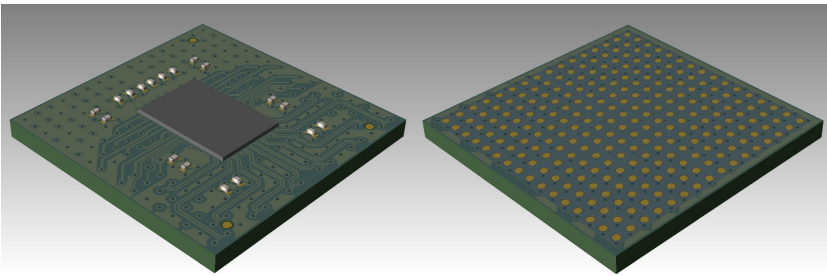
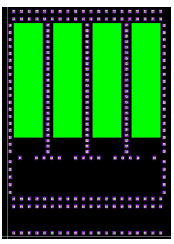
taking ALCOR chip to the ultimate dRICH requirement with 64 channels and a BGA package



ALCOR v3 silicon chip

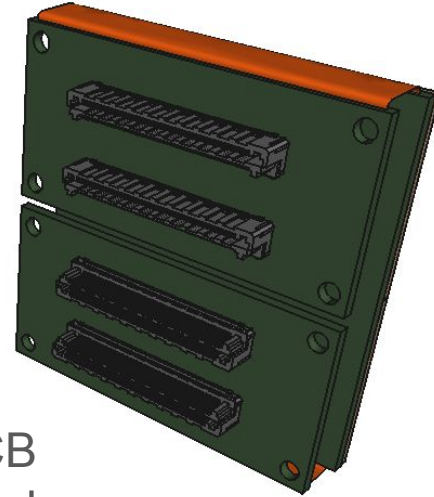
flip-chipped onto interposer complex PCB RDL, design is ready

17x17 mm² BGA chip package with 256 balls, 1 mm pitch

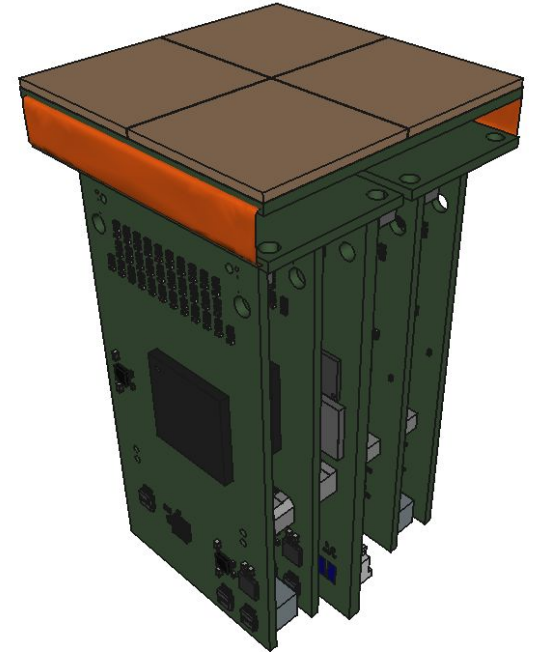


dRICH SiPM photodetector unit engineering and design

evolution from conceptual to final design: in progress



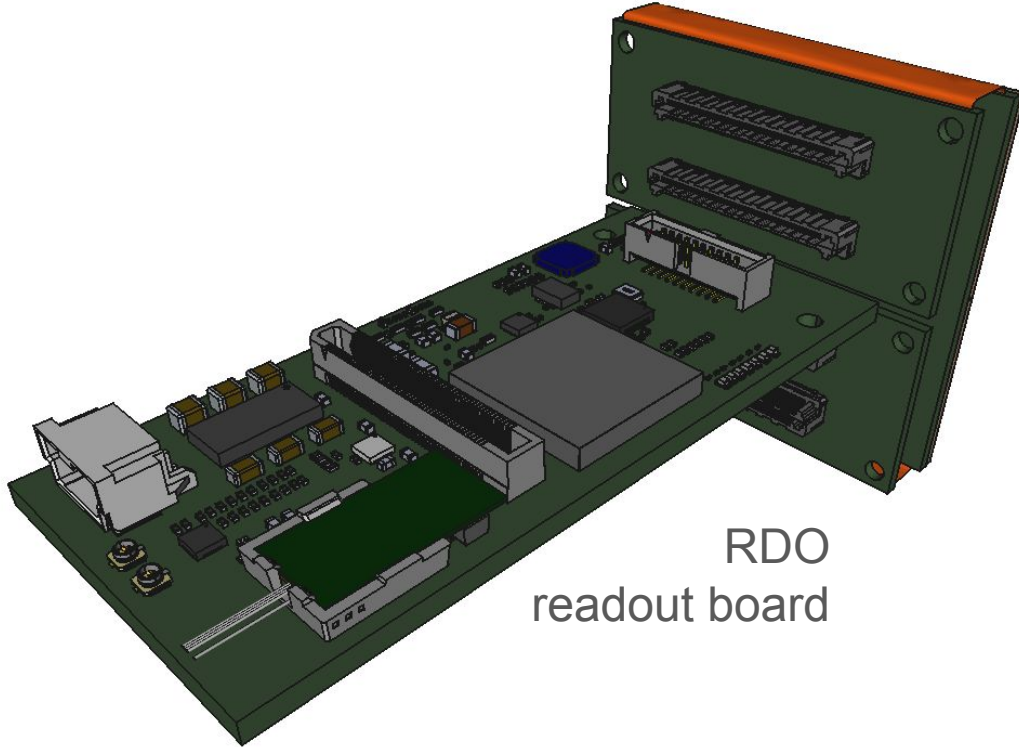
flex-PCB
SiPM carrier board



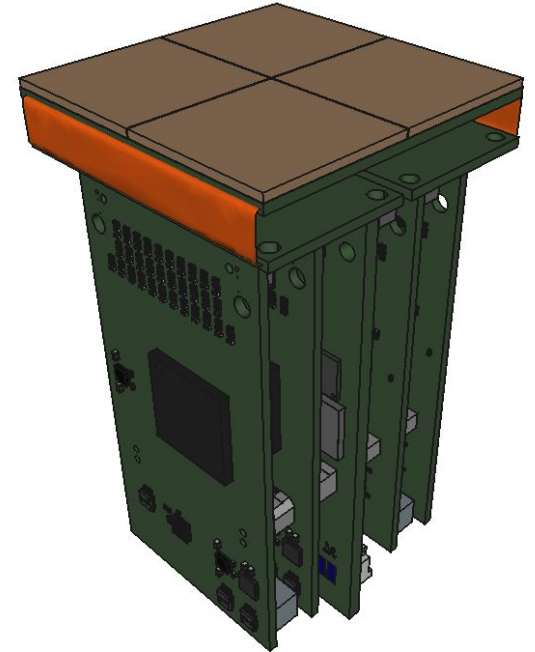
PDU

dRICH SiPM photodetector unit engineering and design

evolution from conceptual to final design: in progress



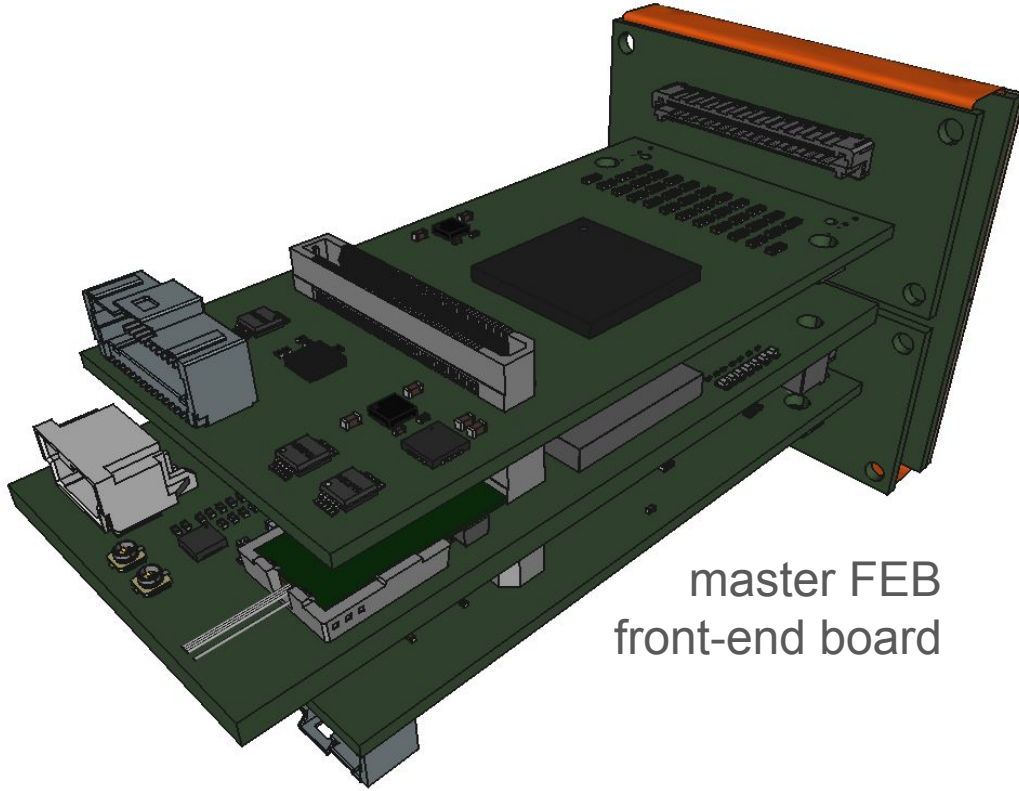
RDO
readout board



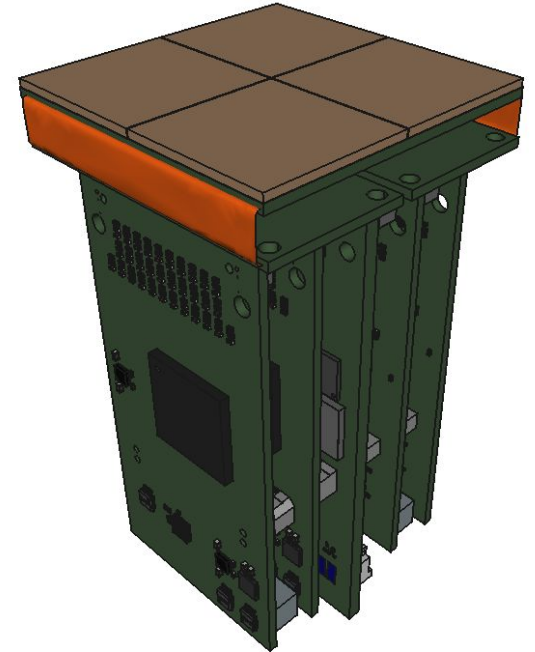
PDU

dRICH SiPM photodetector unit engineering and design

evolution from conceptual to final design: in progress



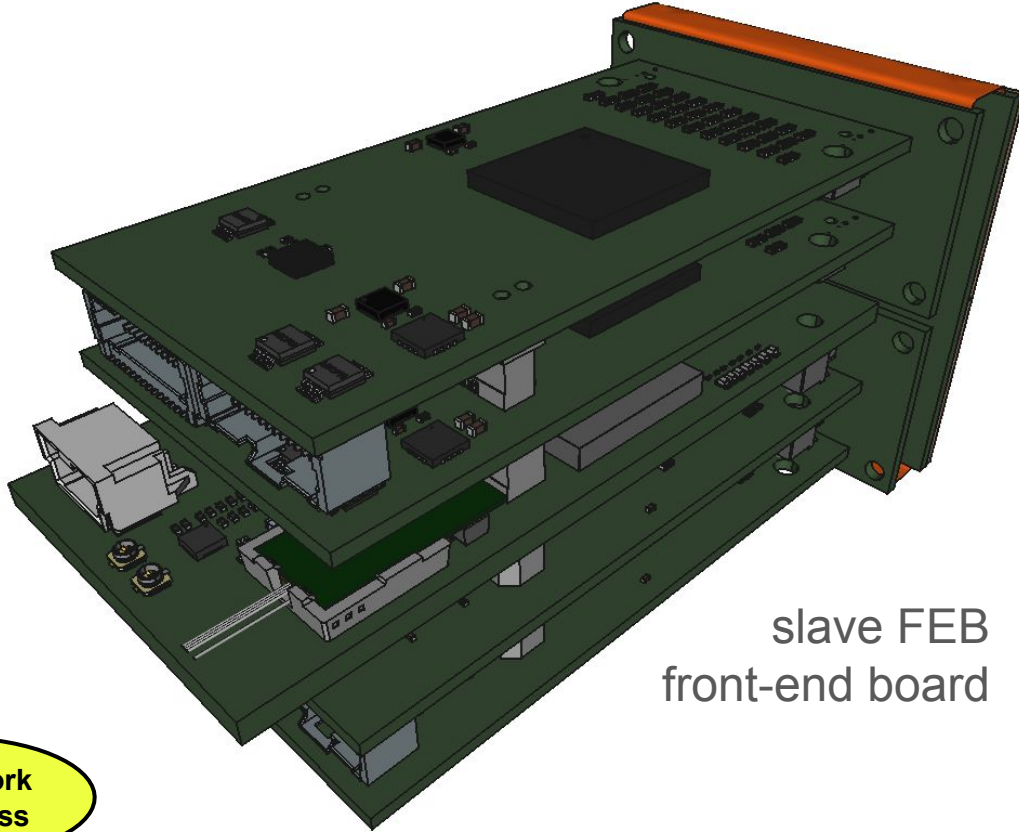
master FEB
front-end board



PDU

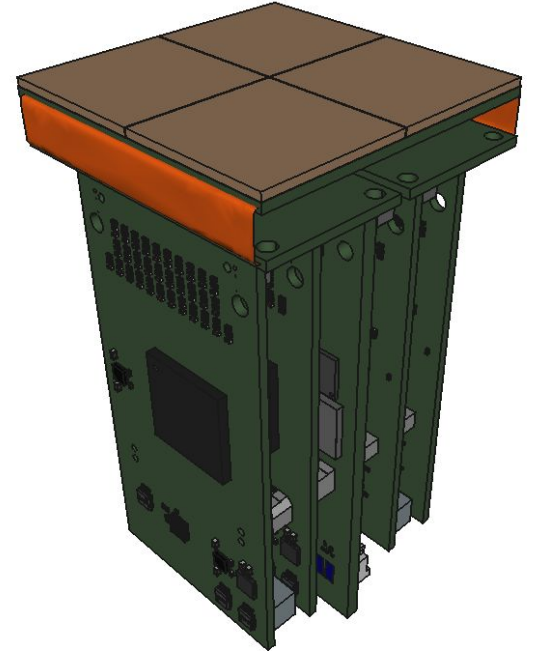
dRICH SiPM photodetector unit engineering and design

evolution from conceptual to final design: in progress



slave FEB
front-end board

PDU



lots of work
in progress

The dRICH MasterPanel board

we developed and operated in the dRICH beam test in October 2023 and May 2024 the MasterLogic v2 card (evolution of the MasterLogic v1 card).

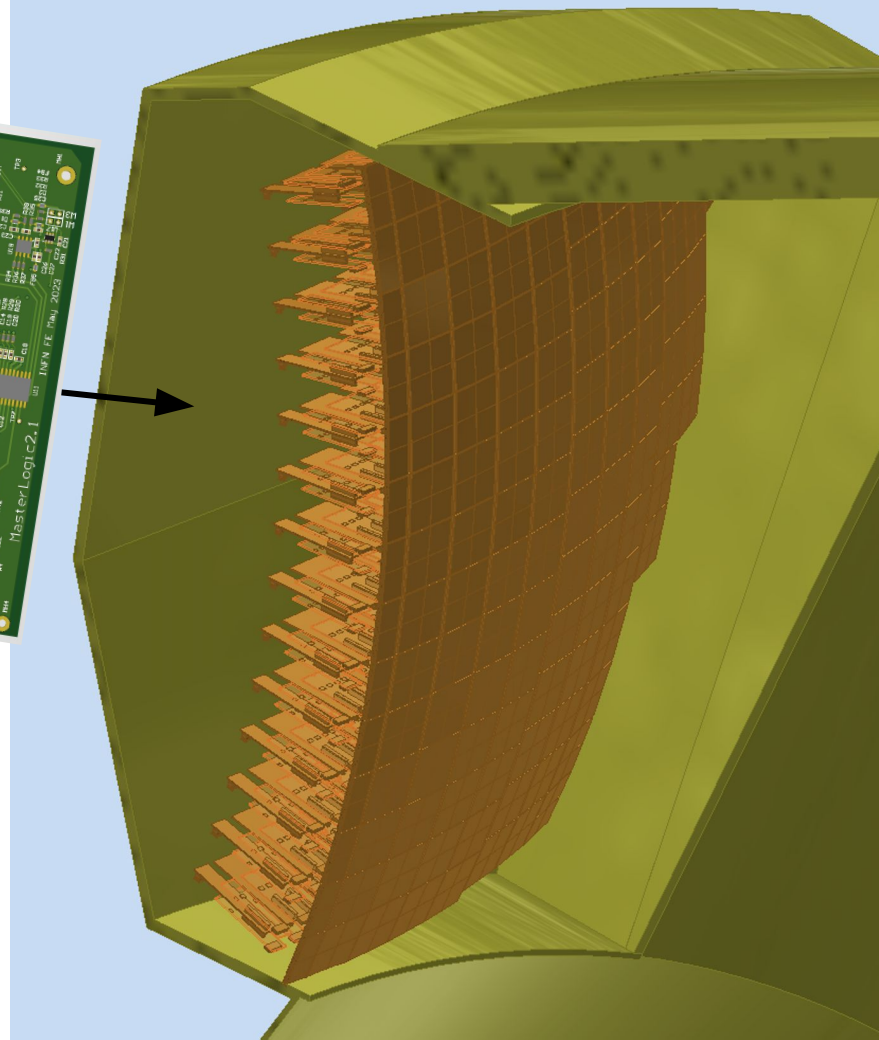
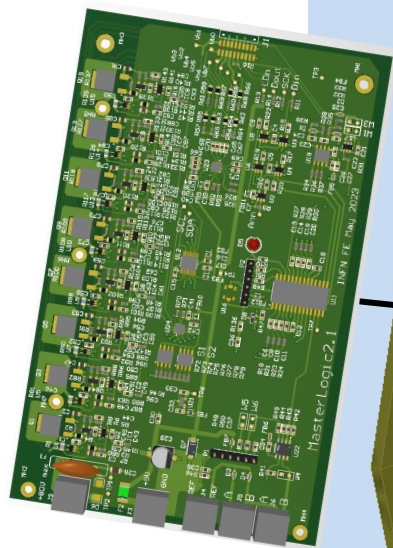
the card hosts

- 8 channels made of identical circuits for linear regulation of Vbias from 0 to V_{in} (80 V max)
- a microcontroller (PIC) for external communication (RS485)
- current monitor

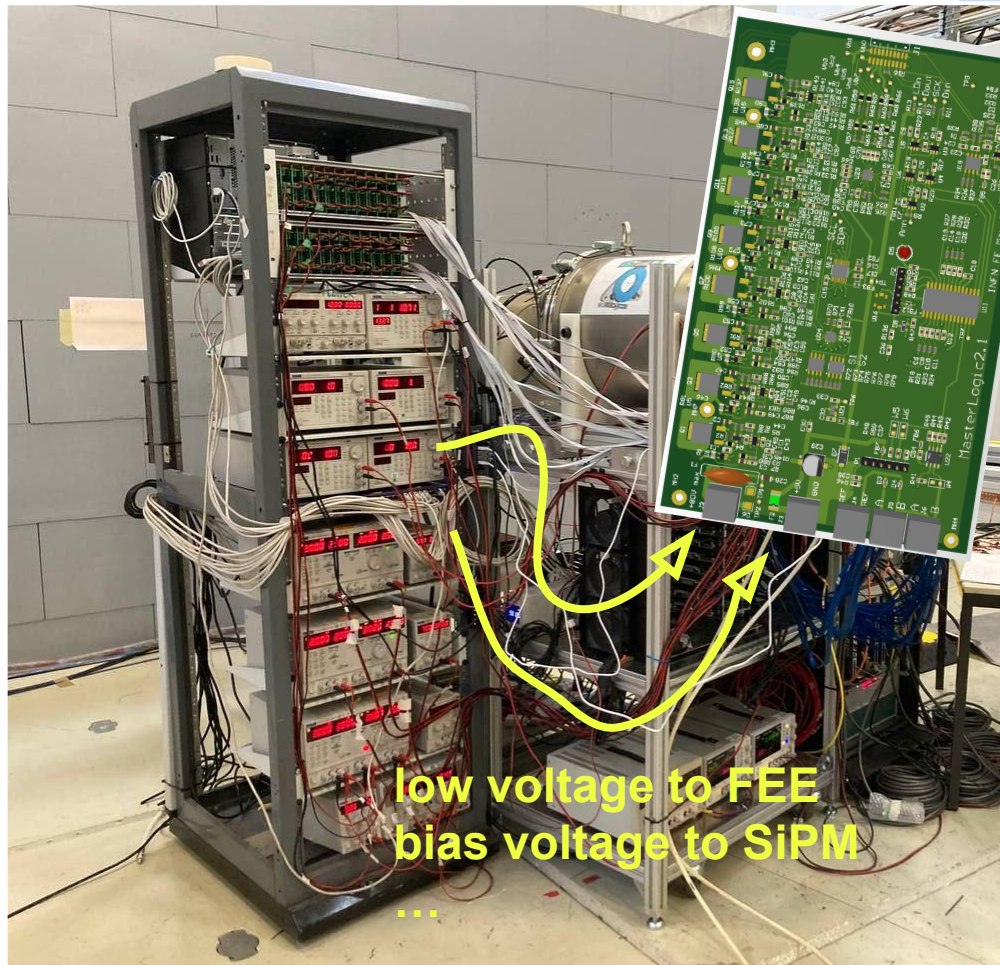
future evolution: MasterPanel card to plug onto the dRICH readout box patch panel for Vbias and Vann control and distribution (and perhaps more features).



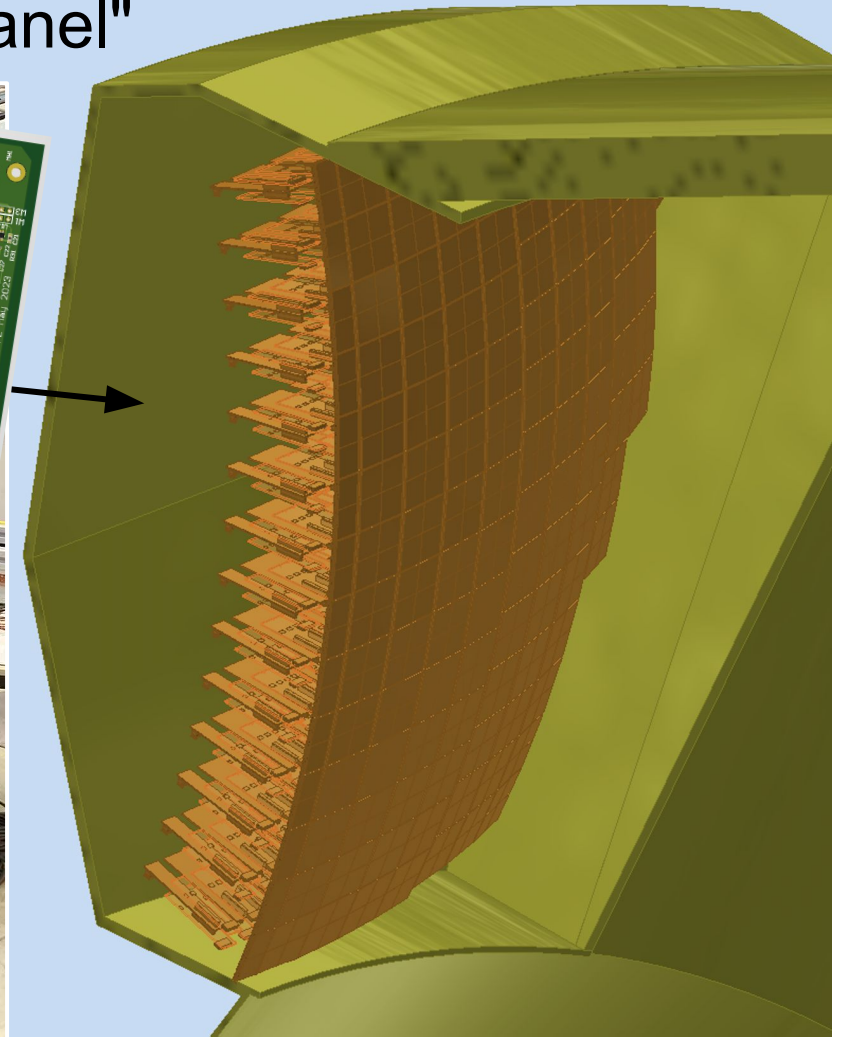
MasterPanel



The dRICH MasterPanel "patch panel"

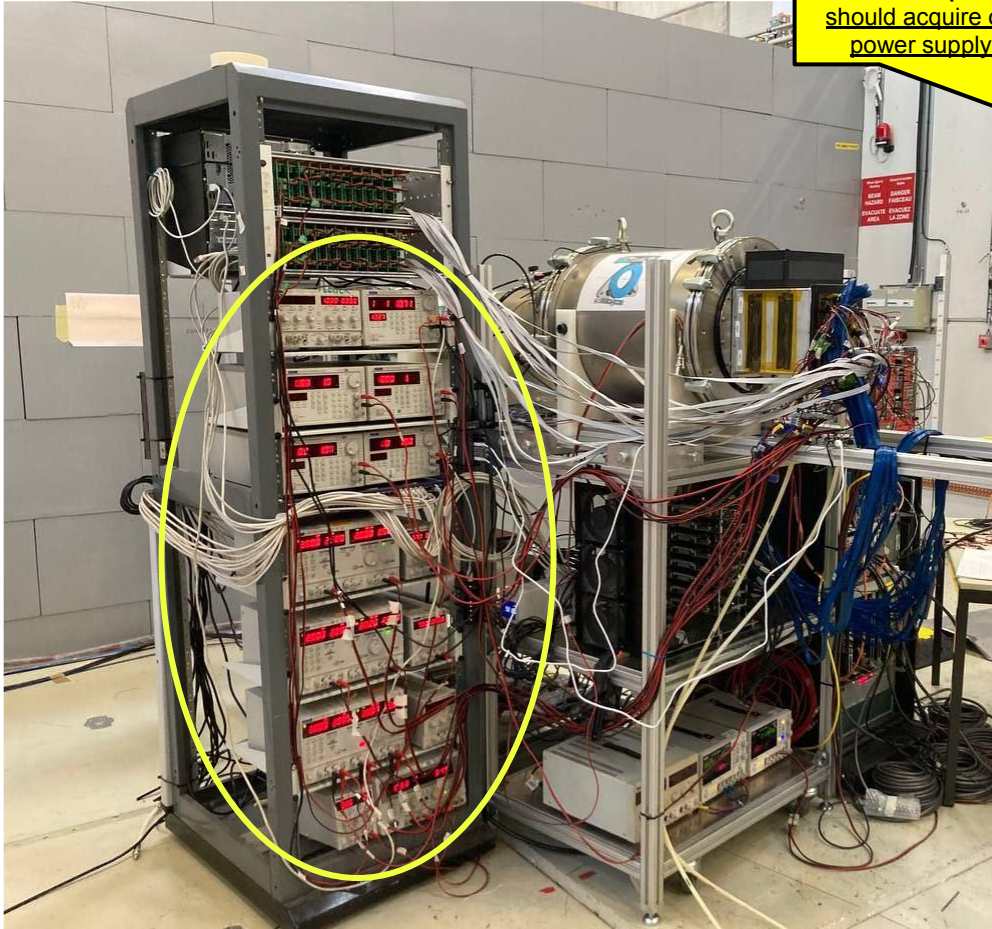


low voltage to FEE
bias voltage to SiPM
...

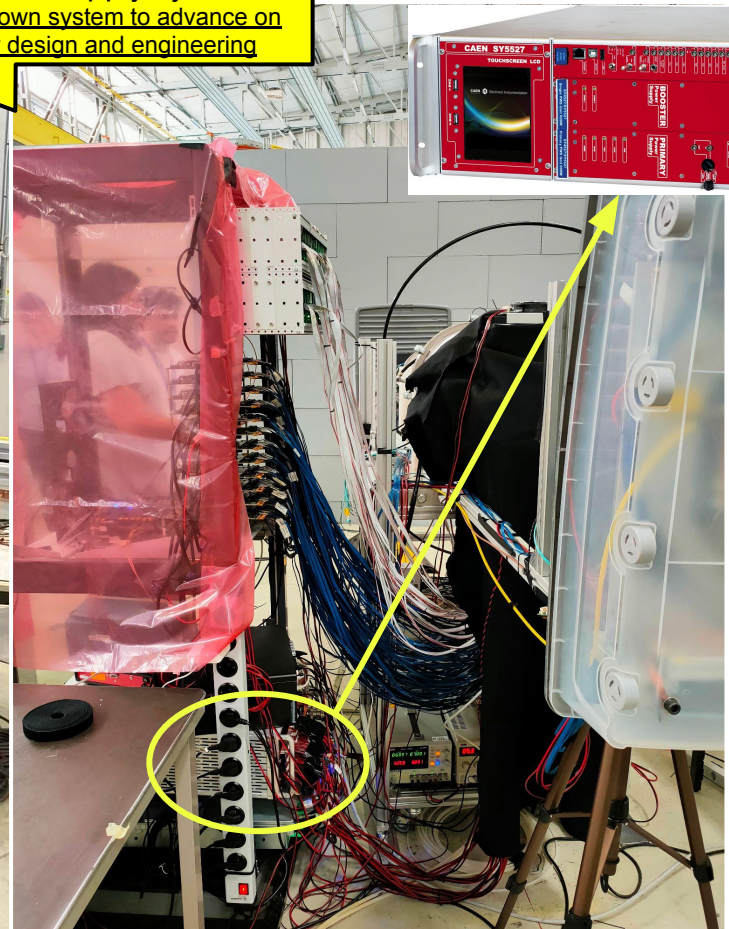


Power supply system

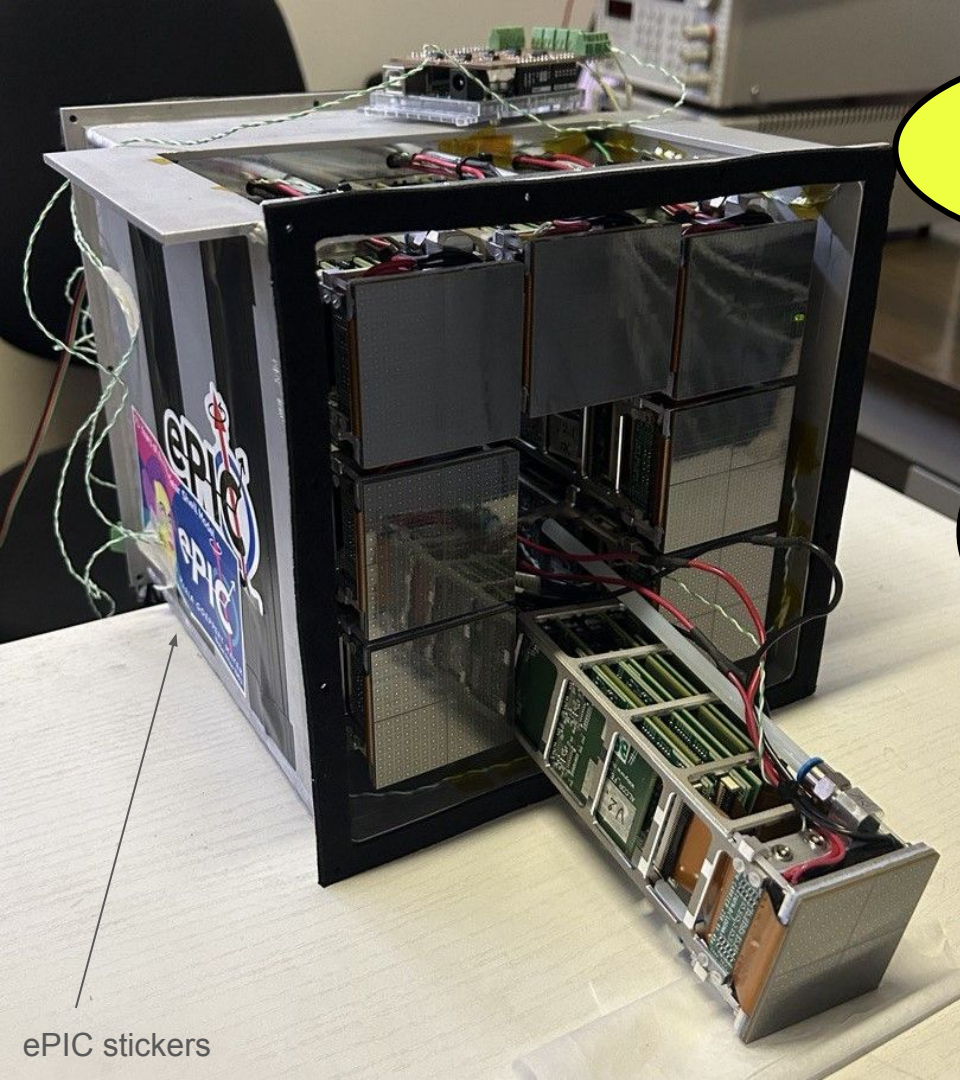
in beam test 2024 used rented
CAEN power supply system
should acquire own system to advance on
power supply design and engineering



many table-top power supplies in 2023



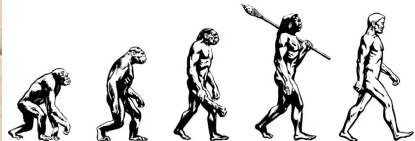
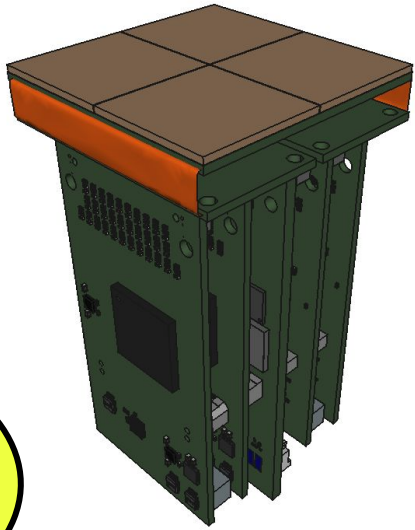
first test with rented CAEN power-supply units in 2024



lots of work done

lots of work in progress

lots of work to be done



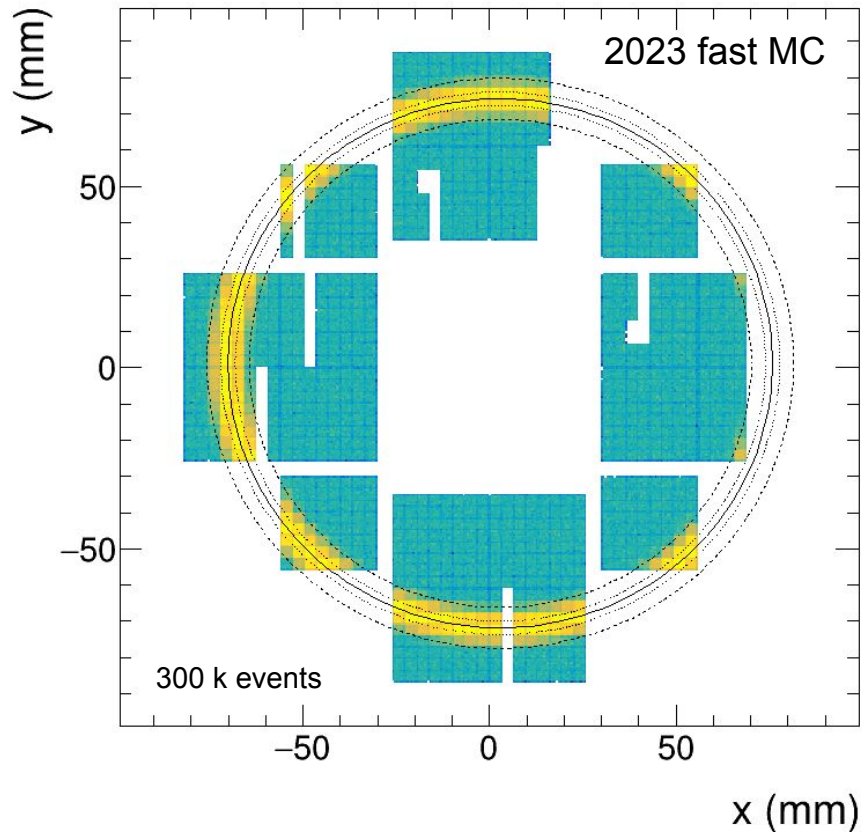
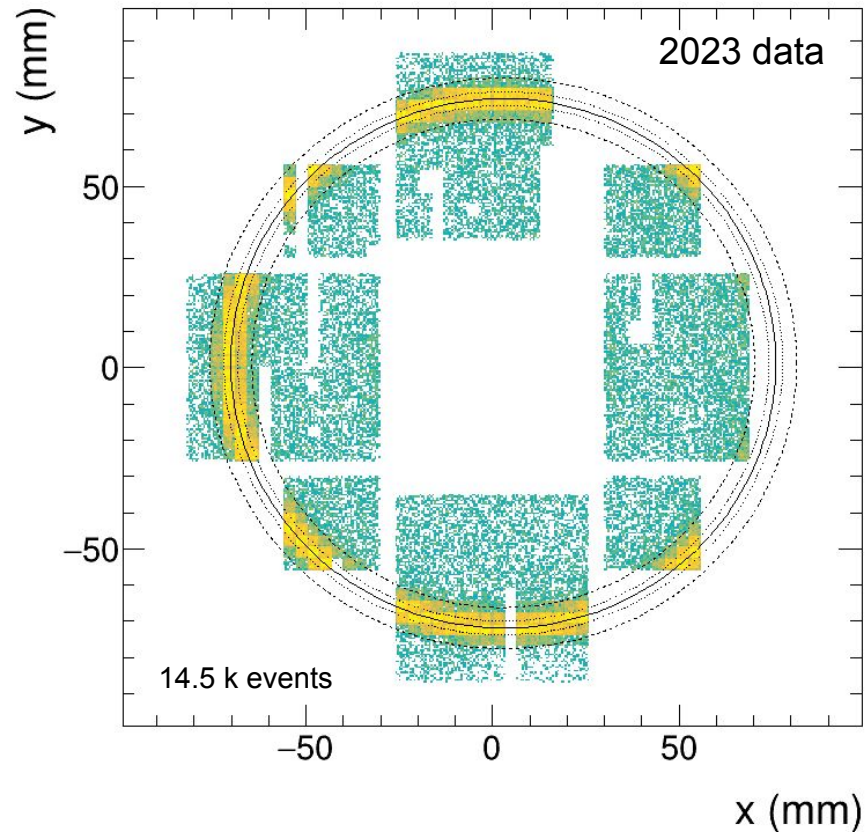
some
beam-test
results



Number of photoelectrons

Nsig	=	23.6048	+/-	0.0154101
X0	=	2.87125	+/-	0.00255149
Y0	=	1.18834	+/-	0.00193679
R	=	73.0013	+/-	0.00166626
sigmaR	=	1.88591	+/-	0.00123206
Nbkg	=	10.3538	+/-	0.0133316

2D fit parameters match accurately fast MC input
notice redefinition of Nsig and Nbkg

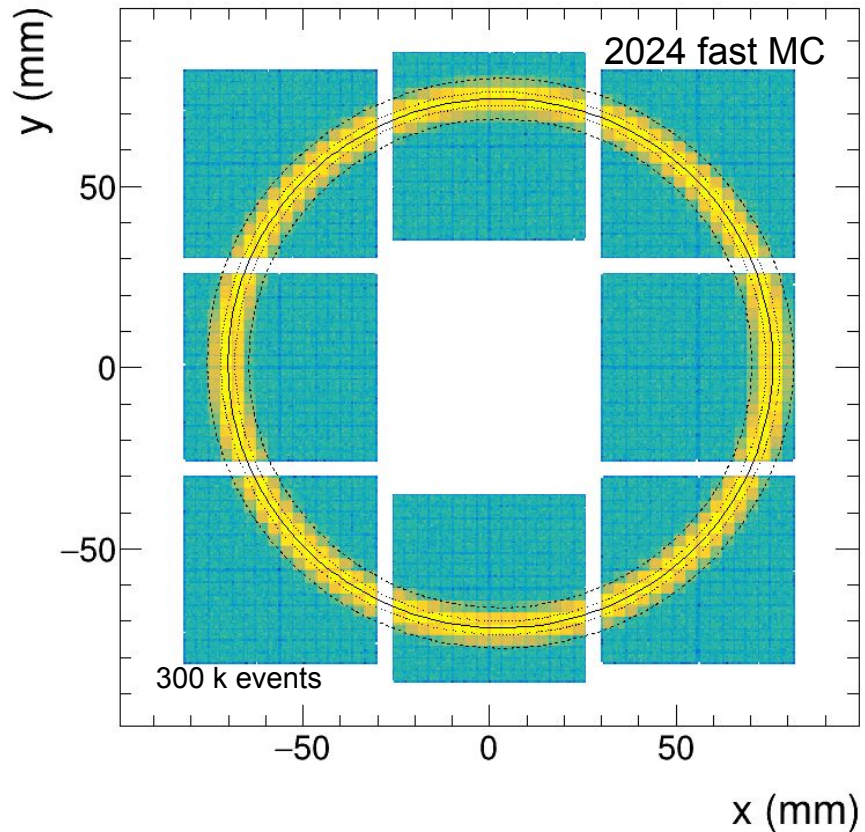
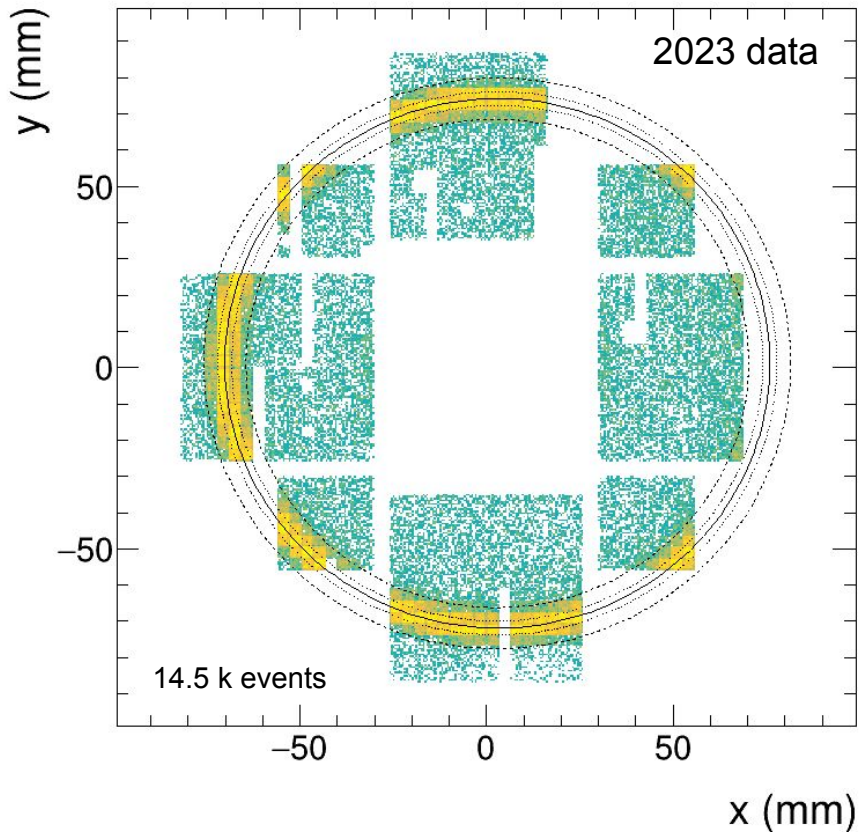


large number of detected aerogel photons in 2023, on average **more than 9 photoelectrons over the active area**

Number of photoelectrons

2D fit parameters match
accurately fast MC input
notice redefinition of Nsig and Nbkg

Nsig	=	23.6048	+/-	0.0154101
X0	=	2.87125	+/-	0.00255149
Y0	=	1.18834	+/-	0.00193679
R	=	73.0013	+/-	0.00166626
sigmaR	=	1.88591	+/-	0.00123206
Nbkg	=	10.3538	+/-	0.0133316

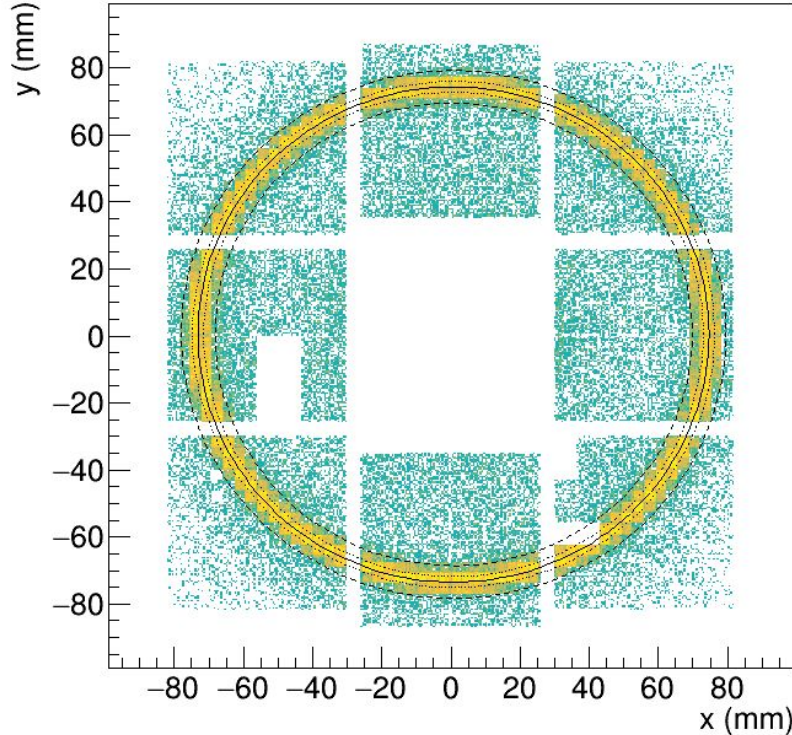


fast MC expectation for a 2024 beam test with 8x full PDUs is a **very large average number of photoelectrons for aerogel > 18**

Number of photoelectrons

is large as expected

11.5 GeV/c negative beam, $n = 1.02$ aerogel (accumulated events)



$$X_0 = 0.75 \pm 0.01 \text{ mm}$$

$$Y_0 = 0.45 \pm 0.01 \text{ mm}$$

$$R = 73.87 \pm 0.00 \text{ mm}$$

$$\sigma_R = 1.63 \pm 0.00 \text{ mm}$$

average number of
signal photons for
100% acceptance
includes SiPM efficiency

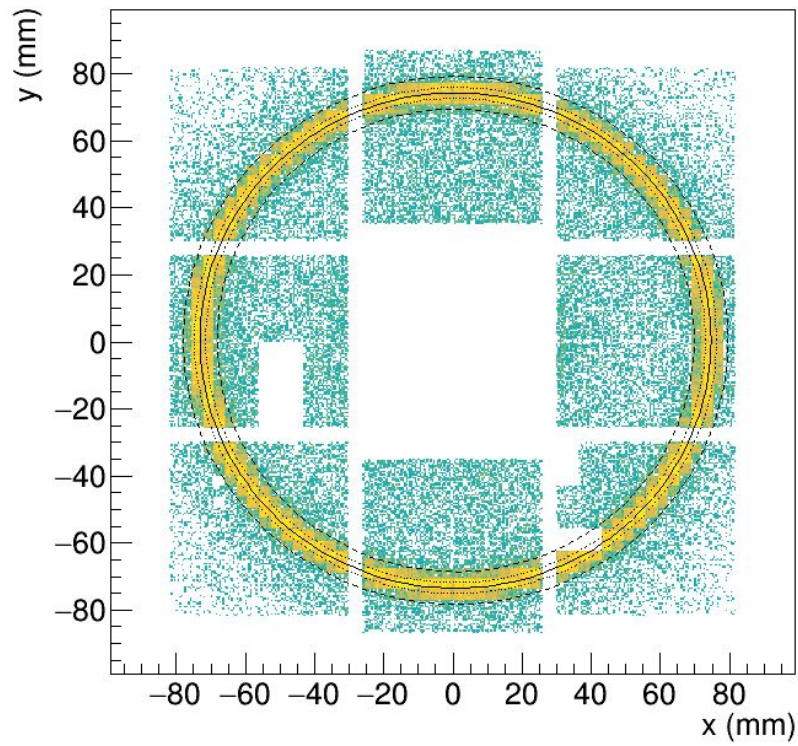
$$N_{\text{sig}} = 29.13 \pm 0.07$$

$$N_{\text{bkg}} = 8.47 \pm 0.05$$

Number of photoelectrons

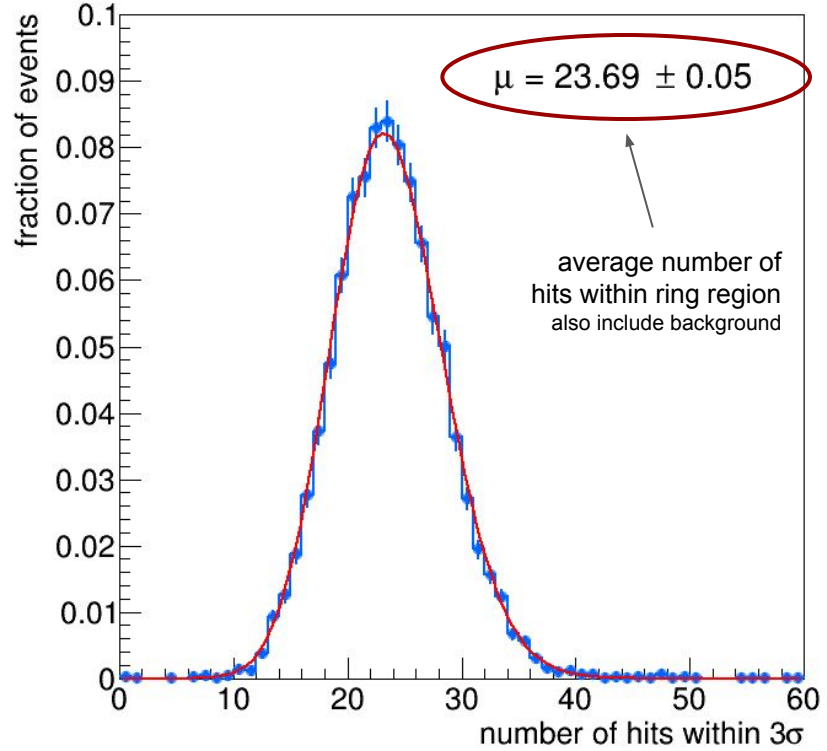
large as expected

11.5 GeV/c negative beam, $n = 1.02$ aerogel (accumulated events)



2D fit to accumulated data with realistic model (ring + background)

event-by-event distribution of hits in the ring



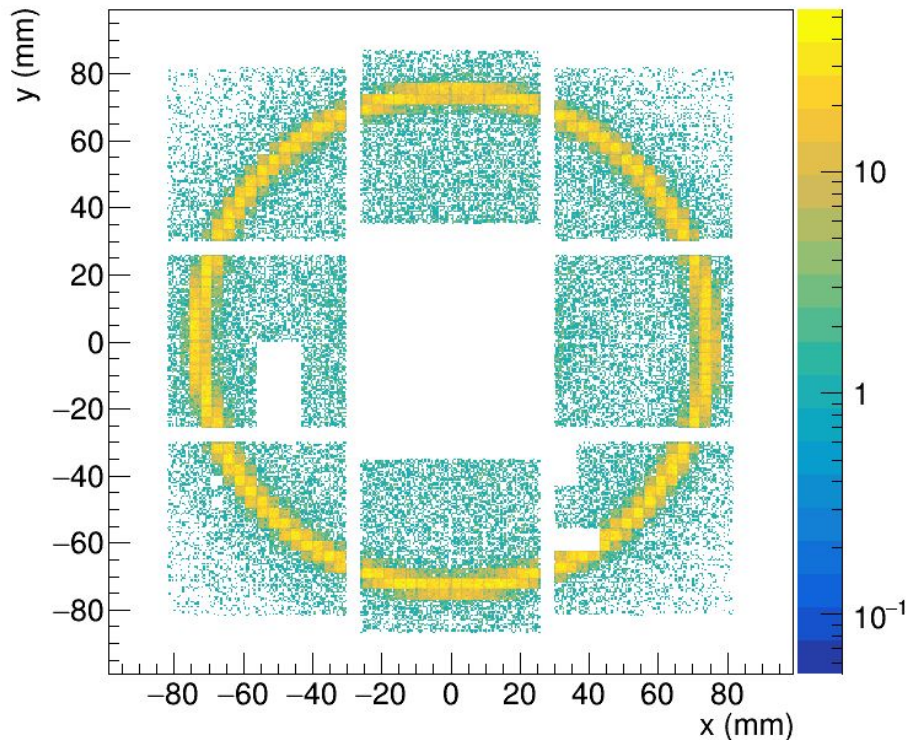
Poisson fit to data, average number of hits is large

Background studies

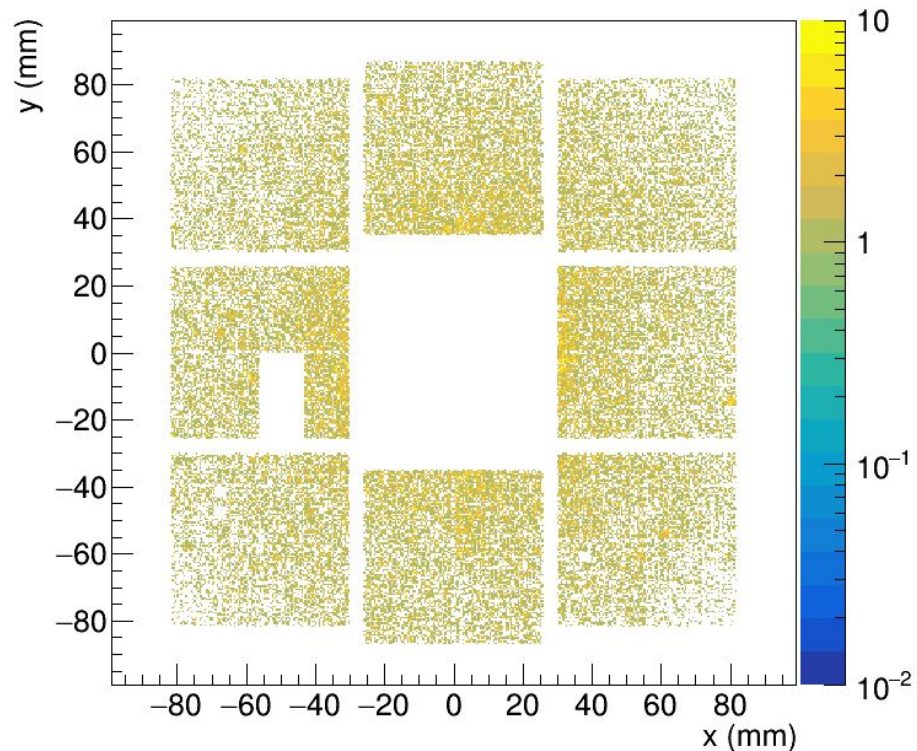
data taken without aerogel radiator



with two $n = 1.02$ aerogel tiles (accumulated events)



without aerogel (accumulated events)



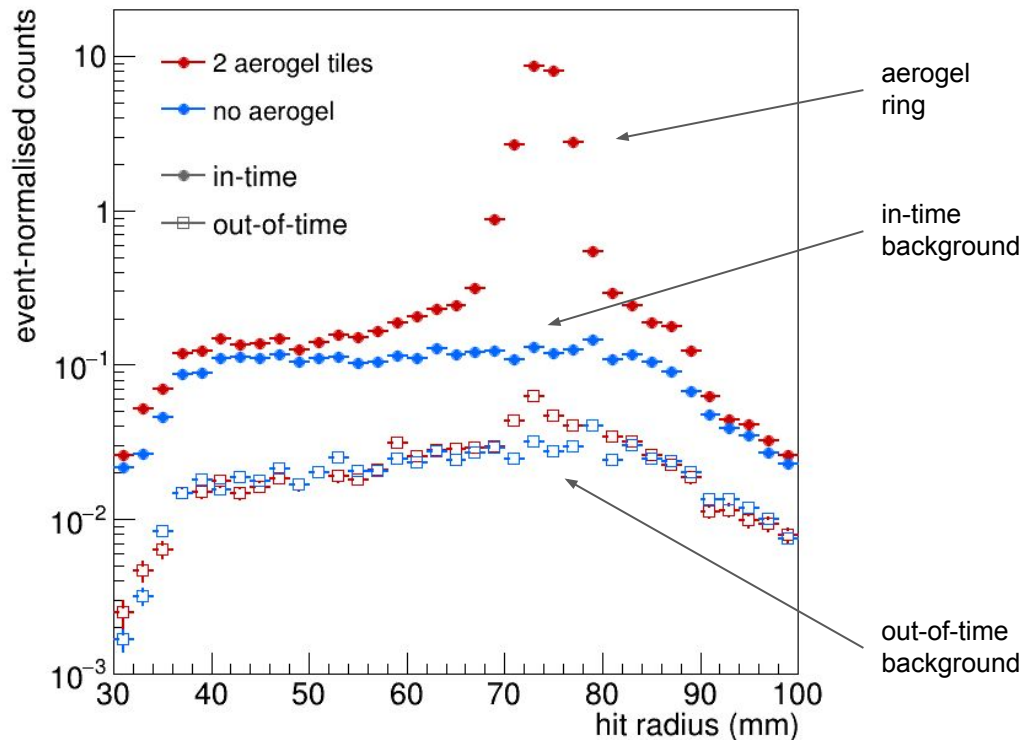
with timing cuts applied, large background as seen in past years

removed the aerogel tile, background remains

Background studies

basically all the background remains after removing aerogel, not from DCR

distribution hit radii with and without aerogel

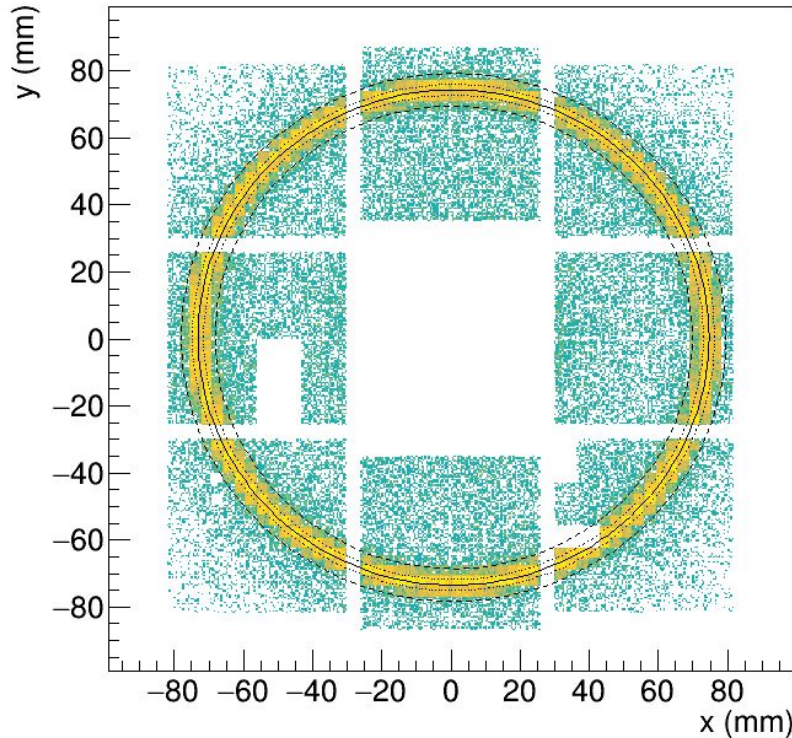


in-time (40 ns window) background is $\sim 10\times$ larger than out-of-time (40 ns window) background (mostly DCR) | origin still unclear | to be understood

Background studies

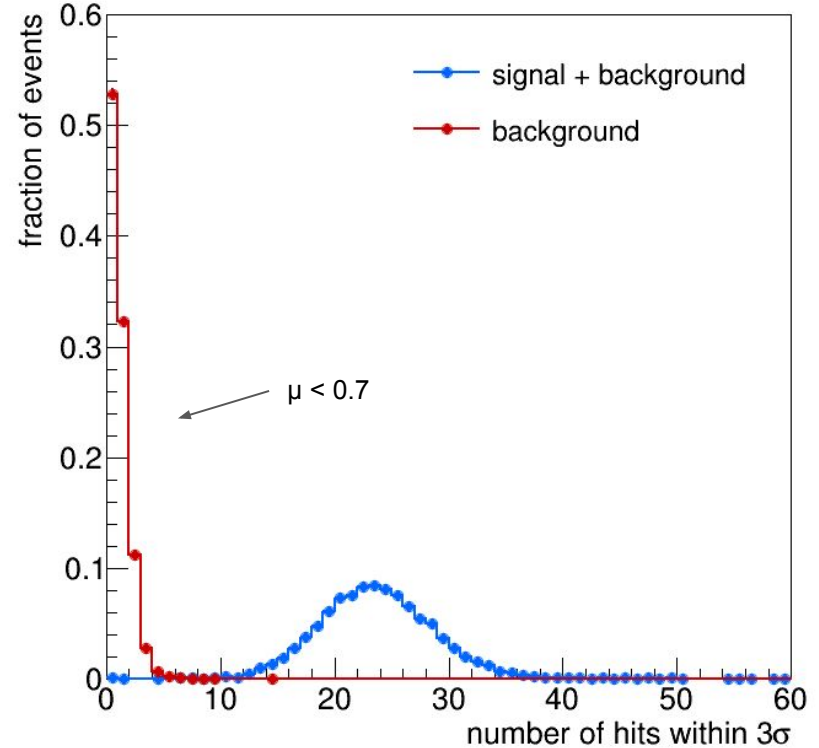
there is often one background hit in the ring, this will impact resolution

11.5 GeV/c negative beam, $n = 1.02$ aerogel (accumulated events)



2D fit to accumulated data with realistic model (ring + background)

event-by-event distribution of hits in the ring



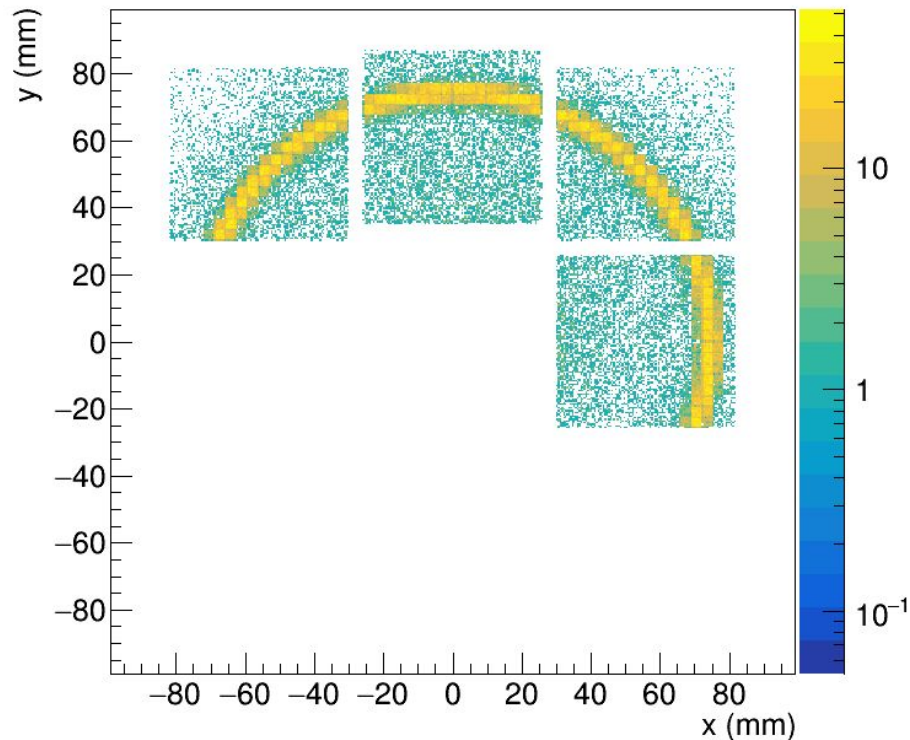
background in ring region estimated with data taken without aerogel

Comparison between different SiPM sensors

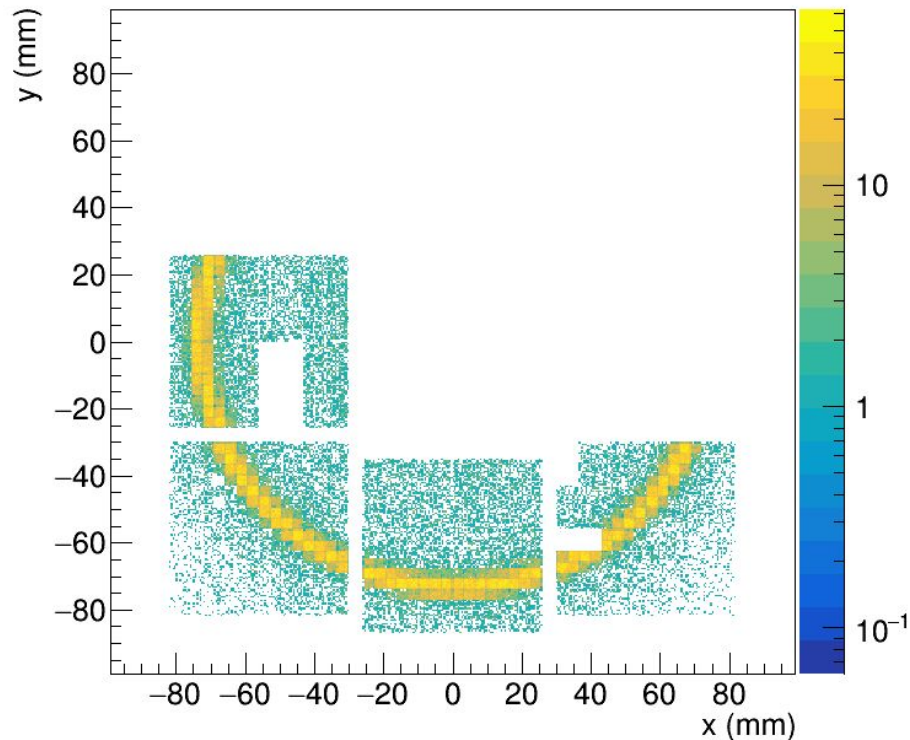


same Hamamatsu technology, different SPAD sizes

Hamamatsu S13360-3050 (50 μm)



Hamamatsu S13360-3075 (75 μm)

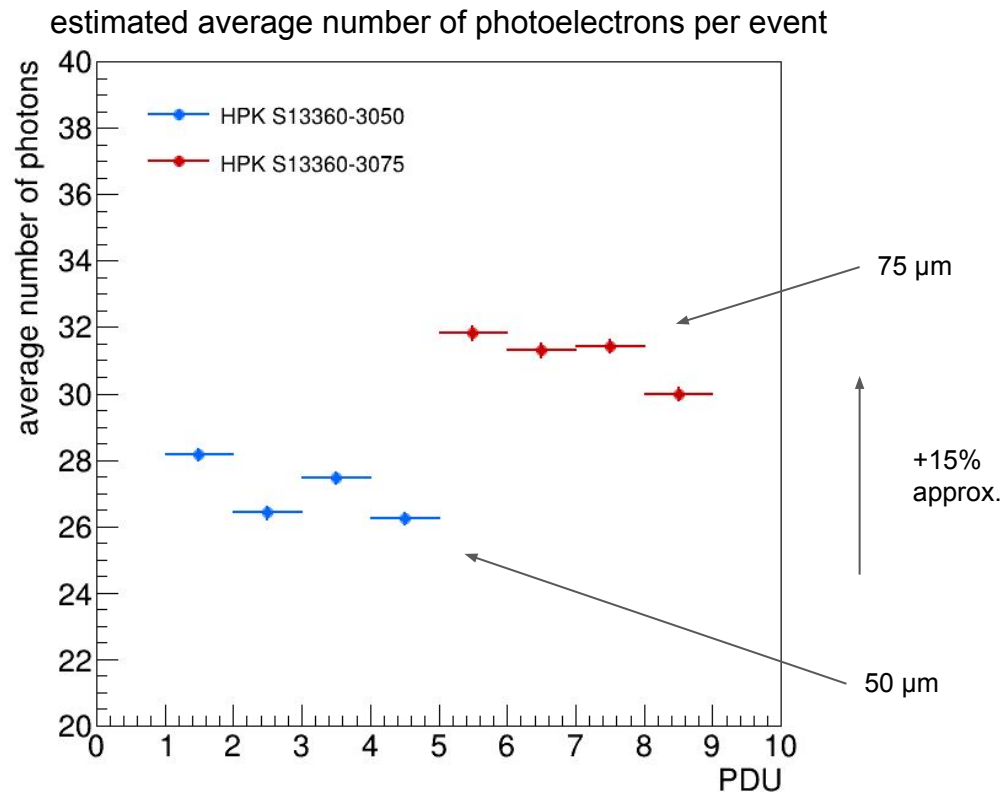


4 PDUs were equipped with one type of sensors

symmetrically, the other four with different sensors

Comparison between different SiPM sensors

same Hamamatsu technology, different SPAD sizes

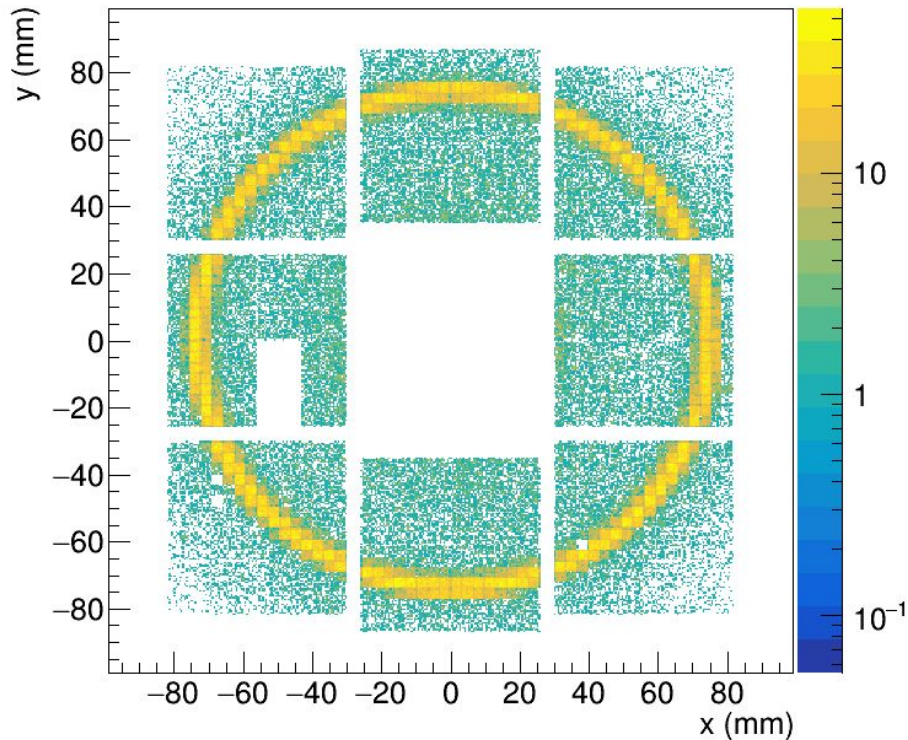


larger SPADs see more light (at the same overvoltage) than smaller SPADs | observed 15% more light | expected 25% higher PDE from datasheet

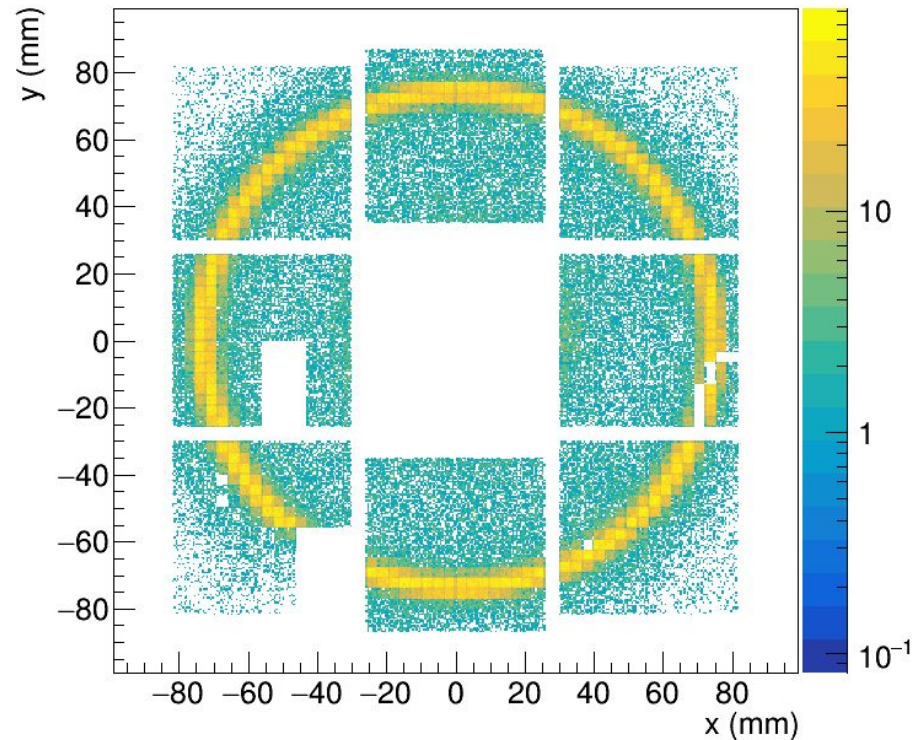
Increasing number of aerogel tiles

$n = 1.02$ aerogel tiles of $L = 2$ cm thickness

one aerogel tile ($n = 1.02$, $L = 2$ cm)

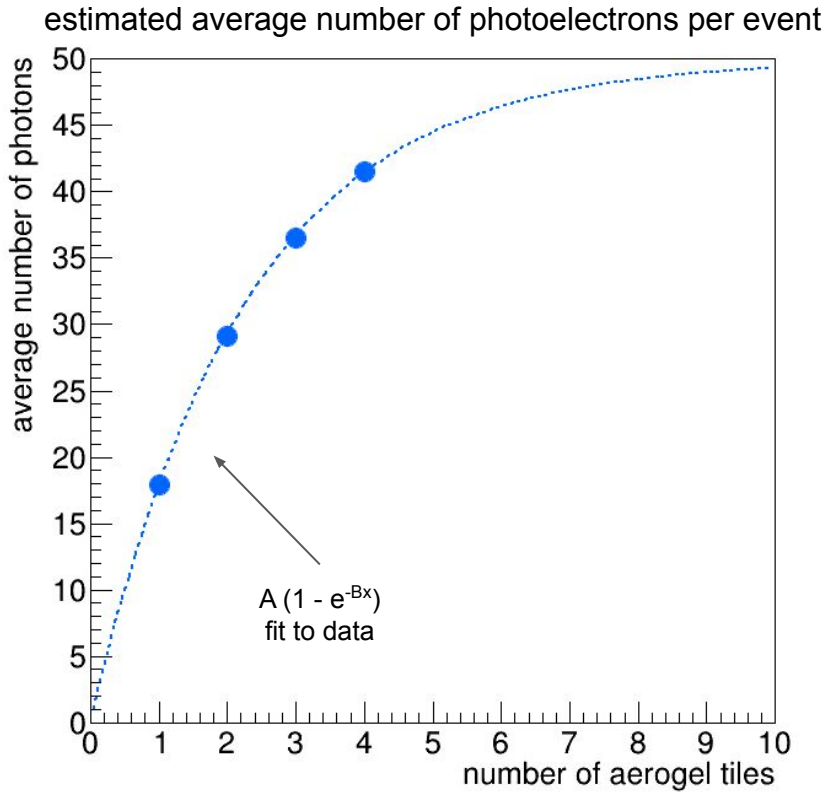


four aerogel tiles ($n = 1.02$, $L = 2$ cm)

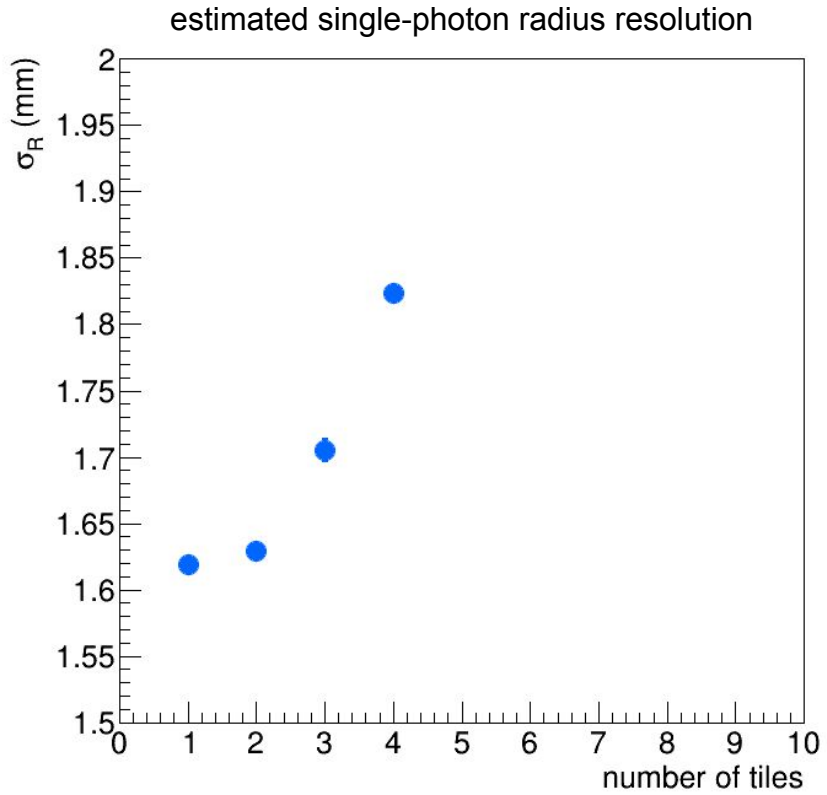


Increasing number of aerogel tiles

$n = 1.02$ aerogel tiles of $L = 2$ cm thickness



adding tiles increases light, less and less effectively (absorption)



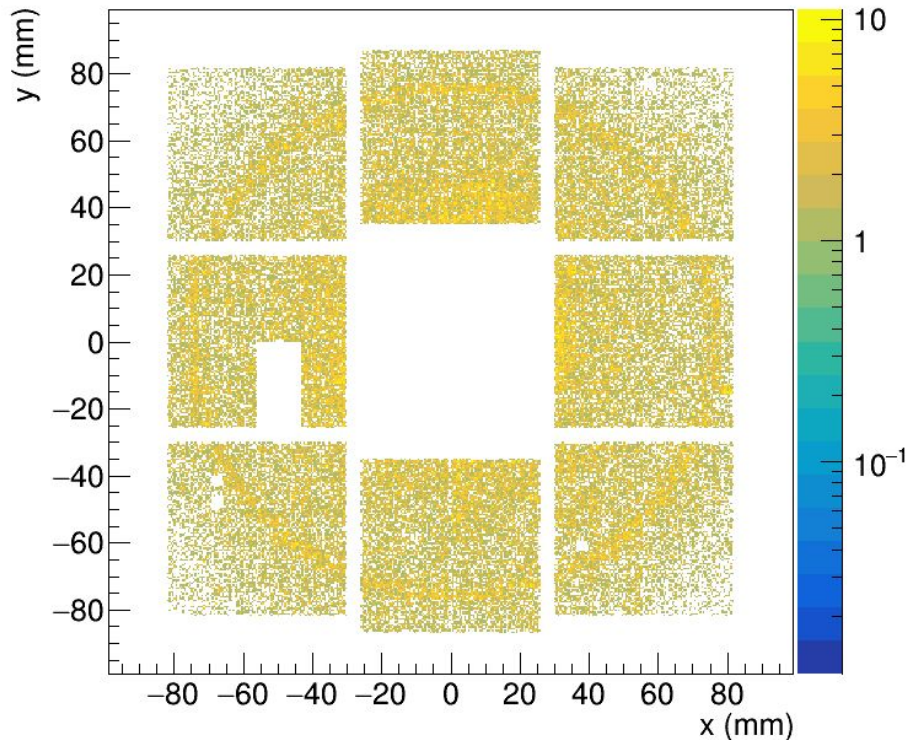
looks like single-photon resolution is degrading, not clear why

Wavelength filters

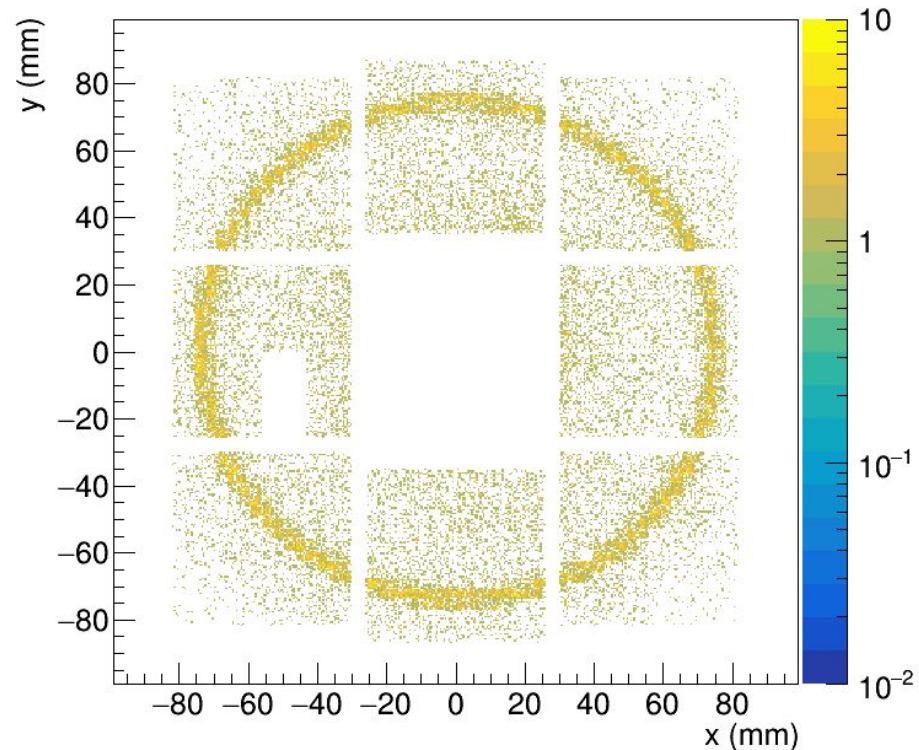
several filters used to select specific wavelength bands



near ultra-violet filter ($\lambda \sim 350$ nm)



blue filter ($450 < \lambda < 500$ nm)

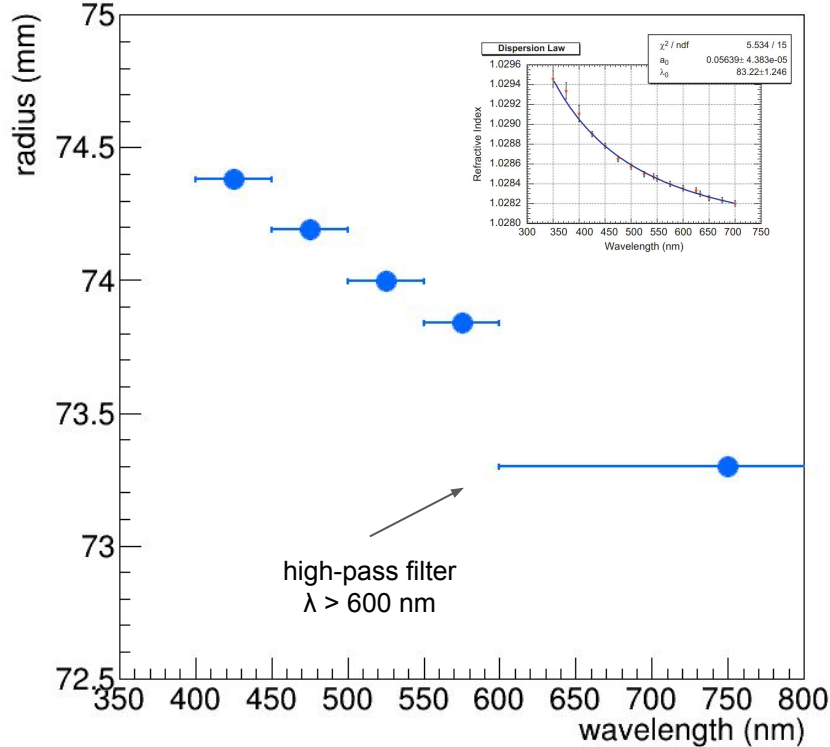


we still see the ring, but the "beam background" makes life difficult

Wavelength filters

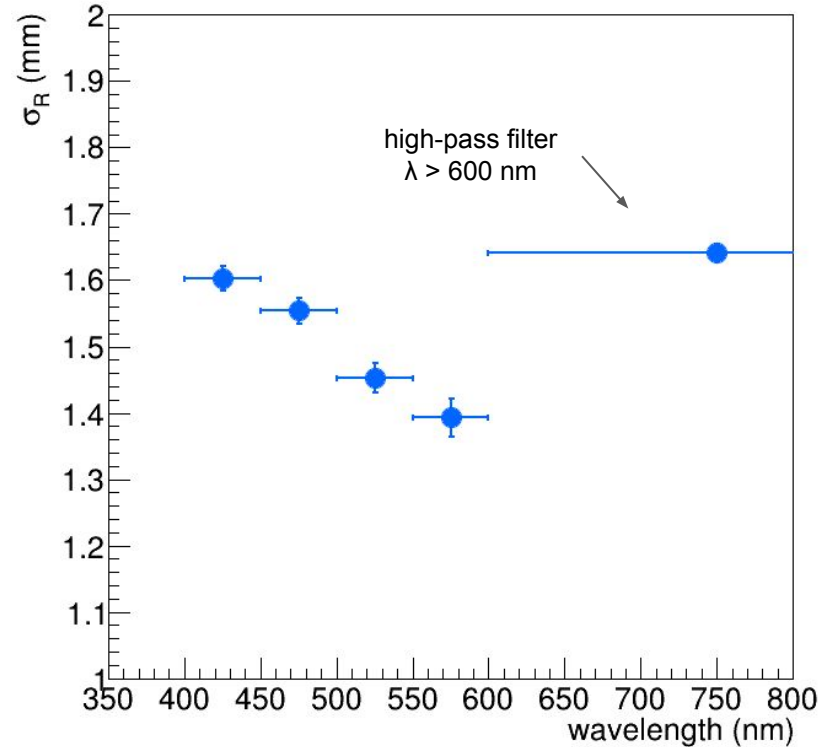
several filters used to select specific wavelength bands

estimated ring radius



ring radius decreases with increasing wavelength

estimated single-photon radius resolution



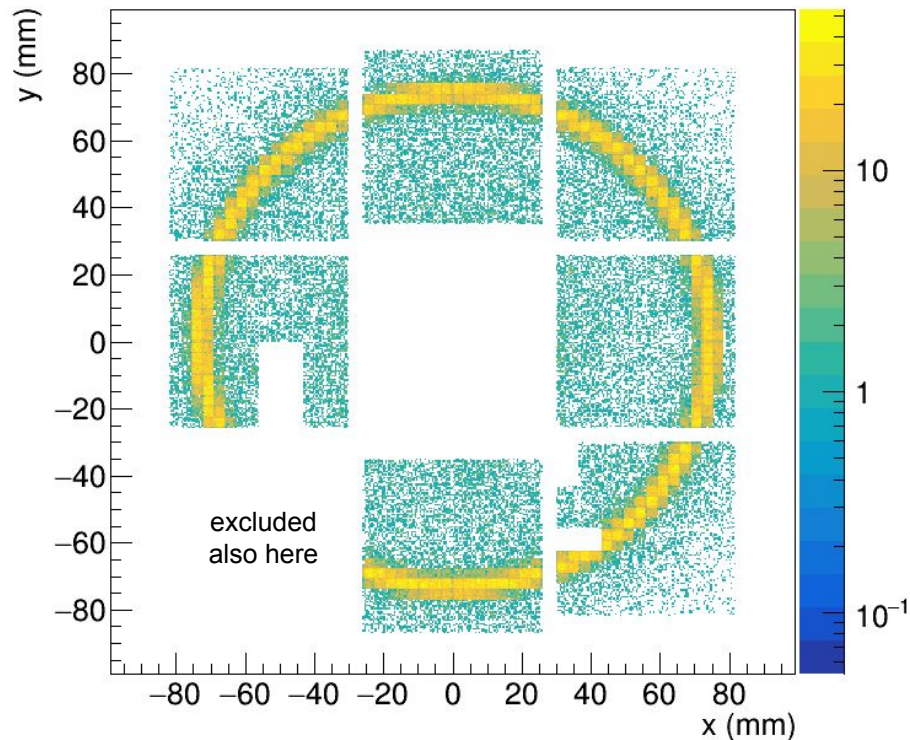
single-photon resolution improves, not clear why

$n = 1.026$ aerogel samples



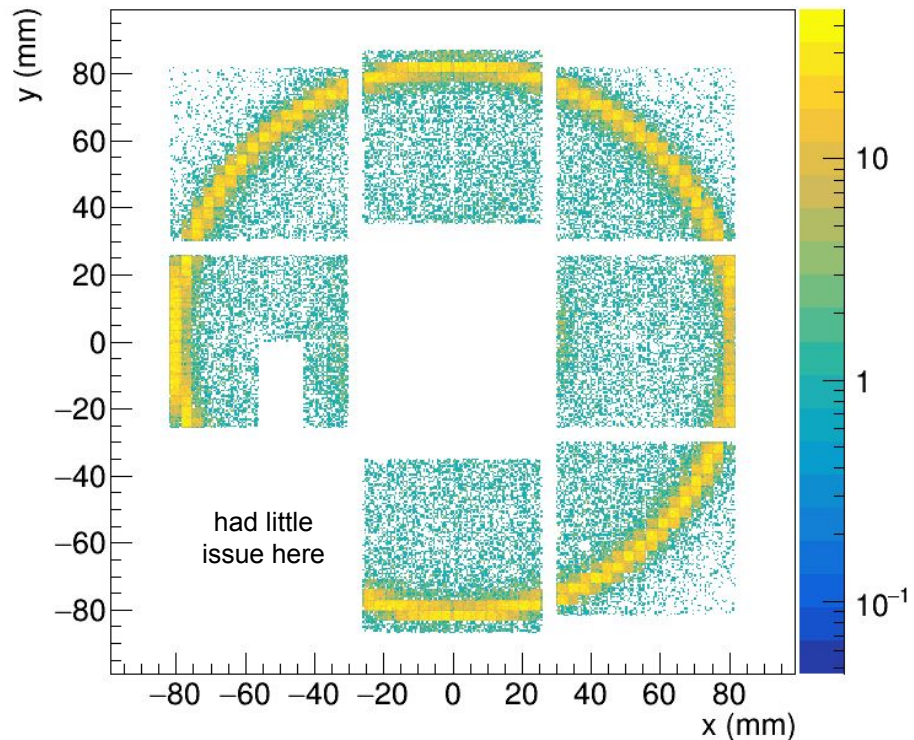
larger refractive index, expected larger rings and more light

two $L = 2$ cm tiles of $n = 1.02$ aerogel



excluded bottom-left corner in these runs because of little issue

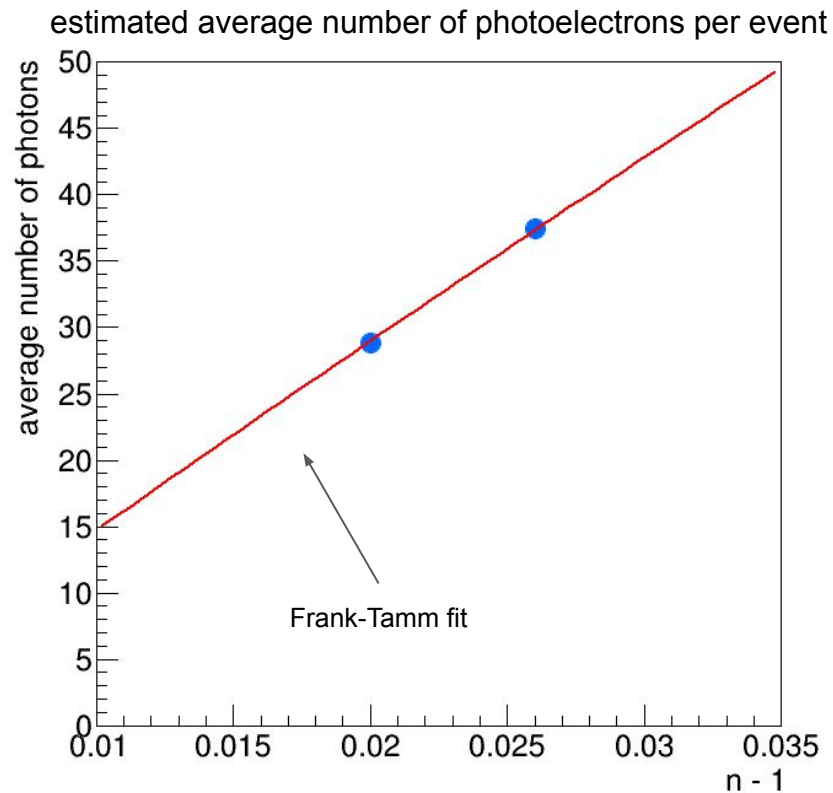
two $L = 2$ cm tiles of $n = 1.026$ aerogel



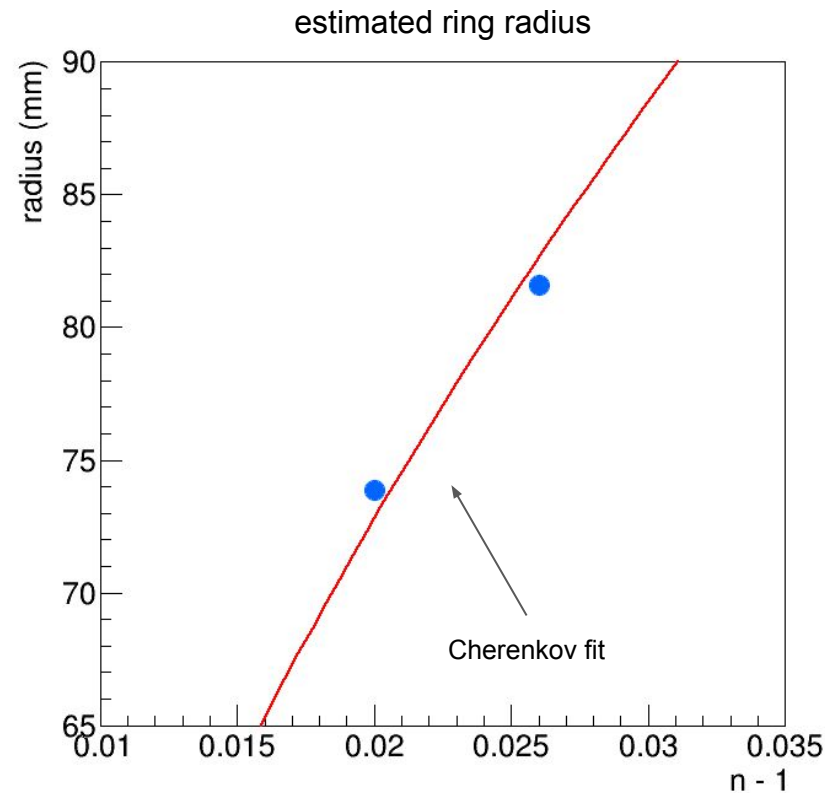
ring is larger, at the limit of the detector acceptance

n = 1.026 aerogel samples

larger refractive index, expected larger rings and more light



increases with refractive index (angle)

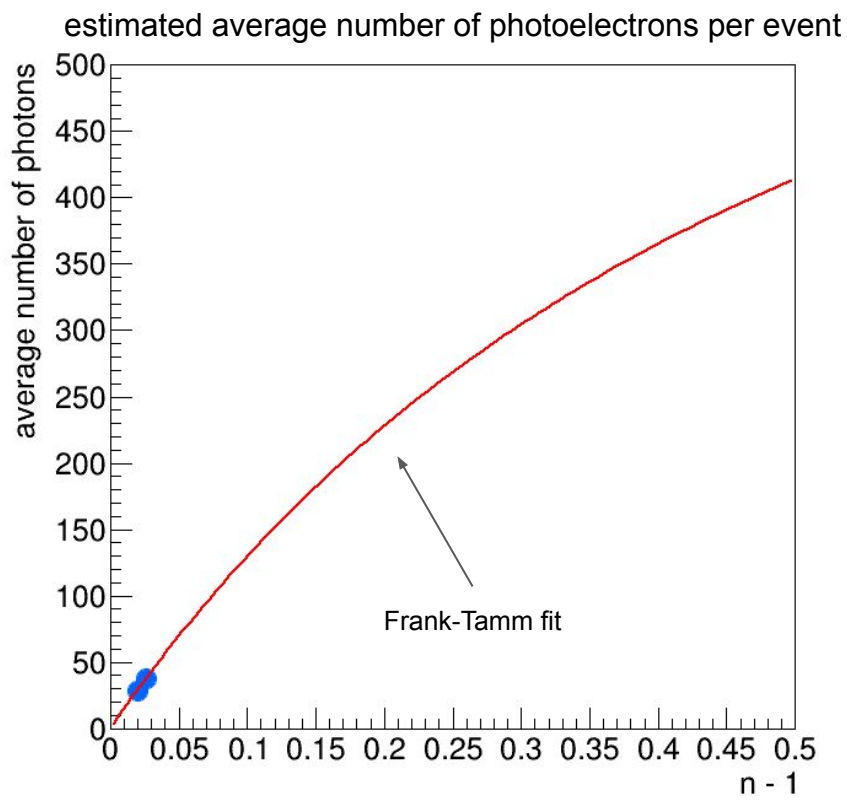


radius increases

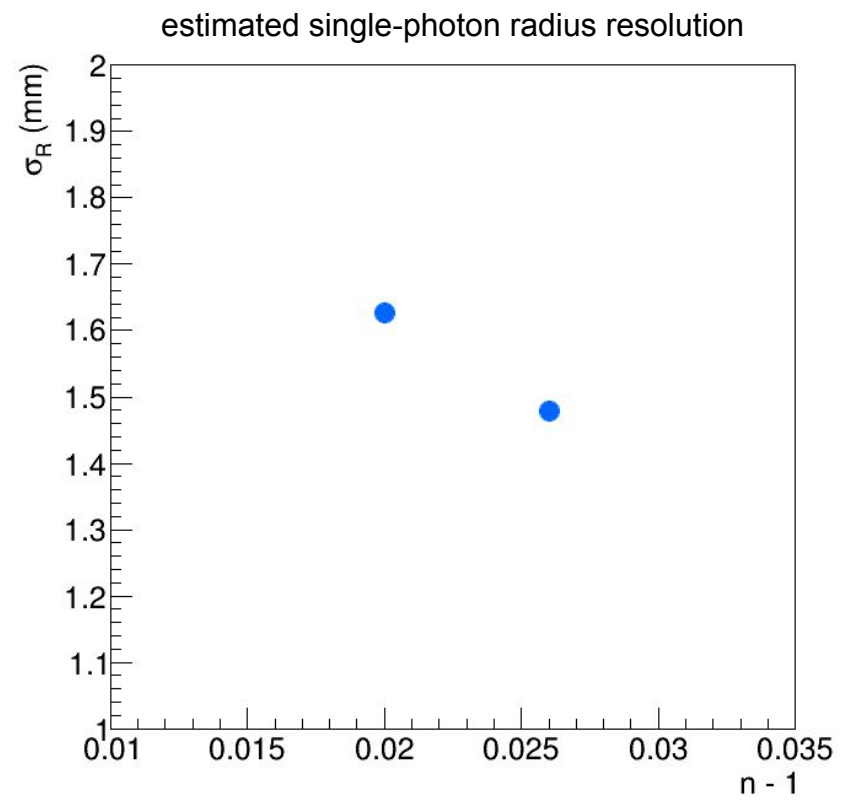
$n = 1.026$ aerogel samples



larger refractive index, expected larger rings and more light



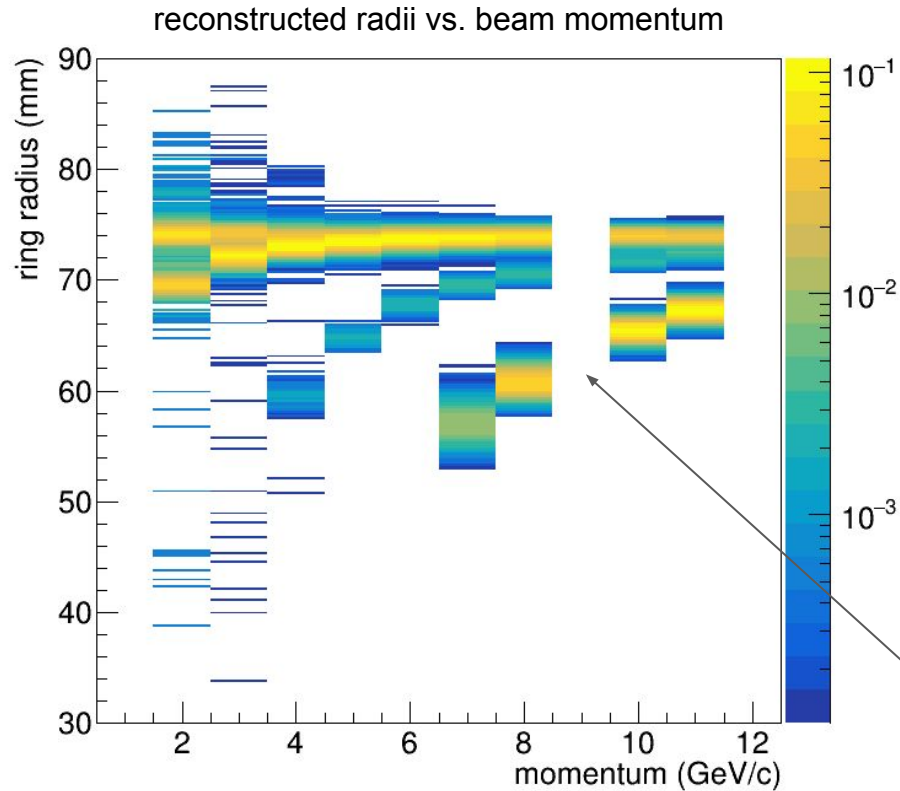
same view with extended range



single-photon resolution improves

Beam momentum scan

positive particles, aerogel only

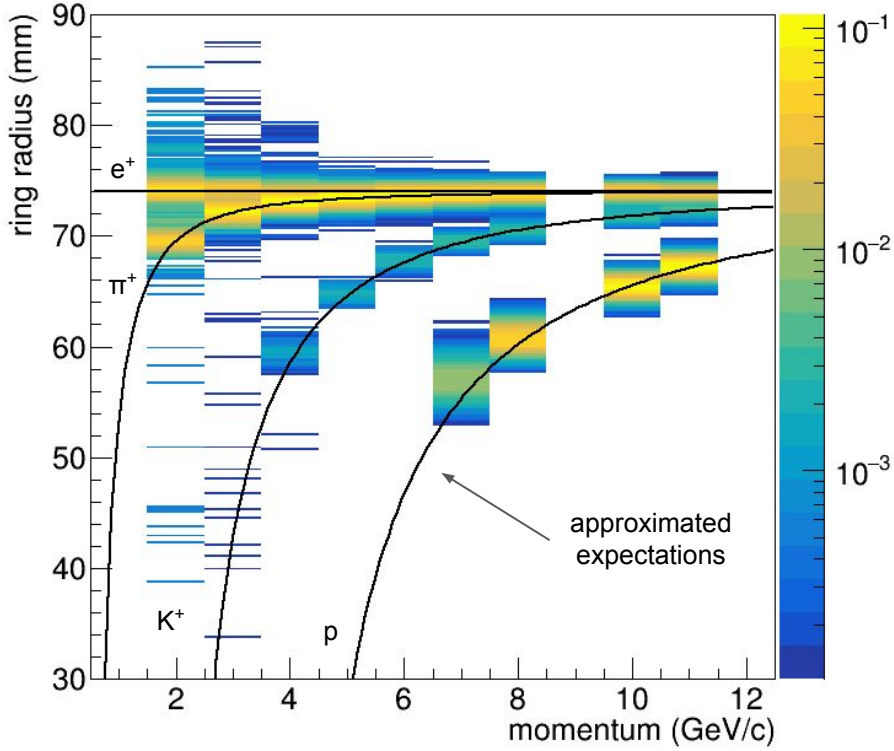


something has gone wrong with the beam configuration for 9 GeV (data not show)

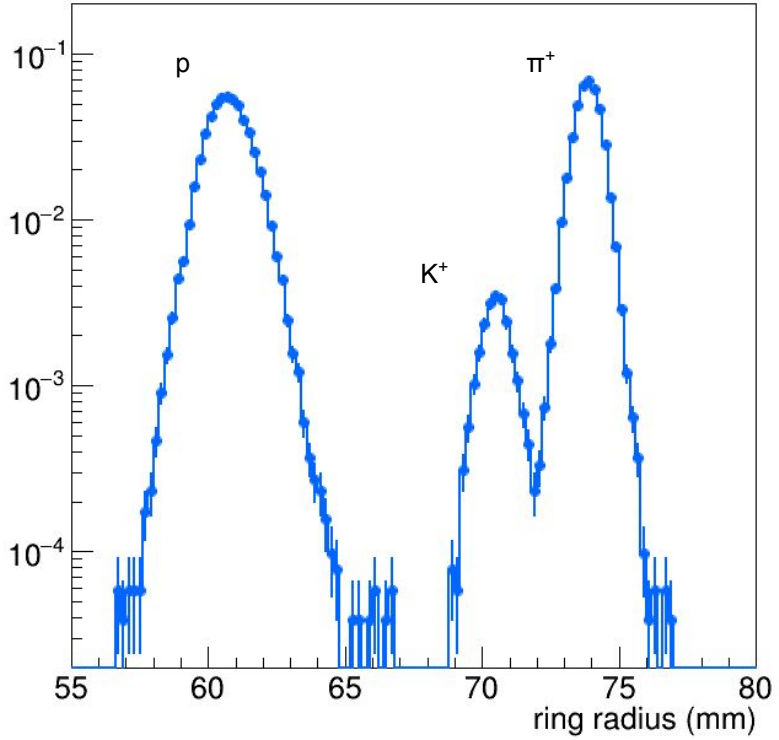
Beam momentum scan

positive particles, aerogel only

reconstructed radii vs. beam momentum



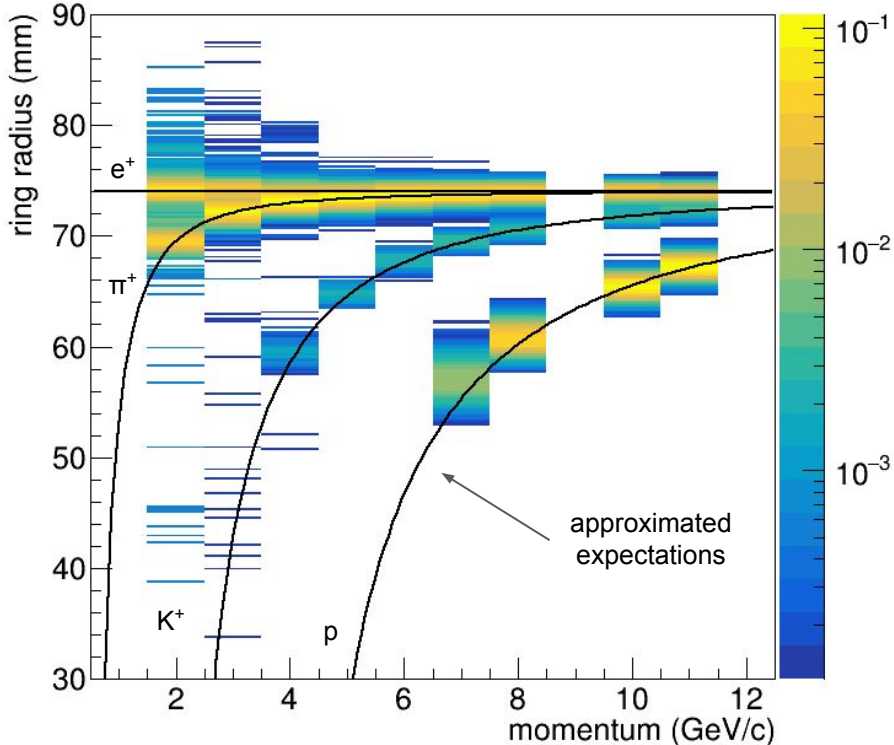
reconstructed radii at 8 GeV/c beam momentum



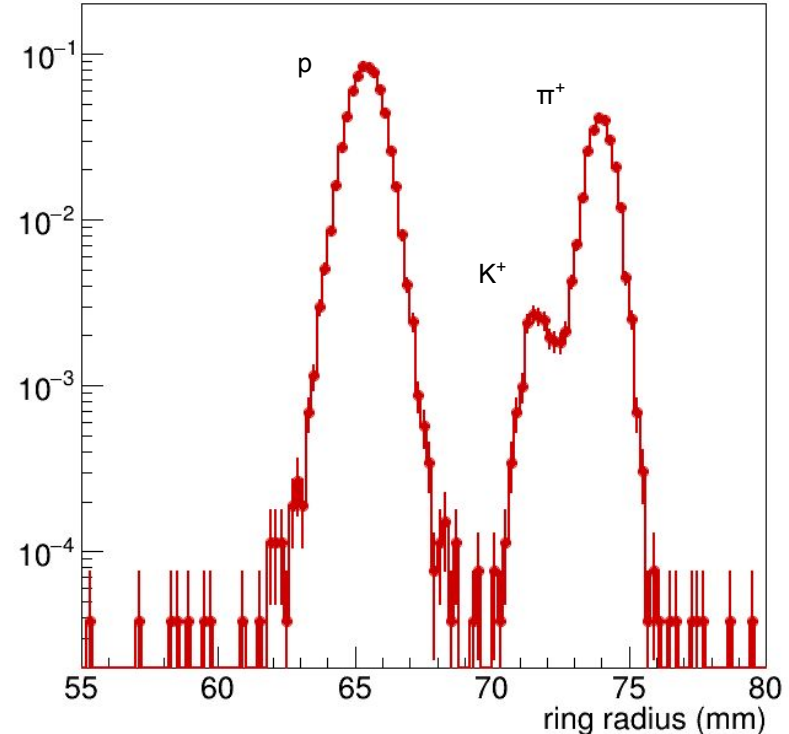
Beam momentum scan

positive particles, aerogel only

reconstructed radii vs. beam momentum



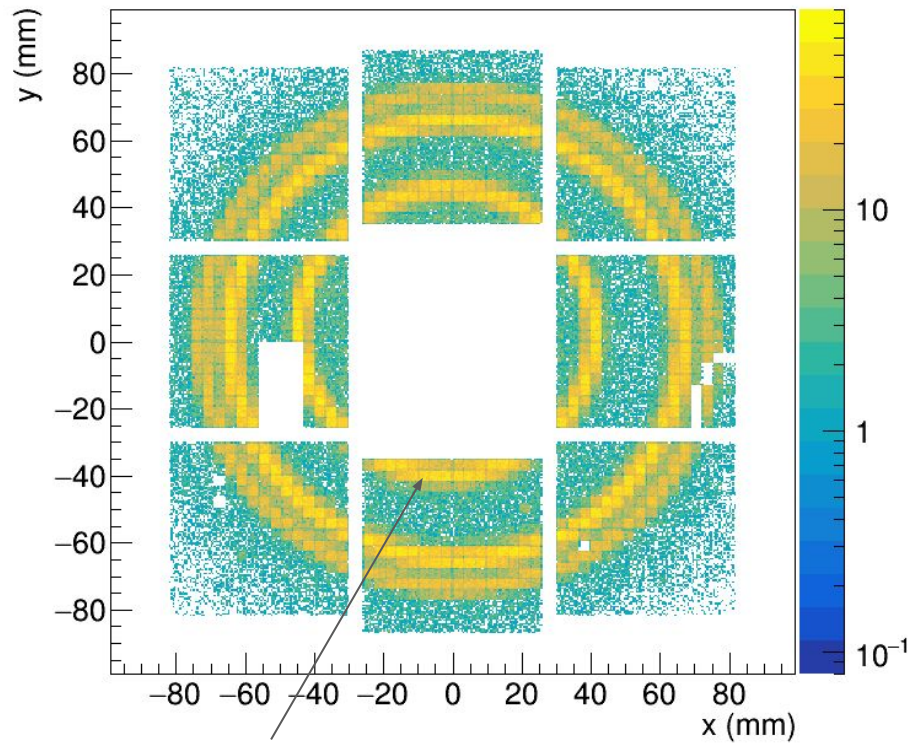
reconstructed radii at 10 GeV/c beam momentum



Interplay between radiators

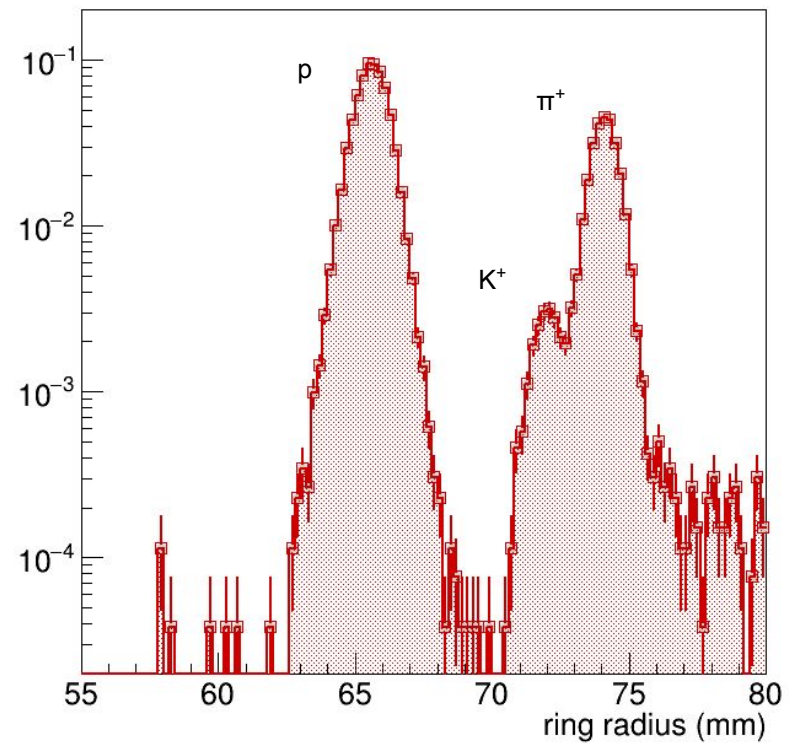
gas ring tags pions, kaons and protons are below threshold

10 GeV/c positive beam with no selection applied



gas ring

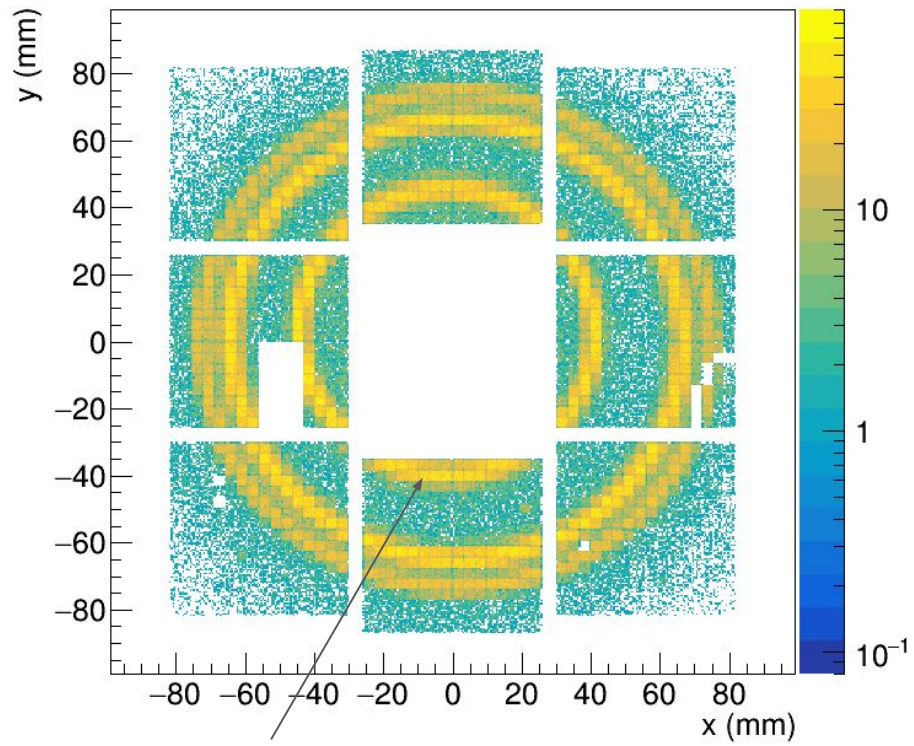
reconstructed radii at 10 GeV/c with no selection applied



Interplay between radiators

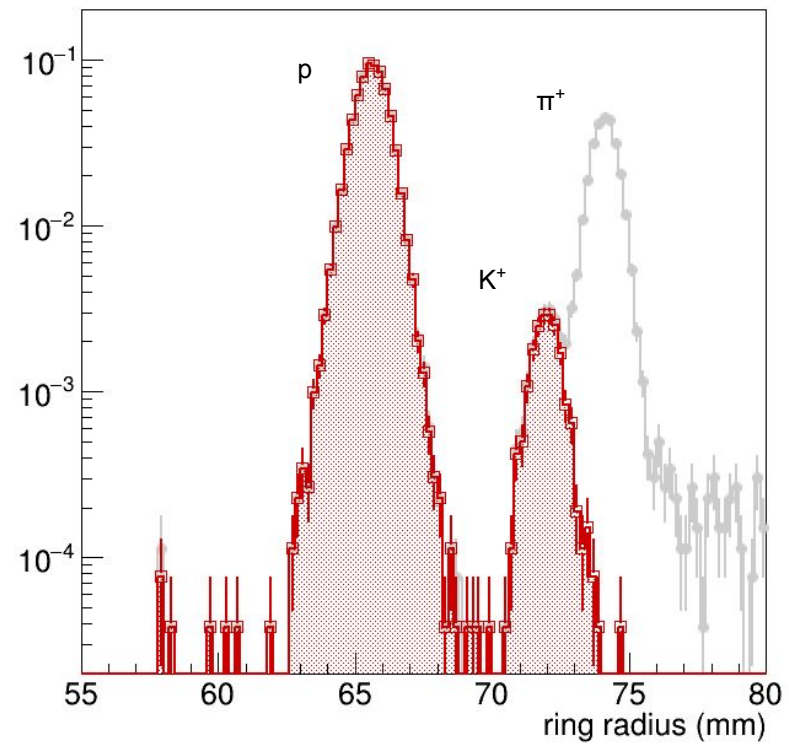
gas ring tags pions, kaons and protons are below threshold

10 GeV/c positive beam with no selection applied



gas ring

reconstructed radii at 10 GeV/c with gas veto



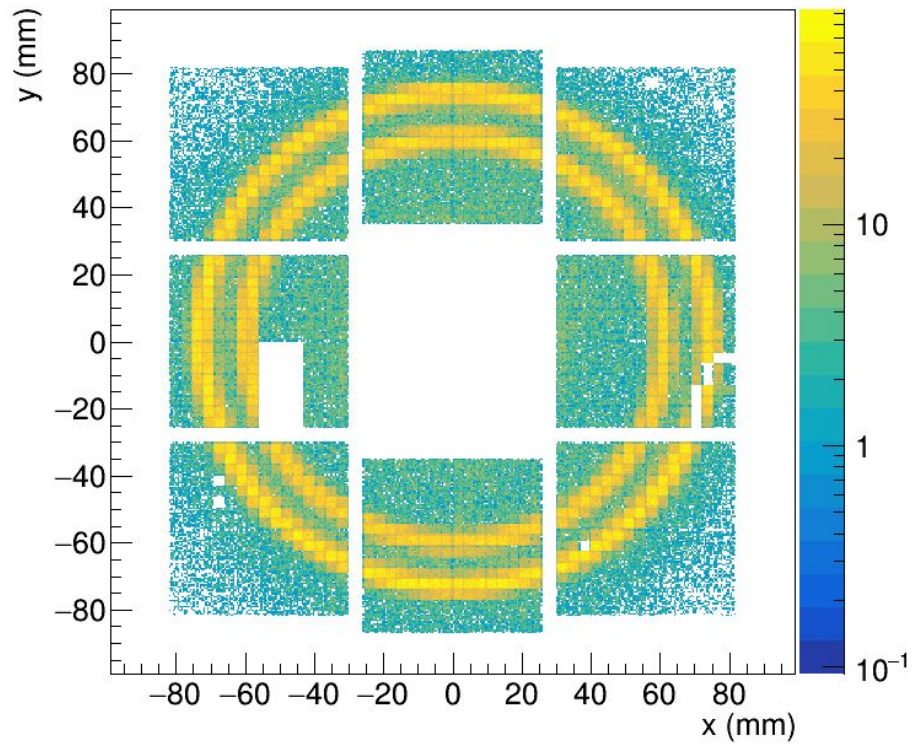
clean kaon identification at 10 GeV/c

Threshold Cherenkov beam counters

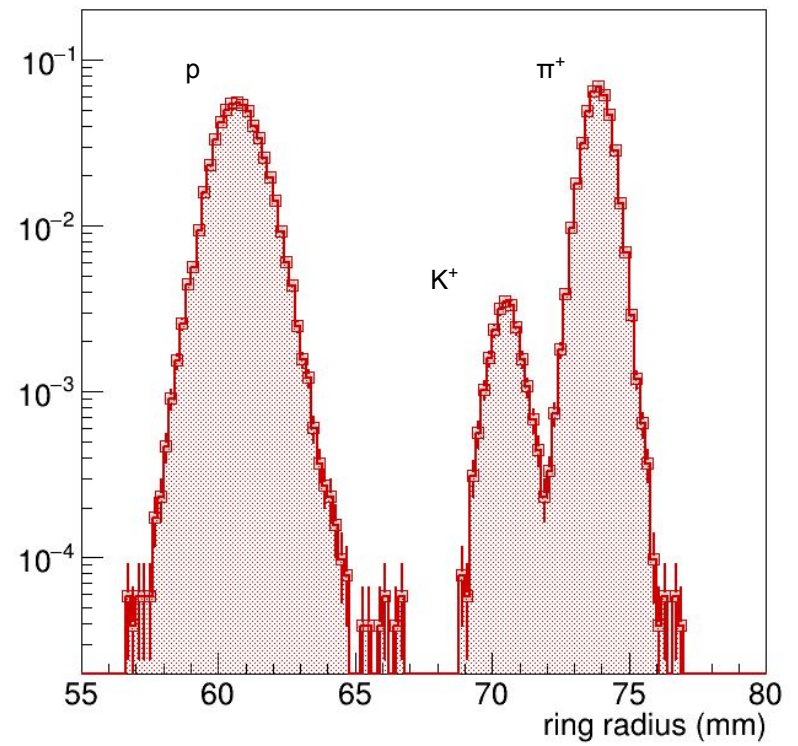


TCh-1 set below kaon threshold, TCh-2 set below proton threshold

8 GeV/c positive beam with no selection applied



reconstructed radii at 8 GeV/c with no selection applied

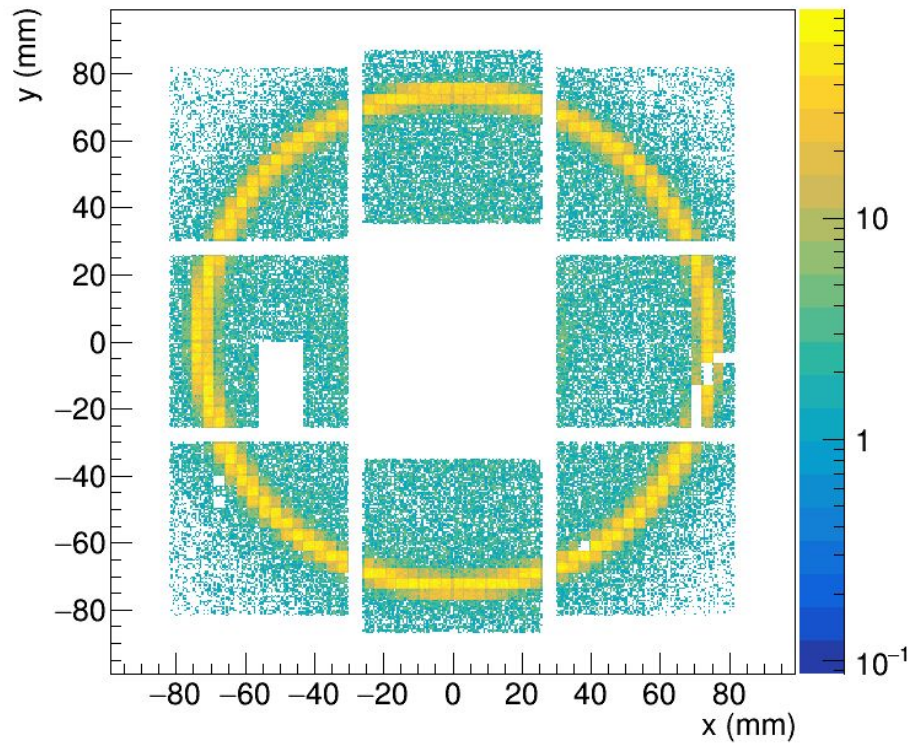


Threshold Cherenkov beam counters

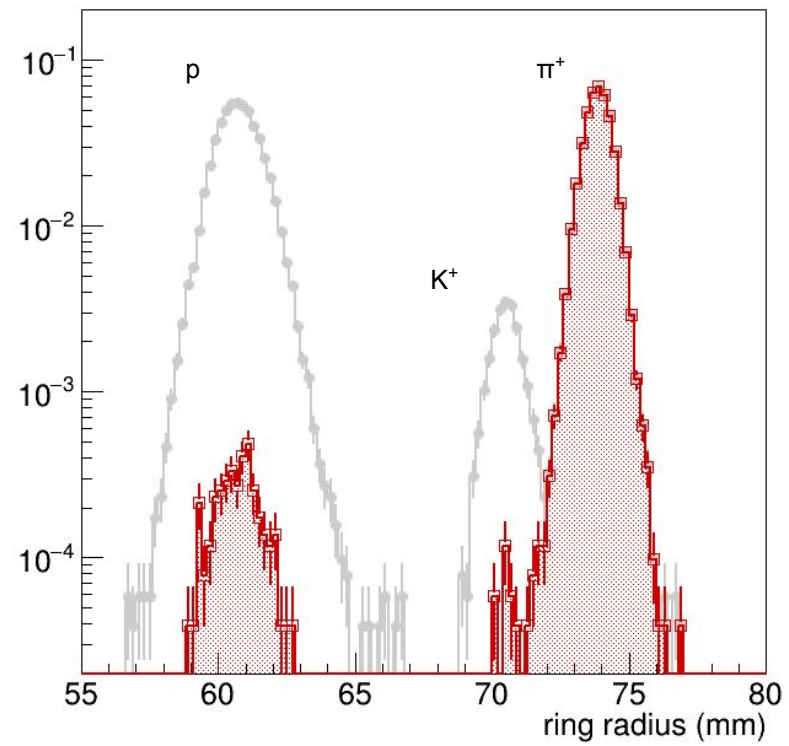


TCh-1 set below kaon threshold, TCh-2 set below proton threshold

8 GeV/c positive beam with pion tag



reconstructed radii at 8 GeV/c with pion tag



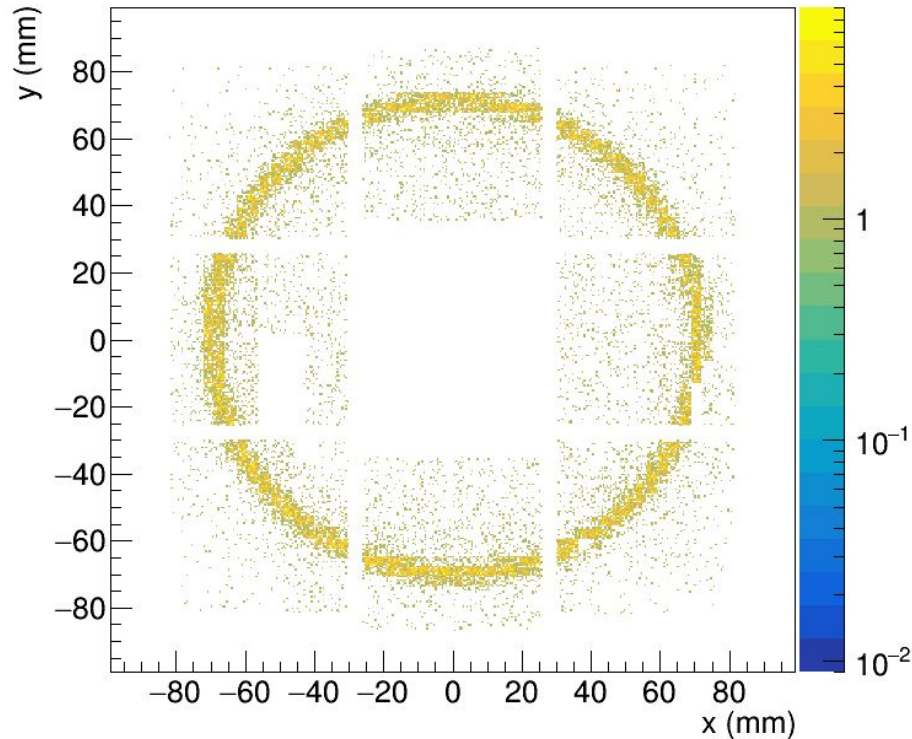
pion tag: TCh-1 required

Threshold Cherenkov beam counters

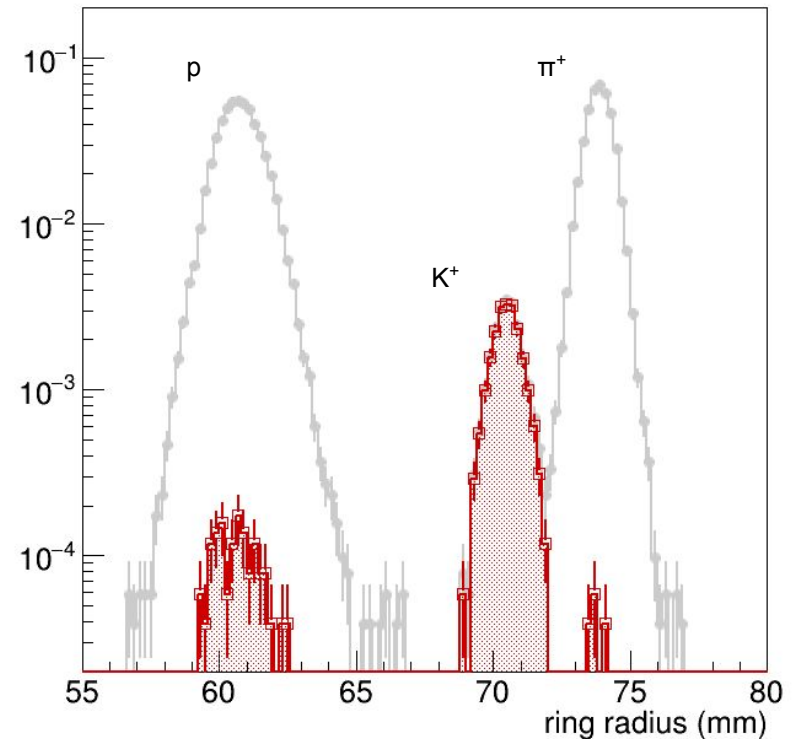


TCh-1 set below kaon threshold, TCh-2 set below proton threshold

8 GeV/c positive beam with kaon tag



reconstructed radii at 8 GeV/c with kaon tag



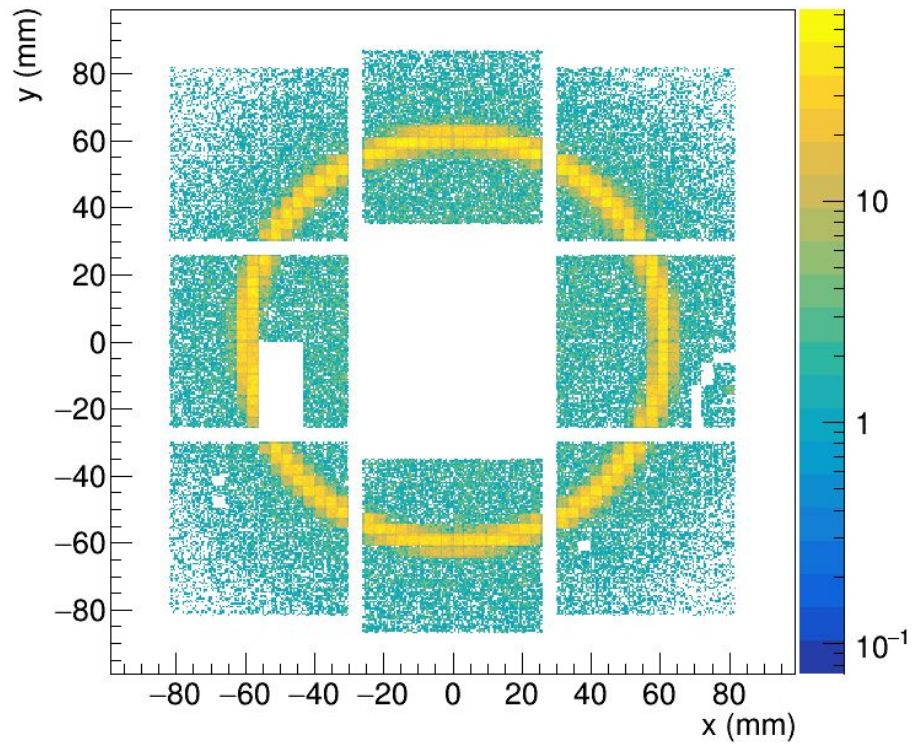
kaon tag: TCh-1 veto and TCh-2 required

Threshold Cherenkov beam counters

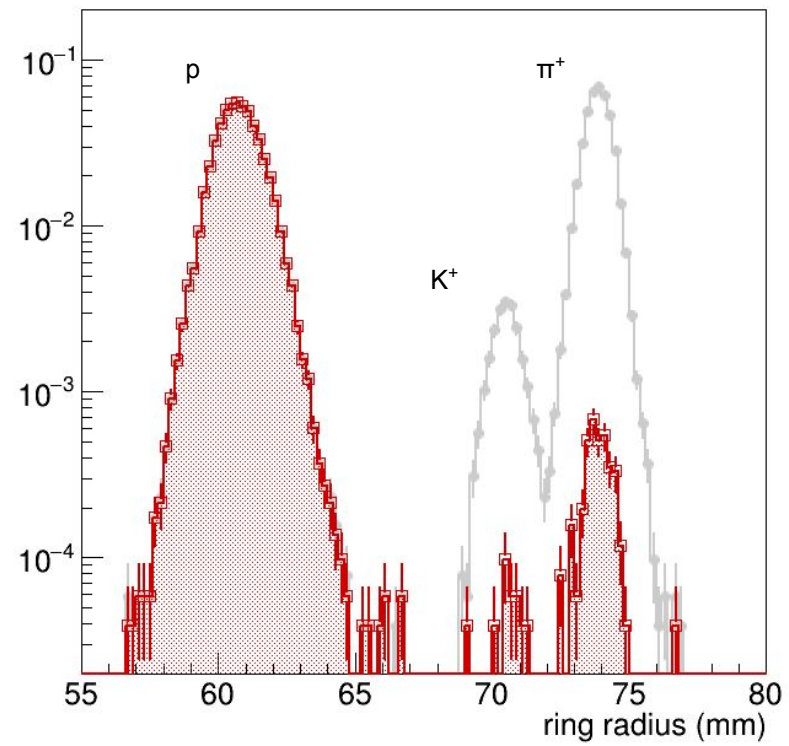


TCh-1 set below kaon threshold, TCh-2 set below proton threshold

8 GeV/c positive beam with proton tag



reconstructed radii at 8 GeV/c with proton tag

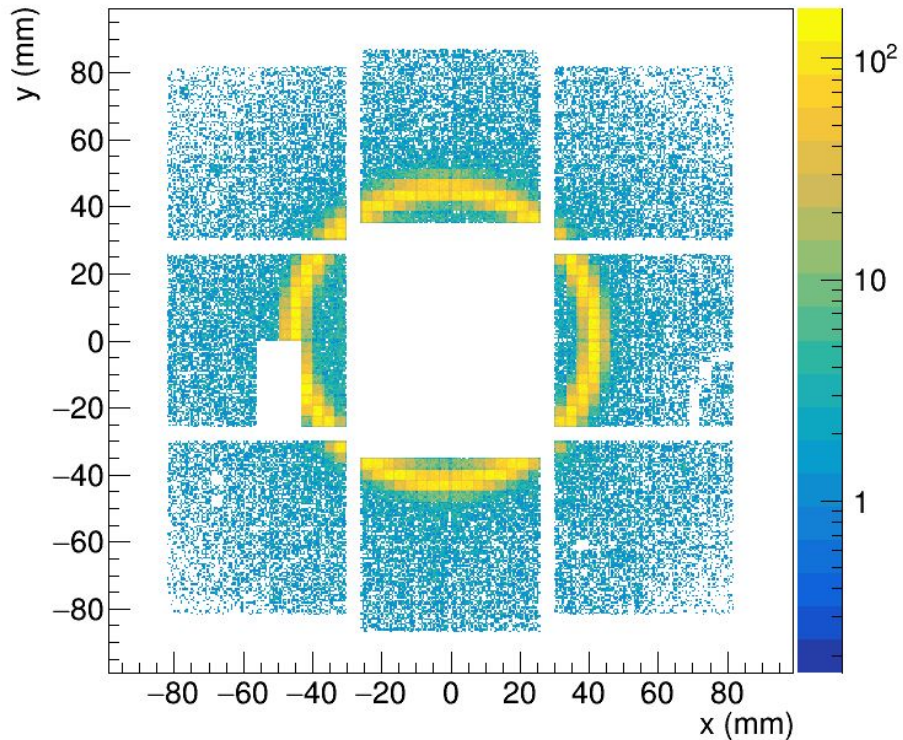


proton tag: TCh-1 veto and TCh-2 veto

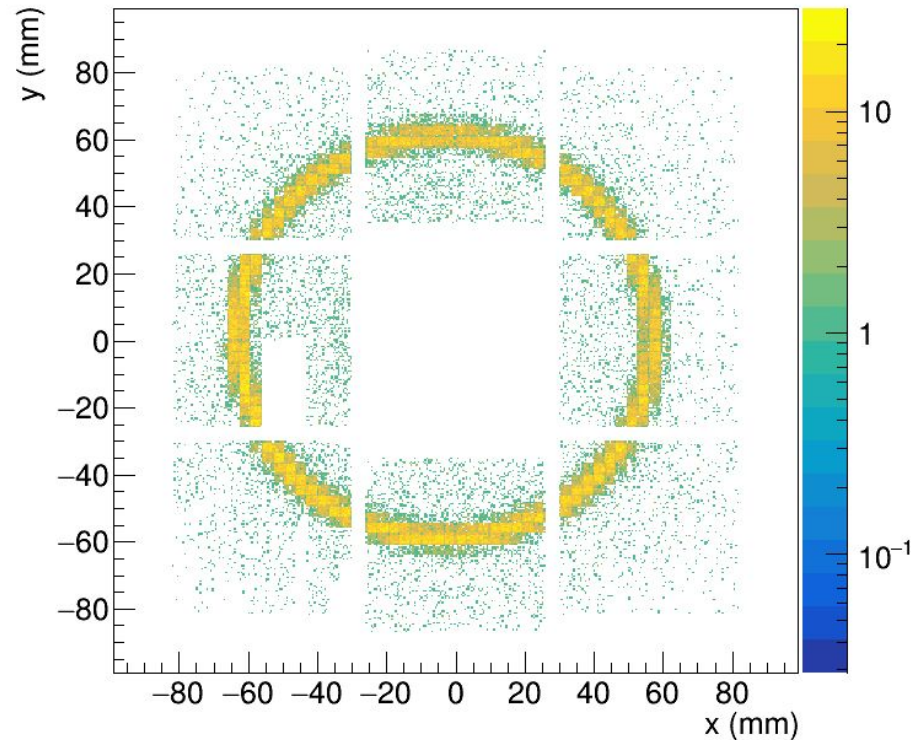
Gas radiators

standard gas C_2F_6 ($n = 1.0008$) and heavier C_4F_{10} ($n = 1.0014$)

C_2F_6 ($n = 1.0008$)



C_4F_{10} ($n = 1.0014$)

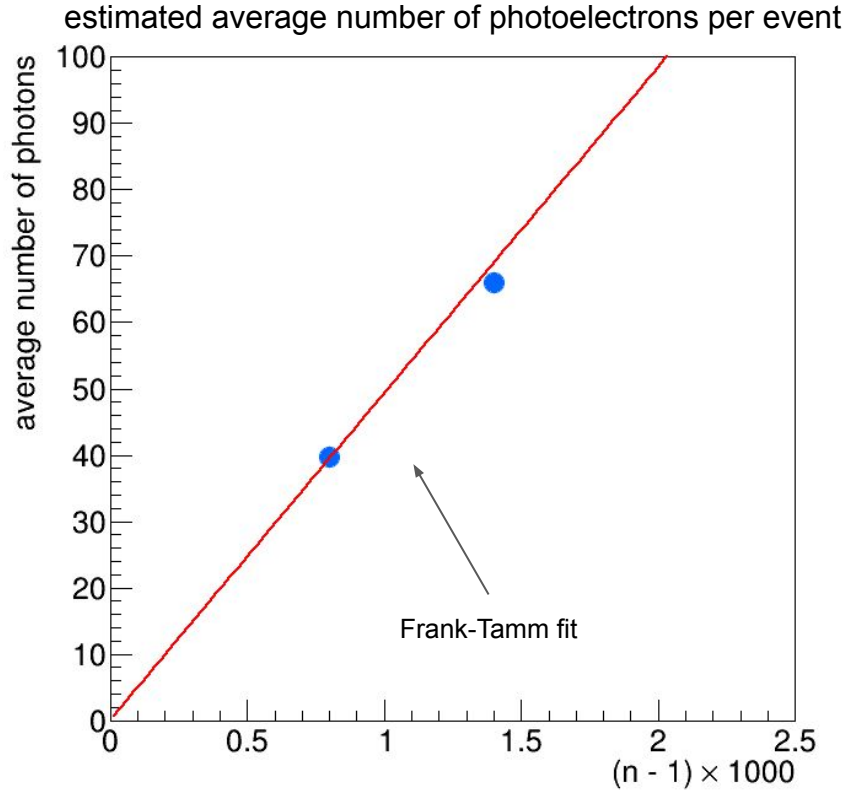


no aerogel in these data

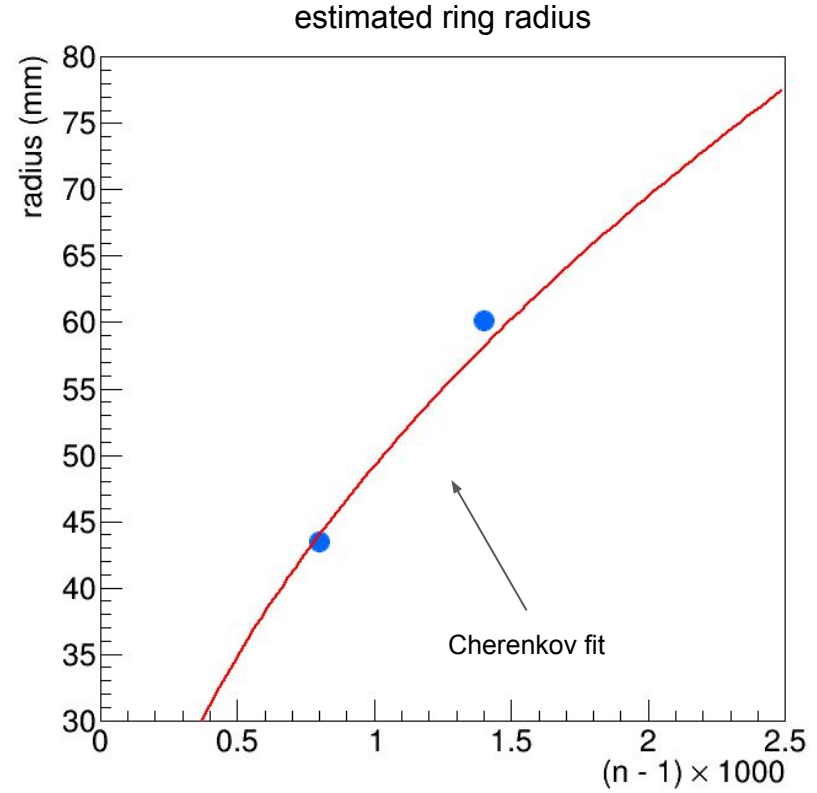
heavier gas, larger refractive index, larger ring

Gas radiators

standard gas C_2F_6 ($n = 1.0008$) and heavier C_4F_{10} ($n = 1.0014$)



increases with refractive index (angle)



radius increases